

CHAPTER 19

Sedimentation Hazards

*Marcelo H. García, Robert C. MacArthur, Richard French, Julianne Miller
with Appendix by Jeffrey Bradley, Tom Grindeland and Hans Hadley*

19.1 INTRODUCTION

In May 1980 Mount St. Helens erupted, removing the upper 404 m (1,324 ft) of the mountain and depositing approximately 2.8B m³ (3.7B cubic yd) of material over an area of 596 km² (230 square mi). The resultant debris avalanche buried the upper 27.2 km (17 mi) of the North Fork Toutle River to an average depth of 46 m (150 ft). Mudflows carried a significant amount of this material downstream into the Toutle, Cowlitz, and Columbia Rivers. It became clear at the time that knowledge about mass sediment movement was extremely limited. This geologic event of catastrophic proportions generated a substantial amount of interest on debris-flows and mudflows. Mount St. Helens is presented as a case study in an appendix to this chapter.

Hyperconcentrated flows had not received much attention in *ASCE Manual 54*, “Sedimentation Engineering”, (Vanoni, 1975; 2006), which was originally published five years before the eruption of Mount St. Helens. In fact, one of the few references to hyperconcentrated flows was about the seminal work by Beverage and Culbertson (1964).

Since 1975, when *Manual 54* was first published, there have been several publications on the subjects of debris-flow (Takahashi, 1991; Lorenzini and Mazza 2004); hyperconcentrated flows (Wan and Wang 1994); mud flows (United Nations 1996; Coussot 1997); alluvial fans (French 1987; NRC 1996a); and landslides (NRC, 1996b). There have also been several international meetings devoted to debris-flows hazards and their mitigation (Walling et al. 1992; Chen, 1997a; Wieczorek and Naeser 2000; Rickenmann and Chen 2003). However, this is clearly an area where much interdisciplinary research is still needed, because there is quite a gap between theoretical analysis, numerical modeling, laboratory experiments and what is observed in the field.

In the past decade, a plethora of models for debris-flows and mud flows have appeared in the literature. Some of them

are coupled to hydrologic models with GIS frameworks for hazard mapping. A recent international conference on debris-flows provides a good source of information on debris-flow modeling, laboratory experiments and field observations (Rickenmann and Chen 2003). Although computational modeling capabilities have increased substantially, it is also important to realize that physical experiments and field observations need to continue at a steady pace so that theoretical and numerical models can be tested and further improved. In this regard, many studies have been conducted at the USGS debris-flow facility located at H. J. Andrews Experimental Forest in Oregon (Iverson et al. 1992; Major and Iverson, 1999; Denlinger and Iverson 2001). Prototype-scale experiments such as these yield high-resolution data that help refine the interpretation of field observations as well the predictions of theoretical and numerical models.

The fact that current knowledge about sedimentation hazards is still rather limited, in particular for hazard assessment and mitigation, was made evident recently in Latin America. The torrential flows that took place in the north coastal range of Venezuela (state of Vargas) in December, 1999 were a unique event in Latin American history, and perhaps in the world. On that day simultaneous extreme debris-flows occurred in about 20 streams (Fig. 19-1) along 50 km of a narrow coastal strip (Lopez et al. 2003). The disaster caused losses of more than \$2 billion and killed an estimated 20,000 people. In terms of human losses this was the worst natural disaster in Venezuelan history and one of the worst in South America (Wieczorek et al. 2001).

As shown in Fig. 19-2, most of the cities along the Venezuelan coastline that were devastated by sedimentation are located in alluvial fans (Lopez and Garcia, 2000). Obviously the people living at these locations were not aware of the potential dangers and the authorities were not aware of the need to have any evacuation or emergency plans. There is a clear need to create public awareness of mudflows and

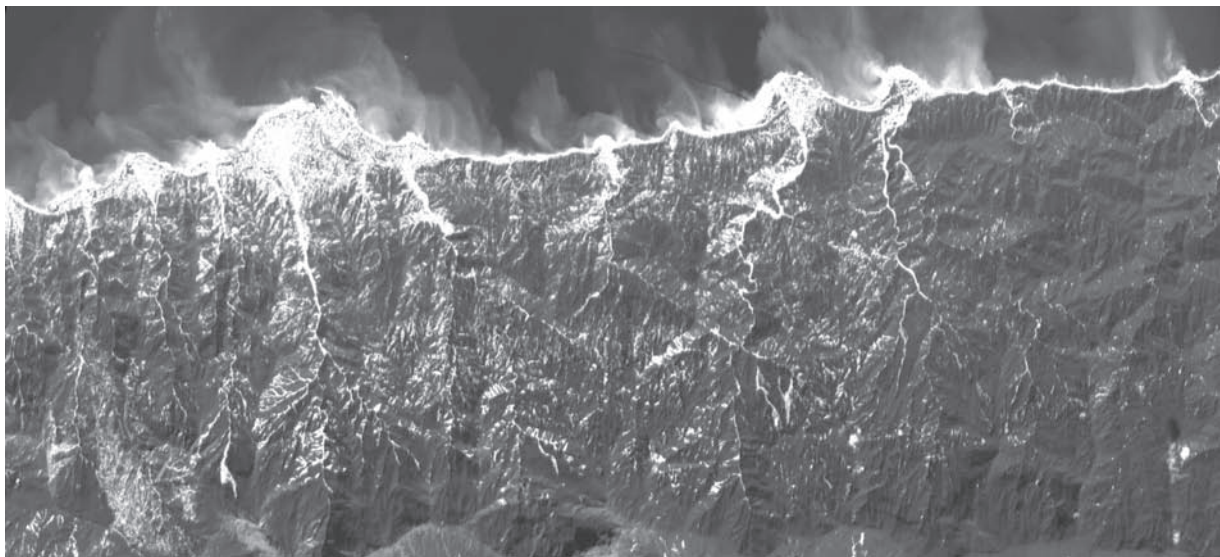


Fig. 19-1. Image of Venezuela northern coastline a few days after catastrophic sedimentation events of December 1999. (Source: SPOT Satellite)



Fig. 19-2. Town of Tanaguarena located in the alluvial fan of the Cerro Grande River in the aftermath of catastrophic sedimentation events, December 1999, Venezuela. (From López and García 2000 with permission).

sediment hazards in general. In a paper published in *Natural Disaster Science*, Takahashi (1981b) pioneered the estimation of potential debris-flow hazards, including the hydrologic and soil conditions leading to them, in Japan. His approach has great potential for the estimation of hazardous areas as well as countermeasures to prevent disasters in other

debris-flow prone areas around the world. More recently, Rickenmann (1999) has advanced a series of useful empirical relationships that can be used by practicing engineers to assess debris flow hazard potential. Obviously the need to conduct field reconnaissance and to search for historic events wherever possible cannot be overemphasized.

In order to mitigate the damage caused by landslides, debris-flows and mudflows, it is necessary to introduce various structural and non-structural measures (United Nations 1996). For this purpose, policy makers, community leaders, and teachers in mudflow-prone regions have important roles to play. At the same time, most universities do not cover in their courses the mechanics of sediment transport during extreme hydrologic or geologic events, when the most destructive sedimentation events take place. Thus there is a need to summarize what is known about the subject of sedimentation hazards in this second volume *Manual 110* "Sedimentation Engineering."

This chapter attempts to summarize what is known about hyperconcentrated flows such as mud-floods, mudflows, and debris-flows, so that hydraulic and sedimentation engineers involved in the planning and design of mitigation measures as well as risk assessment have the best tools available for their use. However, the importance of public information and education to improve sediment hazard awareness and avoidance cannot be emphasized enough.

19.2 SEDIMENTATION HAZARDS—HISTORY AND MAGNITUDE

Throughout recorded history natural disasters have claimed lives and resulted in significant losses of property, income and social stability. Today there is far greater potential for worldwide catastrophic events, and there are far greater impacts from such events, because of a growing population in high-hazard areas, mounting investment and value of structures, dependency upon lines of communication, and the growing economic interdependence of businesses, communities and nations (NRC 1989). People's propensity to occupy areas subject to natural hazards, to alter natural watercourses, to alter land forms, and to engage in other activities that impact natural hydrologic and sedimentation processes creates a need to understand and forecast where and when such hazards may occur and to be able to avoid and mitigate for hazards. The first step for reducing natural sedimentation hazards is to become aware of their likely occurrence and their consequences. This awareness is necessary to motivate financial and scientific resources to prepare means for reducing and mitigating natural hazards.

Worldwide, nearly 3 million people died and approximately 820 million more were injured, displaced, or otherwise affected by natural disasters during the period from 1969 to 1989 (NRC 1989). Nearly 670,000 people were killed and approximately 211 million were adversely affected by natural disasters from 1991 to 2000 (IFRCRCS 2001). During the period from 1965 to 1985, floods and flood-related sedimentation processes were the greatest cause of deaths and property damage by natural disasters in the United States (Rubin, et al. 1986). Global flood disasters accounted for more than two-thirds of the people

adversely affected by natural disasters from 1991 to 2000. Singh (1996) summarizes the historical occurrence of many of the largest worldwide natural and man-induced disasters since the turn of the century.

Singh (1996) also reports that flood damages, which exceeded \$50 million per event in the United States from 1947 to 1964 (22 yrs.), accounted for approximately \$5 billion in 1966 dollar equivalents. In 1968, the U.S. Water Resources Council (WRC) projected annual flood-related damages in the United States from the mid-1950's to 2020. The WRC forecast that during the period from 1966 to 2000, annual flood damages in the United States would double and by the year 2020, the annual damages would triple [from Singh (1996)]. According to the 1987 National Research Council, that forecast was low and the occurrence of significant flood-related damages in the United States and worldwide is growing because of increasing population, dramatic land use changes, and the propensity for people and valuable developments and infrastructure to locate in flood-prone zones.

Deaths and property losses from floods and fluvial processes exceeded those caused by other natural disasters such as earthquakes, hurricanes, tornadoes, tsunamis, landslides and volcanoes. These facts surprise many because floods are not usually thought to be significant causes of destruction and loss of life. This lack of public awareness of the increasing potential danger of floods and other fluvial processes, especially in the vicinity of rivers, channels, alluvial fans and coastal areas, is itself a problem. Rapidly urbanizing communities worldwide are especially susceptible to flooding problems because of the rate at which urbanization and land use are occurring. There is insufficient time to plan developments properly and they are commonly designed and constructed with a severe lack of long-term continuous rainfall and runoff records to document past flood occurrences and the capability of severe storm events to produce high-intensity, large-volume rainfall events in relatively isolated catchments. In regions where special sedimentation hazards occur (e.g., hyperconcentrated flows, flow bulking, and mud and debris-flows), traditional clear-water hydraulic design procedures for flood control works can lead to under sizing of debris retention facilities by 10 to 100 times and flood conveyance channels by 3 to 10 times depending on event sequencing, the severity of the storm event and geomorphic characteristics of the basin (MacArthur et al. 1992).

Landslide and debris-flow hazards often result from earthquakes, volcanic eruptions, and excessively wet rainy seasons, particularly those that immediately follow summer wildfires. Schuster and Flemming 1986 provide a historical review of large landslide and debris-flow events that have occurred in the western hemisphere, including the economic costs and loss of life associated with each event. The largest landslide in recorded history occurred during the May 1980 eruption of Mount St. Helens, a volcano in the state of Washington. The rock slide-debris avalanche contained

approximately 2.8 km³ of material, which traveled as far as 22 km downslope along the North Fork Toutle River. The 1964 earthquake in Anchorage Alaska was one of the largest in recorded history (M9.2) and produced the most economically costly landslides of the 20th century, amounting to nearly \$180 million (\$1 billion in today's dollars) in damage to property and infrastructure in a series of landslides that moved an estimated 260,000 km³ of material (Youd 1978). Earthquake-triggered landslides occurred in Whittier, California, causing property damages exceeding \$350 million when a magnitude 5.9 earthquake struck the area for less than 5 s. In South America, the once prosperous Armero region of Colombia was devastated by mudflows spawned by the November 1985 eruption of Nevado del Ruiz, South America's northernmost active volcano. Though not a great eruption, a pyroclastic flow melted part of the mountain's snow and ice cap, generating mudflows called *lahars* that swept down the valleys flanking the summit (NRC 1989). "Two of the largest flows, augmented by scoured slope and valley debris and moving at more than 30 kph, swept from the mouth of Rio Lagunillas Canyon into the valley cradling the town of Armero. Successive waves of mud surged through the town, tearing homes from their foundations and burying sleeping residents to a depth of up to 3 meters. The peak discharge of the mudflow, estimated from the super-elevation left by the flood mark on a river bend immediately upstream from Armero, was 30,000 m³/s (Takahashi, 1991). At least 22,000 perished, though the eruption had been predicted weeks in advance" (NRC, 1989). Similar eruption-induced mud and debris-flows, lahars and surge release debris torrents occurred at Mount St. Helens, Washington in 1980 and at Mount Pinatubo in the Philippines in 1991, killing many people and dramatically changing the landscape and rivers draining those mountains and floodplains (MacArthur et al.1993).

Massive landslides occurred in many California coastal communities during the heavy rainfall El Nino years of 1983, 1986 and 1995. Copious winter rains raise the local water level and pore pressures within hillslope soil materials, which increase the weight of hillslope materials while reducing the binding forces between layers of soil and bedrock. This often results in large slabs of weathered rock and earthen materials breaking free and sliding as a massive soil slip or rotational landslide or running out as a mud or debris-flow. Mechanisms for these types of rainfall-induced hazard are discussed by Varnes (1958), Campbell (1975), Krohn and Slosson (1976), Cannon and Ellen (1985), and Wilson and Wieczorek (1995). In 1987, California and Oregon experienced summer wildfires that lead to rainy-season fire-flood sequence-associated mud and debris-flows that damaged hundreds of homes and thousands of acres of urbanized area and dramatically affected the economies of many communities for years to come. Additional occurrences of fire-flood-associated landslides and mud and debris-flows have had dramatic effects in the states of Idaho, Wyoming, Montana,

California, Arizona, New Mexico, Oregon, and Washington during the past decade (Bigio and Cannon 2001).

Death tolls and the collapse of homes or buildings often grab headlines after an earthquake or landslide. However, the effects of the quake and slides do not end there. Chassie and Goughnour (1976) of the Federal Highway Administration estimated that more than \$100 million is a conservative total annual cost for landslide damage to highways and roads in the United States as of 1976. Water supply and sewer lines, reservoirs, pipelines, irrigation canals, flood-control channels, energy distribution and communication systems, and other transportation facilities—often referred to as *socio-economic lifelines*—are often directly impacted by landslide events as well.

Developments on alluvial fans may be at risk of severe periodic sedimentation and flooding hazards. During the spring of 1983, widespread flooding and mudflows caused an estimated \$250 million in damages to Davis County communities located on numerous alluvial fans along the base of the Wasatch Mountains in Utah. The destruction was so extensive that 22 of Utah's 28 counties were declared national disaster areas (MacArthur and Hamilton 1988). Flash flooding and mudflows resulted from a rapidly melting snow pack that triggered over 1,000 landslides in the steep canyons above Farmington, Centerville, Bountiful and Salt Lake City. Detailed flood insurance studies had been completed for the communities in Davis County, Utah just prior to the events. Traditional steady-state, clear-water flood insurance study methods were used to delineate potential flood hazard zones. However, these studies did not account for the severe sedimentation processes (hyperconcentrated sediment loading and mud and debris-flows) associated with the events, so they grossly underestimated the magnitude and aerial extent of damage such an event could cause. The City of Rancho Mirage, located in Coachella Valley, California, experienced similar sedimentation hazards and debris-flow flood events on the Magnesia Spring Creek alluvial fan in 1976 and 1979. The occurrences of these destructive, high-velocity sedimentation-associated flood events led to the design and construction of a flood-control project by the U. S. Army Corps of Engineers. Unique to that project, however, was the recognition of the need to develop new methods for estimating severe-event hydrology (peak flows and event volumes) and for the design of mud—and debris-control facilities subject to such episodic, high-energy flood hazards.

Alluvial fan flooding and mud and debris-flow-hazards are often thought to occur in arid ephemeral locations of the world; however, similar hazards occur in warm tropical as well as cold polar regions of the world (Lecce, 1990; HEC, 1993). On New Year's Eve, 1987, severe flash floods and debris-flows occurred in Hawaii. The disaster happened unexpectedly, resulting in significant property loss, injuries, and economic impacts. The event was triggered by intense rainfall occurring in steep saturated basins above residential communities, resulting in several hillslope failures and

initiating significant mud and debris-flows that ran down valley for many miles, slamming into bedroom communities in the middle of the night (see MacArthur et al., 1992). As mentioned earlier, in December 1999 heavy rains in the mountains near Caraballeda, Venezuela caused landslides, debris-flows, and flash flooding on alluvial fans located along the densely populated coast. The community of Caraballeda, constructed on an alluvial fan, was partially buried by over 1.8 million tn of debris. Total damage caused by the storm was estimated at \$1.9 billion with a loss of life exceeding 19,000 (Larsen et al., 2001; Wieczorek et al. 2001). Flash floods, debris-flows, and debris and boulder torrents are also common in steep cold-region catchments of Alaska and British Columbia. Neill, in *Hydrology of Floods in Canada* (Neill 1989), discusses special flood and sedimentation hazards associated with debris torrents and debris jam floods, phenomena typical of steep terrain. Neill (1989) also describes other unique sedimentation conditions associated with glacial outburst floods and ice jam flooding, typically found in cold regions of the world.

Other common types of sedimentation-related flood hazards include the following:

- Coastal flood and erosion hazards, including tsunami, hurricane surges, coastal bluff erosion and retreat, seasonal littoral sand transport, accelerated shoaling, sand dune and barrier island dynamics, and underwater debris-flows and turbidity currents resulting from seismic activity;
- Failure of natural debris dams formed by landslides in mountain areas;
- Collapse of mine-tailings dams. *In Tesero, Italy, a tailings dam collapsed in 1985 and the stored tailings together with the dam body material flowed down the Stava River as a mudflow, claiming the lives of 268 people and washing away 47 houses (Takahashi, 1991).*
- Gullying and hillslope instability due to deforestation, land use modification, road building, and urbanization;
- River and flood control channel instability due to local scour processes;
- Bridge pile, footing, and abutment instability due to local scour processes;
- Excessive accumulation of sediment and debris resulting in channel blockage and avulsion;
- Dam-break or glacial outburst-flood-induced debris-flows.

Even though much is yet to be learned about physical processes and consequences of sedimentation-related flood hazards, much has been learned on these esoteric topics since the first publication of *Manual 54* in 1975. During the past 30 yr, local, state, and federal researchers have advanced our abilities to identify hazard-prone zones and to estimate risks associated with sedimentation-related hazards. Since the passage of the Flood Control Act of 1936, the U. S. Corps of Engineers has been the leading federal agency responsible

for regulating flood flows and building projects to reduce flooding damage. Beginning in the late 1970's and early 1980's, the U.S. Army Corps of Engineers, in cooperation with the Federal Emergency Management Agency (FEMA) and many private and state researchers, began to develop new study and design procedures to better account for sedimentation processes that affect fluvial systems during severe floods (MacArthur and Hamilton 1988; HEC 1993). Beginning in 1987, the United Nations General Assembly initiated the International Decade for Natural Disaster Reduction (IDNDR) to run from 1990 to 2000. Its aim was to reduce the loss of life, property damage, and social and economic disruption caused by natural disasters, including those attributed to sedimentation processes. The Decade concluded that floods cause about one-third of all deaths, one-third of all injuries and one third of all damage from natural disasters worldwide (Askew 1997). The IDNDR called for action by governments and international organizations to put greater emphasis and financial commitments to disaster prevention. Today, therefore, we see more awareness and understanding of flooding and special sedimentation hazards and improved study methods for forecasting their risk of occurrence and for designing mitigation measures are becoming available.

19.3 MECHANICS OF MUDFLOWS, DEBRIS-FLOWS, AND MUD-FLOODS

19.3.1 Definition of Hyperconcentrated Flow

Hyperconcentrated sediment flows can be initiated by numerous causes including intense rainfall, rapid snowmelt, and volcanic and man-made activities (Wan and Wang, 1994). The sediment load may also be increased by hill-slope failure and bank collapse during flood events. The volume and properties of the fluid matrix, which is composed of the fluid and the sediment particles, govern flow hydraulics, flow cessation, and runout distances of hyperconcentrated sediment flows. The fluid matrix properties are usually dependent on sediment concentration, size fraction and clay content. A hyperconcentrated flow can be defined as a fluid in movement in which a high percentage of solid material is transported. The mean solid concentration by volume is defined as the ratio between the volume occupied by the solid fraction and the total mixture volume:

$$C_V = \frac{V_{\text{solid}}}{V_{\text{solid}} + V_{\text{liquid}}}, \text{ in which } V_{\text{solid}} \text{ and } V_{\text{liquid}} \text{ are the}$$

volume of the solid fraction and that of the liquid fraction of the mixture, respectively.

To avoid misinterpretation, the term *concentration* requires clarification, particularly for the case of hyperconcentrations. The units used in the measurement of sediment concentration vary with the range of concentrations and the standard measurement techniques utilized in different countries. The most common unit for sediment concentration is milligrams

per liter, which describes the ratio of the mass of sediment particles to the volume of the water-sediment mixture. Other units include kilograms per cubic meter ($1 \text{ mg/l} = 1 \text{ g/m}^3$), the volumetric sediment concentration C_V , the concentration in parts per million C_{ppm} , and the concentration by weight C_W , which are defined as follows:

$$C_V = \frac{\text{sediment volume}}{\text{total volume}} \quad (19-1a)$$

$$C_W = \frac{\text{sediment weight}}{\text{total weight}} = \frac{C_V G}{1 + (G - 1) C_V} \quad (19-1b)$$

in which $G = \gamma_s/\gamma$ is the specific gravity of the sediment and

$$C_{\text{ppm}} = 10^6 C_W \quad (19-1c)$$

Note that the percentage by weight C_{ppm} is given by 1,000,000 times the weight of sediment over the weight of the water-sediment mixture. The corresponding concentration in milligrams per liter is then calculated by the following formula:

$$C_{\text{mg/l}} = \frac{1 \text{ mg/l } G C_{\text{ppm}}}{G + (1 - G) 10^{-6} C_{\text{ppm}}} = 10^6 \text{ mg/l } G C_V \quad (19-1d)$$

The conversion factors in going from C_{ppm} to $C_{\text{mg/l}}$ are given in Table 19-1. Note that there is less than 10% difference between C_{ppm} and $C_{\text{mg/l}}$, at concentrations $C_{\text{ppm}} < 145,000$.

Table 19-1 Equivalent Concentrations for C_V , C_W , C_{ppm} , and $C_{\text{mg/l}}$

C_V	C_W	C_{ppm}	$C_{\text{mg/l}}$
Suspension			
0.001	0.00264	2,645	2,650
0.0025	0.00660	6,598	6,625
0.005	0.01314	13,141	13,250
0.0075	0.01963	19,632	19,875
0.01	0.02607	26,070	26,500
0.025	0.06363	63,625	66,250
Hyperconcentration			
0.05	0.12240	122,402	132,500
0.075	0.17686	176,863	198,750
0.1	0.22747	227,468	265,000
0.25	0.46903	469,027	662,500
0.5	0.72603	726,027	1,325,000
0.75	0.88827	888,268	1,987,500

Note: Calculations are based on mean density of water of 1g/ml and specific gravity of sediment $G = 2.65$.

Source: from Julien (1995) with permission.

In the laboratory, the sediment concentration $C_{\text{mg/l}}$ is measured as 1,000,000 times the ratio of the dry mass of sediment in grams to the volume of the water-sediment mixture in cubic centimeters ($1 \text{ cm}^3 = 1 \text{ ml}$). Two methods are commonly used: evaporation and filtration. The evaporation method is employed when the sediment concentration of samples exceeds 2,000 to 10,000 mg/l; the filtration method is preferred at lower concentrations. The lower limit applies when the sample consists mostly of fine material (silt and clay), and the upper limit when the sample is mostly sand. For samples having low sediment concentration, the evaporation method requires a correction if the dissolved solids content is high (Julien 1995).

Mud-floods are typically hyper concentrations of non-cohesive particles (e.g., sand). They display very fluid behavior for a range of sediment concentrations by volume C_V as high as 40%. *Mud-floods* are turbulent and flow resistance depends on boundary roughness, as for turbulent flows with clear water. At volumetric sediment concentrations $C_V > 0.05$ the sediment concentration of small particles tends to become more uniform than described by the Rousean vertical concentration profiles for dilute suspensions presented in Chapter 2. Increased buoyancy and fluid viscosity reduce the settling velocity of sediment particles. A detailed analysis of hyperconcentrations of sands was presented by Woo et al. (1988). Turbulent diffusion and settling fluxes are dominant despite an increase in specific weight and viscosity of the mixture. An example of a *mud-flood* is shown in Fig. 19-3. Notice the instabilities in the free surface of the flow as predicted by Engelund and Wan (1984).

Mudflows are characterized by a sufficiently high concentration of silts and clays (sediment size $< 0.0625 \text{ mm}$) to change the properties of the fluid matrix and help support large clastic material. *Mudflows* behave as a highly viscous fluid mass, which at high concentrations is capable of rafting boulders near the flow surface. Based on laboratory results, the volumetric sediment concentration of a mudflow fluid matrix is in the approximate range $45\% < C_V < 55\%$ (O'Brien, 1986). *Mudflows* exhibit high viscosity and yield stress, can travel long distances on mild slopes at slow velocities, and leave lobate deposits on alluvial fans. A detailed analysis of *mud-flow* properties has been presented by O'Brien and Julien (1988); Major and Pierson (1992); and Coussot (1997). An example of a *mud-flow* deposit is shown in Fig. 19-4.

Debris-flows are mixtures of clastic material, including boulders and woody debris, where lubricated interparticle collision is the dominant mechanism for energy dissipation. Knowledge of debris-flows is based largely on the contributions of Bagnold (1954) and Takahashi (1978). A recent review of debris-flows is given by Hutter et al. (1996). Granular flows (non-cohesive) flows without a lubricating fluid) constitute a sub class of debris-flows in which the exchange of momentum between the flow core and the boundary occurs exclusively through particle collision and friction.



Fig. 19-3. Example of mud flood (From Julien and Leon, 2000, with permission).



Fig. 19-4. Example of mudflow frontal deposit (from O'Brien et al., 1993, with permission).

Debris-flows involve the motion of large clastic material and debris characterized by destructive frontal impact surging and flow cessation on steep slopes (Fig. 19-5). Dispersive stresses arising from the collision of clastic particles control the exchange of flow momentum and energy dissipation.

Debris-flows are much less fluid than mud-floods. The fluid matrix viscosity is comparatively small corresponding to the small concentration of fine sediments. The fluid matrix is essentially non-cohesive. The interstitial fluid does not significantly inhibit particle contact, permitting frequent collisions and impact between the solid clasts. Using a linear stability analysis, Lanzoni and Seminara (1993) have explored the conditions for the development of *debris waves* similar to the commonly observed *roll waves* in steep channels conveying clear water (Chow 1959).

19.3.2 Main Classification Criteria

In the past, the main classifications of hyperconcentrated flows were based on criteria obtained from direct observations, experimental process evaluations, and morphological analysis of deposits, physical models, and theoretical studies. Some investigators have focused on the classification of hyperconcentrated flows based on sediment concentration. Another group have categorized hyperconcentrated flows based on the triggering mechanism responsible for generation of these flows, and the third group of researchers have classified these flows according to the rheological and kinematic behavior. Classifications based on sediment concentration date back to the seminal study of Beverage and Culberson (1964). Motivated by the wide spectrum of sediment-laden flows observed in the aftermath of Mount St. Helens eruption, Bradley and McCutcheon (1987) were among the first to provide a comprehensive review on the classifications of hyperconcentrated flows. Their summary of commonly used classifications is shown in Table 19-2.

The first mass-wasting classifications concentrated in particular on landslides, a phenomenon that is of great interest to any new urban settlement (NRC 1996b). Sharpe (1938) considered two main parameters, relative velocity and sediment concentration and despite the fact that he did not specify transition boundaries, this classification has been widely used and refers to the following process categories: *debris avalanches*, *mudflows*, *earthflows*, *solifluction*, *soil creep* and *streamflows*.

Two decades after the Sharpe (1938) classification scheme first appeared in the literature, Varnes (1958) presented a classification that became a main reference point for the terminology of these processes. Varnes' classification is based on two main characteristics, the type of material and the type of movement involved, whereas velocity and mixture composition are used for subclassification purposes. Therefore, for coarser materials it identifies the phenomena as block streams, debris avalanches, debris-flows (mudflows if the coarser material content is lower than 50%), solifluction, and creep, and for finer materials: blends of dry sands and silt, blends of wet sands or silt, and *earthflows*. In the Chinese literature (Wan and Wang 1994), the term "hyperconcentrated" is generally used to indicate a material having measurable yield strength and therefore debris-flows

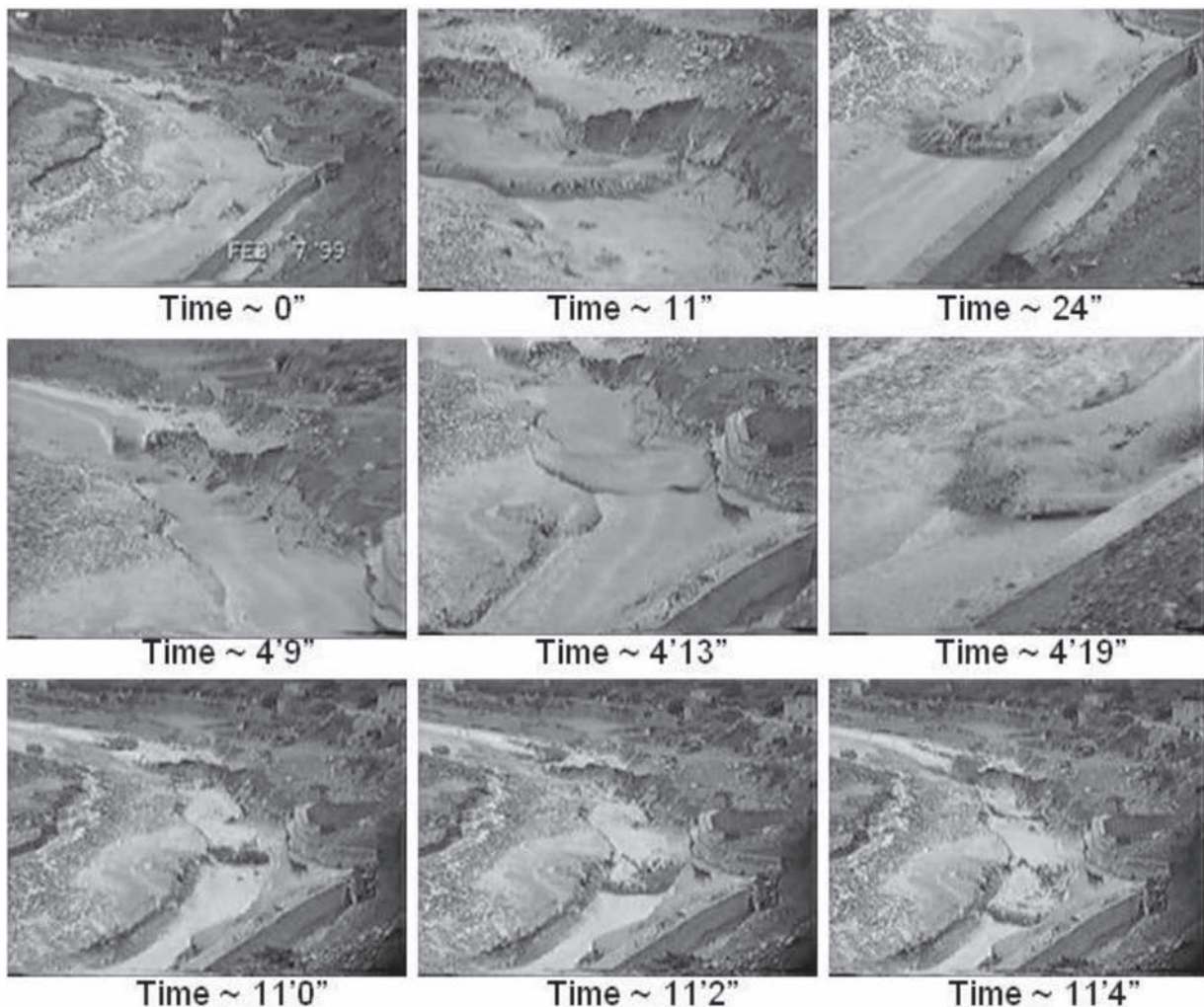


Fig. 19-5. Video images of debris flows passing by town of Iruya, Salta, Argentina, February 7, 1999 (courtesy of Daniel Brea and Pablo Spalletti).

are considered as hyperconcentrated flows. However, more recent classifications have attempted to systemize established terminology by introducing quantitative criteria.

Takahashi (1991) defines mass wasting as the fall, slide, or flow of a conglomerate or dispersed mixture of sediment in which gravity moves all the particles and the interstitial fluid, so that the relative velocity between the solid and fluid phases in the main direction of motion plays a minor role, whereas in a fluid flow the forces of lift and resistance caused by relative velocity are essential for the transport of each single particle. In this approach, the following four phenomena can be distinguished on the basis of the mechanism that supports the clasts, the properties of the interstitial liquid, velocity, and distance reached: *falls*, in which the single particles move separately with relatively small internal deformation; *sturz-stroms*, particularly rapid and destructive events; *pyroclastic flows*, which are rapid and explosive events originated by volcanic eruptions, in which the suspension mechanism is linked to the expansion of the gas trapped within the flow; and,

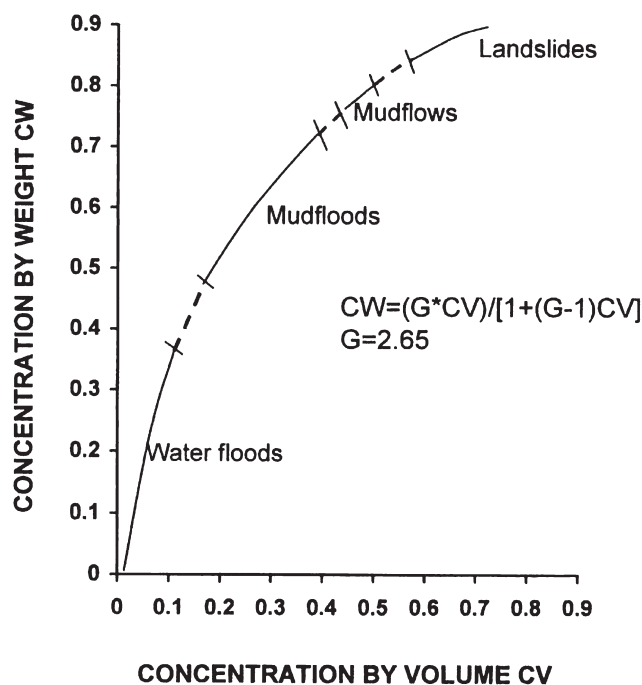
finally, *debris-flows*, in which the grains are dispersed in a water-clay interstitial fluid. These last three processes can be termed collectively *gravitational sediment flows* (Takahashi 1991) and constitute continuous processes that require a certain force for grain suspension.

In the case of debris-flows, the approach of Bagnold (1954) and Takahashi (1978) considers the dispersive pressure that results from the exchange of momentum between grains as predominant; if the interstitial fluid is particularly dense, large clasts can be suspended with relatively low dispersive pressures by floating in the fluid phase. Another approach, first advanced by Johnson (1970), considers that the viscous stress of the interstitial fluid is predominant and neglects interactions between grains.

Following a number of laboratory experiments with samples from Colorado, O'Brien and Julien (1985) classified hyperconcentrated flows according to the properties controlled by sediment concentrations, as *water floods*, *mud-floods*, *mudflows*, and *landslides* (Fig. 19-6). The characteristic

Table 19-2 Classification of High Sediment Concentration Flows (After Bradley and McCutcheon 1987).

Source	Concentration percent by weight (100% by WT = 1,000,000 ppm)									
	23	40	52	63	72	80	87	93	97	100
Concentration percent by volume (G. = 2.65)										
Beverage and Culbertson (1964)	High	Extreme	Hyperconcentrated				Mud Flow			
Costa (1984)	Water Flood		Hyperconcentrated				Debris Flow			
O'Brien and Julien (1985) using National Research Council (1982)	Water Flood		Mud Flood	Mud Flow		Landslide				
Takahashi (1981)	Fluid Flow			Debris or Grain Flow				Fall, Landslide, Creep, Sturzstrom, Pyroclastic Flow		
Chinese Investigators (Fan and Dou, 1980)					Debris or Mud Flow					
Sediment Laden						Hyperconcentrated Flow				
Pierson and Costa (1984)	STREAMFLOW			SLURRY FLOW			GRANULAR FLOW			
	Normal: Hyperconcentrated			(Debris Torrent), Debris Mud Flow, Solifluction			Sturzstrom, Debris Avalanche, Earthflow, Soil Creep			

**Fig. 19-6.** Classification of hyperconcentrated flows after O'Brien and Julien (1985).

stresses of such processes are yield stress, viscous stress, turbulent stress in the fluid, and dispersive stress caused by the inertial impact of the coarser sediments. Which of these stresses dominates depends on the volumetric concentration of sediment and the percentage of the fine fraction. Despite

the fact that the transition between the types of flow is difficult to determine, according to this approach they can be divided into three categories, which lie between conventional stream flooding on the one hand and landslides on the other end.

Mud-floods are hyperconcentrated flows of cohesionless particles (mainly sand) with limited quantities of cohesive particles, which show characteristics that are typical of fluids, with sediment concentrations by volume of 20 to 45% (Winterwerp et al. 1990). From a hydrodynamic point of view, *mud-floods* have characteristics that are typical of a conventional turbulent flow and resistance to motion depends on the roughness of the channel in which the flow occurs. Moreover, they are not able to support stress without deforming and show no yield stress. Sediment concentration tends to be uniformly distributed throughout the flow depth, because the viscosity of the interstitial fluid reduces the velocity of particle sedimentation.

Mudflows are hyperconcentrated flows composed, to a large extent, of cohesive silt and clay particles (smaller than 0.0625 mm), in which sediment concentration by volume varies between 45 and 55%. This composition alters the properties of the interstitial fluid, making it extremely viscous and giving it considerable yield strength. Consequentially, in the free surface area, *mudflows* can hold clasts of considerable size in suspension for long distances even on slight slopes, resulting in the formation of lobe-shaped deposits. Typical resistance to motion is a characteristic of pseudoplastic fluids that appears with high viscosity (Huang and Garcia 1998).

Debris-flows are mixtures of clastic material with high coarse particle contents, in which collisions between particles and therefore dispersive stresses are the dominant mechanisms in energy dissipation. Cohesionless granular debris-flows are a subcategory of debris-flows, in which momentum exchange takes place due to friction and collisions. These phenomena occur depending on the simultaneous occurrence of the following conditions:

- high volumetric concentration of sediments (>0.5);
- high shear rates ($>100 \text{ s}^{-1}$);
- large particle dimensions ($>5\%$ compared to streamflow depth).

Coussot (1992) considers two types of debris-flow: *granular* ones, which have a fine particle fraction quantity (dimension smaller than $40 \mu\text{m}$) 10% lower than the entire solid mass, and *muddy* ones in which the fine fraction exceeds 10%. Coussot's classification is given in terms of dimensional grain distribution, as shown in Fig. 19-7.

When the rheological behavior of granular mixtures is used for classification purposes, two further studies must be considered. Savage (1984) identified three flow regimes for granular mixtures, each one characterized by a value of the solid fraction, interstitial viscosity, and deformation rate: the *macroviscous* regime, in which the viscous effects of the interstitial fluid and solid particle interactions cause the stresses; the *quasistatic* regime, in which dry friction and prolonged contacts between particles are important, whilst inertial effects are negligible; and last, the *inertial-granular* regime, in which the inertia associated to the individual particles prevails. Iverson (1985) developed a constitutive equation for the idealized behavior of mass wasting, based on linear and nonlinear rheological models, which range from the purely plastic case to the purely viscous one; this equation represents an important analytical relationship for differentiating between various types of flow.

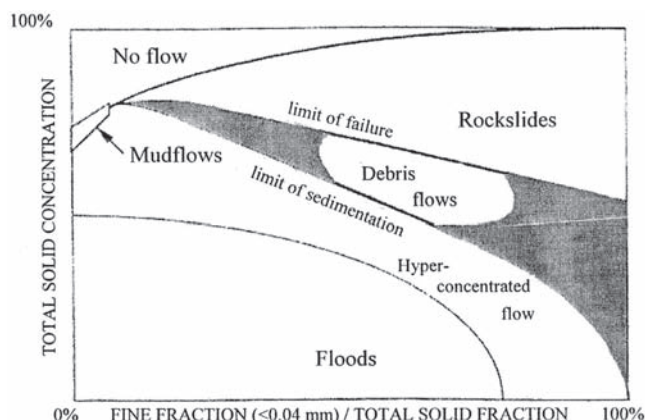


Fig. 19-7. Coussot's (1992) conceptual classification of hyper-concentrated streamflows.

A rheological classification of the various types of flow using a two-dimensional matrix (Fig. 19-8) that considers the mean flow velocity and sediment concentration was proposed by Pierson and Costa (1987). This classification makes it possible to distinguish each process from the others, if mean flow velocity is known or can be estimated and additional information is available on the existence of yield strength and stream capacity to suspend large clasts, characteristics that can be determined by an analysis of sediment deposits. This approach distinguishes between a dilute, ordinary streamflow and a hyperconcentrated streamflow according to whether the flow is Newtonian or non-Newtonian, and between a slurry and a granular flow, the limit being a function of sediment size and particle gradation. In the graph shown in Fig. 19-8, vertical rheological divisions A, B, and C depend on grain size and concentration. From left to right, boundary A represents the appearance of yield strength; boundary B marks sudden increase in yield strength rapid increase that enables the static suspension of granules and the onset of liquid behavior; boundary C marks the cessation of liquid behavior. The horizontal velocity limits, which are also functions of

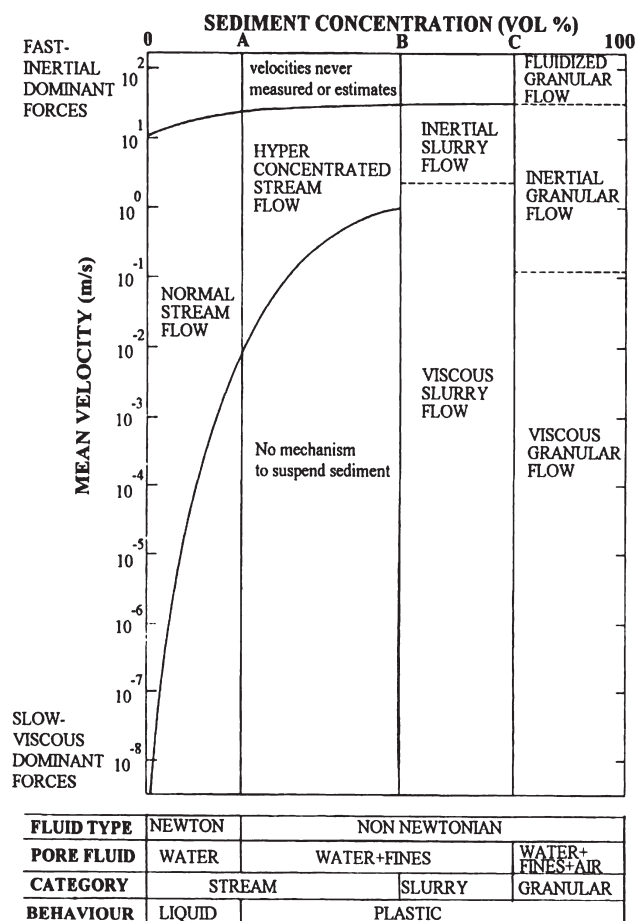


Fig. 19-8. Classification of water-sediment mixtures proposed by Pierson and Costa (1987).

grain-size distribution and sediment concentration as well as particle density, are determined by how shear stress is transmitted between particles during the flow. In the case of cohesive materials or those that contain a high proportion of fine materials, the vertical lines on the graph, that divide the various rheological behavior types, must be shifted to the left; the opposite is true if the mixture contains mainly well-sorted, coarse clasts. It is therefore possible to identify two large-flow categories: one that includes *ordinary streamflows* and *hyperconcentrated streamflows* and a second one that includes *slurry flows* and *granular flows*.

According to Davies (1986; 1988), who reviewed numerous debris-flow descriptions, basically three different debris-flow types can be distinguished:

Type 1: low-density, steadily moving turbulent flows, carrying coarse particles as bed load only and with the fluid made up of a slurry.

Type 2: high-density, laminar flows, carrying fine and coarse particles uniformly distributed over the depth, of unsteady nature with pulse-like motion.

Type 3: the same as Type 2 but consists of a single pulse or wave.

The latter two types have a higher viscosity than the first one, and selective deposition of the coarser particles does not seem possible. Due to their larger flow depths and velocities their destructive power is considerable. In order to distinguish between steady- and unsteady-type debris-flows, Davies (1997) proposed a density of 1.6 to 1.8 tn/m³, corresponding to sediment concentrations of about 36 to 49% by volume. He pointed out that the transition seems to be rather abrupt if a particular flow changes from one type to another. This transition is also reflected in the sediment deposits of either a “water flood” or a debris-flow (Costa 1984).

One of the main problems in the development of a unifying classification scheme relates to the fact that the physical properties of debris-flows, and hyperconcentrated flows in general, vary over a wide range in the field (Iverson, 2003). A summary of physical properties of debris-flows prepared by Costa (1984) is reproduced in Table 19-3. It can be observed that the dynamic viscosity as well as the density of these flows can be much larger than in the case of dilute suspensions. Except for the fast-moving *mudflows and debris flows* observed in China, it is interesting to observe that most flows are laminar as pointed out by very low values of the estimated Reynolds number (Coussot, 1994).

An interesting graph showing a continuous spectrum of sediment concentrations from sediment-laden rivers to debris-flows first proposed by Hutchinson (1988) is shown in Fig. 19-9. What makes this graph particularly useful is that it includes information on conditions observed in the field (some of which are mentioned in Table 19-3), ranging from *streamflows* carrying modest amounts of sediment

all the way to *landslides* having very low water content and very large solids concentrations (Bagnold 1956). This graph includes also the water content in the sediment-water mixture, a parameter that is relatively easy to measure in the field. This is important because soil saturation with water is an important factor in the triggering of *landslides* that might evolve into *debris* and *mud flows*. As shown therein, debris-flows are often of very high density, over 80% solids by weight, and may exceed the density of freshly-mixed concrete. They can therefore move boulders that are meters in diameter as shown in Fig. 19-10. The equation shown in Fig. 19-9 is given by the following expression,

$$\gamma_{\text{sat}} = G \gamma_w \left[\frac{1+W}{1+WG} \right]$$

where γ_{sat} is the specific or unit weight of a saturated soil (sediment plus water) sample, $G = \gamma_s/\gamma_w$ is the specific gravity of the sediment defined earlier as the ratio between the specific weight of the sediment and the specific weight of water. This parameter can have values between 2.6 and 2.75. The water content $W = M_w/M_s$ in the sample is defined as the ratio between the water mass M_w and the sediment mass M_s in the soil sample. It is clear that when the water content W is very large $\gamma_{\text{sat}} \rightarrow \gamma_w$ corresponding to a dilute open-channel suspension; and when the water content decreases and the sediment concentration increases $\gamma_{\text{sat}} \rightarrow \gamma_s$ corresponding to *hyperconcentrated flows* such as *mudflows and debris flows*.

As observed in Fig. 19-10, the impact of large boulders can cause substantial destruction of buildings so it can be useful to estimate potential impact loads resulting from *debris flows*. Impact loads result from objects entrained in the flow striking a structure surface with a velocity component perpendicular to the flow direction (Julien and O'Brien 1997). To compute the impact load, consideration should be given to the evidence of debris and boulders transported on the fan by recent flood events. To be conservative, the largest boulder transported by a flow should be used to determine the impact load. The impact loading P_I is given by:

$$P_I = \frac{wV}{(Ag\Delta t)}$$

where w is the weight of the object (largest boulder), g is the gravitational acceleration, V is the flow velocity, A is the area of impact assumed to be a percentage of the cross sectional area of the object and Δt is the duration of impact. It has been observed that the largest boulders in a given flow have a tendency to accumulate on the frontal area of debris flows (Suwa 1987), where they can be expected to have the largest effect when impacting a structure. Recently, the effect of particle segregation and its implications for debris flows have been studied experimentally by Zanuttigh and Di Paolo

Table 19-3 Physical Properties of Observed Debris-Flows Compiled by Costa (1984)

Location	Velocity [m/s]	Slope [%]	Bulk density [g/cm ³]	μ [poise]	Clay [%]	Depth [m]	Solids [% wt.]	Reynolds No.
Rio Reventado, Costa Rica	2.9–10	4.6–17.4	1.13–1.98	—	1–10	8–12	20–79	—
Hunshui Gully, China	10–13	—	2–2.3	15–20	3.6	3–5	80–85	40,000
Bullock Creek, New Zealand	2.5–5.0	10.5	1.95–2.13	2,100–8,100	4	1.0	77–84	28.57
Pine Creek, Mount St. Helens	10–31.1	7–32	1.97–2.03	2,000–3,200	—	0.13–1.5	—	200
Wrightwood Canyon, California	1.2–4.4	9–31	2.4	2,100–6,000	<5	1.2	79–85	23.8
Wrightwood Canyon, California	0.6–3.8	9–31	1.62–2.13	100–60,000	—	1.0	59–86	1.33
Mayflower Gulch, Colorado	2.5	27	2.53	30,000	1.1 (<0.004 mm)	1.5	91	3.2
Dragon Creek, Arizona	7.0	5.9	2.0	27,800	—	5.8	80	29.2
Jian-jia Ravine, China	8.0	0.06	2.3	15.5–1,736	—	1.4	89	148–11,561

(2006). There is also a FEMA Manual (1994) that provides equations for the computation of the hydrostatic and hydrodynamic loads on structures.

19.3.3 Rheology of Hyperconcentrated Sediment Flows

The general flow behavior of hyperconcentrated sediment flows can be inferred from an examination of the physical processes triggering hyperconcentrations in a watershed, an assessment of sediment availability and sediment source, an investigation of historical flood events on the same or neighboring watershed, and a rheological and particle size analysis of deposits. Deposits from historical or recent events can be brought to the laboratory for a rheological investigation at various sediment concentrations. As discussed above, hyperconcentrated sediment flows can be classified, in general, as mud-floods, mudflows, and debris-flows. Distinct physical processes differentiate these types of hyperconcentrations based on the rheology of the water-sediment mixture.

Various researchers have developed and applied models of mud and debris-flow rheology. These models can be classified as Newtonian models (Johnson 1970; Hunt 1994; Aguirre-Pe et al. 1995); linear and nonlinear viscoplastic models (Johnson 1970; O'Brien and Julien 1988; Liu and Mei 1989; Huang and Garcia 1997a; 1997b; 1998; Imran et al. 2001); dilatant fluid models (Bagnold 1954; Takahashi

1978; Mainali and Rajaratnam 1994); dispersive or turbulent stress models (O'Brien et al. 1993); and frictional models (Iverson 1997).

Rheology is the science of describing the deformation and flow of matter. More specifically, the graphical measure of the shear stress applied at a given rate of deformation of a fluid defines a rheogram. In clear water flows, the shear stress increases linearly with the rate of deformation (i.e., velocity gradient) in the laminar flow regime and the fluid is said to be Newtonian (i.e., $\tau = \mu du/dz$). The dynamic viscosity of a sediment-water mixture μ is then defined as the slope of the rheogram.

There is substantial evidence indicating that mud at high enough concentrations shows non-Newtonian rheological behavior (e.g., Coussot 1994). Videos taken by Davies (1988) during his laboratory experiments show that there are both a thin shear layer near the bed and an upper plug-like layer in which the particles are nearly locked together. This upper plug-like layer is a property of non-Newtonian fluids, and is clearly associated with some yield stress. Rheological studies by Krone (1963), Migniot (1968), and Wan (1982) indicate that mud from different sources behaves approximately as a Bingham plastic fluid whose yield stress, τ_y , and viscosity, μ , increase monotonically with clay concentration. The ranges of values commonly observed for such parameters values are $10^{-6} \text{ m}^2/\text{s} < \mu/\rho < 1.2 \times 10^{-3} \text{ m}^2/\text{s}$ and $10^{-3} \text{ N/m}^2 < \tau_y < 10^2 \text{ N/m}^2$, whereas sediment concentration varies in the

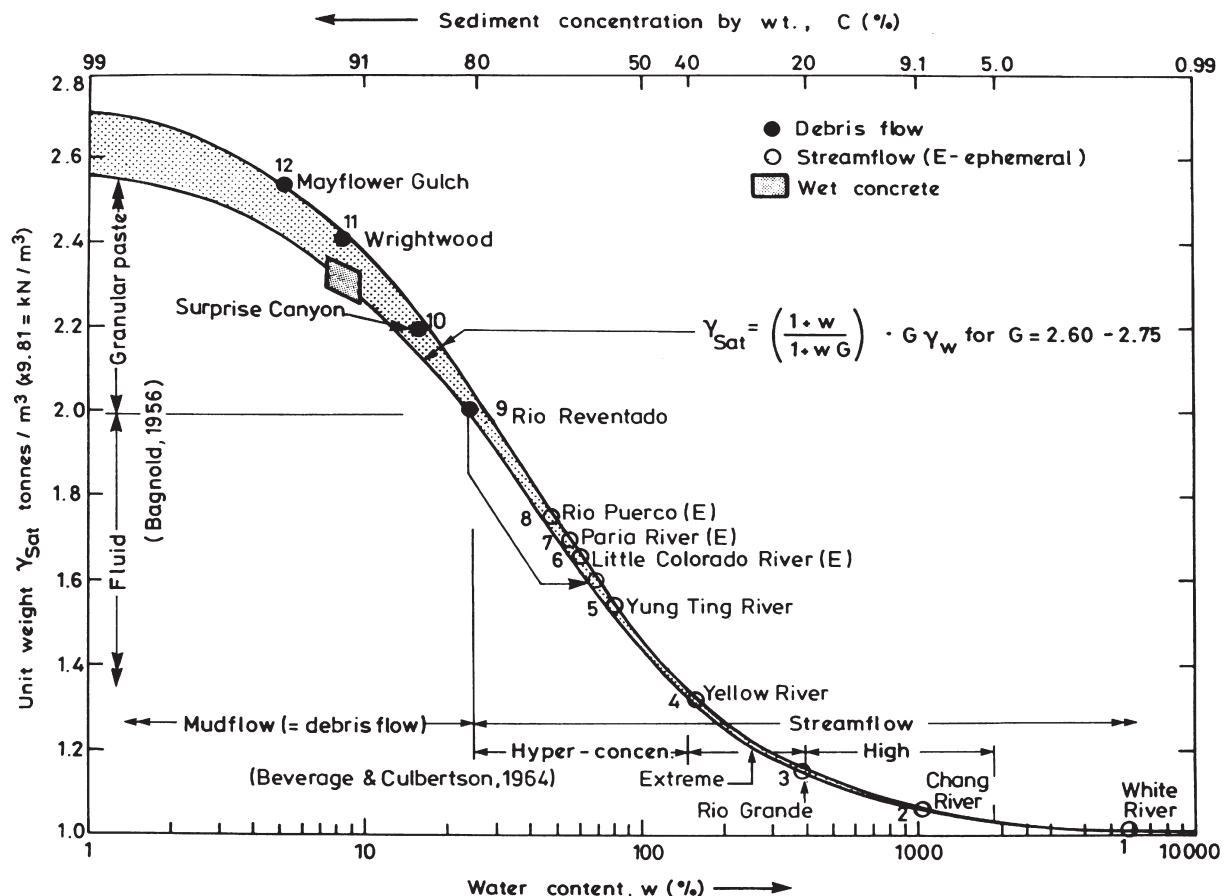


Fig. 19-9. Continuous spectrum of sediment concentrations and water content from sediment-laden rivers through ephemeral streams to mudflows and debris flows (Hutchinson 1988).

range from 2 to 700 kg/m³. Such a fluid at rest is capable of resisting any shear stress less than the yield stress. When the yield stress is exceeded, the fluid structure changes and the material behaves like a Newtonian fluid driven by the excess of the shear stress beyond the yield stress. When the shear stress falls below the yield stress, the fluid structure changes again, and there is no fluid flow. There is also evidence that fine-grained debris-flows (Mainali and Rajaratnam 1991; 1994; Dominique and Coussot, 1997), liquefied mine tailings materials (Jeyapalan et al. 1983), molten lava (Johnson 1970), and snow avalanches (Dent and Lang, 1983) can be modeled as Bingham plastic fluid flows (Huang and García 1997b).

The Bingham rheological model is to some extent a limiting or idealized rheological model. Beyond a finite shear stress (i.e. *yield stress* τ_y) the rate of deformation, du/dz , is linearly proportional to the excess shear stress. The constitutive equation is

$$\tau = \tau_y + \mu \frac{du}{dz} \quad (19-2)$$

The Bingham plastic model is well suited to homogeneous suspensions of fine particles, particularly at low rates of deformation. Experimental laboratory results of Qian and Wan (1986) and others confirm that under rates of deformation observed in the field, fluids with large concentrations of fine particles behave like Bingham plastic fluids. Huang and Garcia (1997b) extended the perturbation-technique approach first proposed by Hunt (1994) for Newtonian flows and proposed a Bingham model to estimate the run-out distance of mudflows. However, it should be clear that rheological models can only provide a first-order approximation for the purpose of modeling hyperconcentrated flows in the field. A number of non-Newtonian rheological models have been proposed for debris-flows and mudflows, including Herschel-Bulkley's viscoplastic model (Chen 1988; Liu and Mei 1989; Huang and García 1998; Imran et al. 2001). It is difficult to say which constitutive equation best represents the behavior of a mud flow.

The analysis of coarse sediment mixtures as observed in debris-flows is somewhat more complex and involves an additional shear stress due to particle-particle interaction (MacTigue 1982; Shen and Ackermann 1982; Mih 1999).



Fig. 19-10. Boulders deposited by debris flows in the alluvial fan of the San Julian River, Venezuela, December 1999 (from López and García 2000 with permission).

Bagnold (1954) pioneered laboratory investigations on the impact of sediment particles. He defined the dispersive shear stress τ_d induced by the collision between sediment particles as

$$\tau_d = c_B \rho_s \left[\left(\frac{0.615}{C_v} \right)^{1/3} - 1 \right]^{-2} D_s^2 \left(\frac{du}{dz} \right)^2 \quad (19-3)$$

where

- C_v = volumetric sediment concentration;
- D_s and ρ_s = sediment particle diameter and density, respectively; and
- c_B = an empirical impact coefficient defined by Bagnold ($c_B \approx 0.01$).

Takahashi (1980) has found experimentally that the impact coefficient ranges between 0.35 and 0.5; an order

of magnitude larger than the value suggested by Bagnold (1954).

The dispersive shear stress is shown to increase with three parameters: the second power of the particle size, the volumetric sediment concentration, and the second power of the rate of deformation. It is important to recognize that the dispersive stress is proportional to the product of these three parameters; therefore, high values of all parameters are required to induce a significant dispersive shear stress. An excellent analysis of constitutive equations for debris-flows and their applicability can be found in Egashira et al. (1997).

The non-Newtonian nature of hyperconcentrated sediment flows results from several physical processes and sediment-water mixture properties (Julien and O'Brien 1997): the cohesive yield strength τ_c , which accounts for the cohesive nature of fine sediment particles; the Mohr-Coulomb shear τ_{mc} , which accounts for the internal friction between grains; the viscous shear stress τ_v , which accounts for the fluid-particle viscosity; the turbulent shear stress τ_t ; and finally,

the dispersive stress τ_d , which accounts for the collision of the largest particles or clasts. Then the total fluid shear stress τ in a hyperconcentrated sediment flow results from the sum (*assuming that all the shear stresses can be linearly added*) of the five shear stress components:

$$\tau = \tau_{mc} + \tau_c + \tau_v + \tau_t + \tau_d \quad (19-4)$$

A quadratic rheological model has been proposed by O'Brien and Julien (1985) and Julien and Lan (1991), which describes the flow continuum through the range of sediment concentrations for these shear stresses. When written in term of shear rates, or velocity gradient du/dz , τ_{mc} and τ_c are independent of velocity gradient, τ_v varies linearly with velocity gradient, and both τ_t and τ_d vary with the second power of the velocity gradient. The resulting quadratic constitutive equation is given by

$$\tau = \tau_y + \mu_m \frac{du}{dz} + \zeta \left(\frac{du}{dz} \right)^2 \quad (19-5)$$

where

$\tau_y = \tau_{mc} + \tau_c$ = yield stress;
 μ_m = dynamic viscosity of the sediment-water mixture; and ζ = the turbulent-dispersive parameter. The last term of the quadratic model combines the effects of turbulence with the dispersive stress induced by the inertial impact of sediment particles. Combining the conventional expression for the turbulent stress in sediment-laden flows with Bagnold's dispersive stress gives

$$\zeta = \rho_m l_m^2 + c_B \rho_s \lambda_B^2 D_s^2 \quad (19-6)$$

where

ρ_m and l_m = the mass density and mixing length of the mixture, respectively; D_s and ρ_s = sediment particle diameter and density, respectively;
 λ_B = Bagnold's linear sediment concentration (defined below);

and

c_B = Bagnold's empirical impact coefficient ($c_B \approx 0.01$). The mass density of the mixture, ρ_m , is calculated from $\rho_m = \rho + (\rho_m - \rho)C_v$, where C_v is the volumetric sediment concentration and ρ is the density of water. Bagnold's (1954) linear sediment concentration is estimated as

$$\lambda_B = \frac{1}{\left(\frac{0.615}{C_v} \right)^{1/3} - 1} \quad (19-7)$$

Viscosity μ_m and yield stress τ_y have generally been explained through increasing exponential functions of the volumetric

sediment concentration (Julien 1995; Lorenzini and Mazza 2004). O'Brien and Julien (1988) measured the rheological properties of natural silt and clay mudflow deposits from the Colorado Rocky Mountains. The yield stress and the viscosity increase by three orders of magnitude as the volumetric concentration increases from 0.10 to 0.40.

It is important to consider that the occurrence of granular debris-flows as prescribed by a dispersive stress relationship alone requires that the following three conditions be simultaneously satisfied: the flow has (1) very large sediment concentrations, typically $C_v > 0.5$; (2) large velocity gradients, typically exceeding 100 s^{-1} ; and (3) very large sediment particles, typically coarser than 5% of the flow depth.

Yield stress is a factor that not only influences debris-flow mobilization, but also is indirectly connected to the resistance that causes stoppage in the final stages of movement. During experiments one can observe that yield stress is always higher for initiation of motion than the corresponding values in stoppage conditions. Thus the yield stress presents a certain form of hysteresis, which must be considered in forecasting the overall distance covered by a debris-flow (*runout*) for a given topography (Contreras and Davies 2000). In fact, by using the yield stress associated with initiation of motion in a runout-distance forecasting model, one is likely to seriously underestimate it.

19.3.4 Dimensionless Rheological Model

To establish a rheological classification for hyperconcentrated flows, Julien and Lan (1991) and Julien and O'Brien (1997) proposed a dimensionless formulation of the quadratic rheological model presented above (Eq. 19-5) in the form

$$\tau^* = 1 + (1 + T_d^*) c_B D_v^* \quad (19-8a)$$

in which the three dimensionless parameters τ^* , D_v^* and T_d^* are defined as follows:

1. Dimensionless excess shear stress

$$\tau^* = \frac{\tau - \tau_y}{\mu_m \frac{du}{dz}} \quad (19-8b)$$

When $\tau^* = 1$, the mixture behaves as a Bingham fluid.

2. Dimensionless dispersive—viscous ratio

$$D_v^* = \frac{\rho_s \lambda_B^2 D_s^2}{\mu_m} \left(\frac{du}{dz} \right) \quad (19-8c)$$

This is essentially the Bagnold number (Hanes and Bowen 1985). When D_v^* is large, the flow is dispersive; when D_v^* is small, it is viscous.

3. Dimensionless turbulent-dispersive ratio

$$T_d^* = \frac{\rho_m l_m^2}{c_B \rho_s \lambda_B^2 D_s^2} \quad (19-8d)$$

When T_d^* is large, the flow is turbulent; when T_d^* is small, it is dispersive.

Julien and Lan (1991) tested the dimensionless model and the results are in agreement with the data sets from Bagnold (1954), Govier et al. (1957), and Savage and McKeown (1983), as shown in Fig. 19-11. The quadratic model is valid for all values of the parameter D_v^* and reduces to the Bingham model when $D_v^* < 30$ and to turbulent-dispersive formulations when $D_v^* > 400$.

The transition between grain-flow and fluid-mud is not easy to characterize, even in the realm of laboratory experiments (Parsons et al., 2001). Thus the limiting conditions should be used with caution in trying to distinguish between *mudflows* and *debris-flows*.

To relate the parametric delineation to the classification of hyperconcentrated sediment flows, the following guidelines are suggested (Julien and O'Brien 1997):

1. *Mud-floods* occur when the turbulent shear stress is dominant, as given by $D_v^* > 400$ and $T_d^* > 1$;
2. *Mudflows* occur when yield and viscous stresses are dominant, as given by $D_v^* < 30$;
3. *Debris-flows* or *granular flows* are expected when the dispersive stress is dominant, as given by $D_v^* > 400$ and $T_d^* < 1$.

A transition regime exists in the parameter range $30 < D_v^* < 400$, for which all the terms of the quadratic equation are not negligible. A series of examples showing the relative magnitudes of these terms can be found in Julien (1995).

Coussot et al. (1998) have proposed a laboratory test to obtain the rheological characteristics of a debris-flow that occurred on Moscardo Torrent, Italy. They added successively coarser particles obtained from the debris-flow deposits to clear water. At each addition different suspensions were obtained and tested with different rheometric

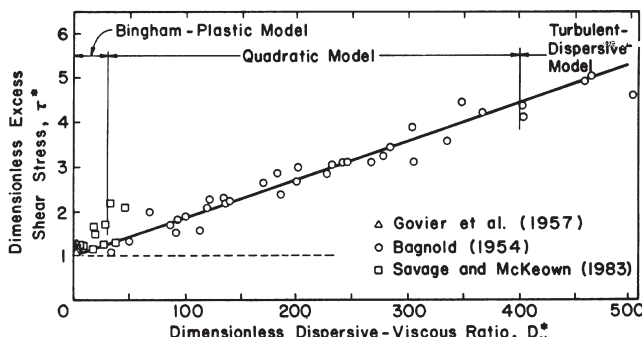


Fig. 19-11. Comparison of dimensionless model with Experimental Data (from Julien and Lan, 1991 with permission).

techniques, such as a laboratory rheometer, inclined plane test, a large-scale rheometer, and field tests. The behavior was found to be viscoplastic and well represented by a Herschel-Bulkley model (Huang and Garcia, 1998). Schatzmann et al. (2003) have presented a new rheometer, the ball measuring system, to determine the behavior of fluids with large particles. In the absence of direct rheological measurements, Locat (1997) has shown that the liquidity index can provide a good first approximation for both mixture viscosity and yield stress of fine-grained mud flows. Bin and Huilin (2000) have advanced a methodology to determine the rheological properties of debris flows in the field which is similar to the one proposed earlier by Phillips and Davies (1991).

19.4 ALLUVIAL FAN FLOODING AND SEDIMENTATION

19.4.1 Introduction

It is generally acknowledged that the delineation of flood hazards and the design of flood mitigation structures in the semi-arid and arid western United States, and in similar environments throughout the world, is more difficult than in the humid areas of the country. The primary reason is that the southwestern United States remains sparsely settled, and most of the population and economic growth is concentrated in a few widely separated urban areas. Further, most of the development in the Southwest has taken place over the last five decades. Given this pattern of economic and population development and the episodic nature of precipitation and runoff events, few precipitation or flow gauges have records that could be characterized as either long-term or reliable; see, for example, French (1989). Also, flooding in the arid environment is less dependent on the magnitude of the event and more dependent on the ferocity, quickness, and sheer volume of materials moved. Compounding these challenges is that much of the development in arid environments has taken place on alluvial fans, which are complex landforms where ephemeral channels may be neither well-defined nor stable.

The classic definition of an alluvial fan (Doehring 1970) is

"An alluvial fan is a relatively thick deposit of coarse, poorly sorted, unconsolidated, clastics found as a semi-conical mass whose apex is adjacent to a mountain front. It has a relatively smooth subaerial surface which declines away from the mountain front."

From the viewpoint of hydraulic engineering, a more descriptive definition by the U.S. Federal Emergency Management Agency (FEMA) of an alluvial fan (Federal Register 1989) is

Alluvial fans are geomorphic features characterized by cone- or fan-shaped deposits of boulders, gravel, sand,

and fine sediments that have been eroded from mountain watersheds, and then deposited on the adjacent valley floor. Flooding that occurs on an active alluvial fan is characterized by fast-moving debris and sediment laden shallow flows. The paths followed by these flows are prone to lateral migration and sudden relocation to other portions of the fan. In addition, these fast moving flows present hazards associated with erosion, debris-flow, and sediment transport.

The FEMA definition itemizes the hydraulic processes expected to occur on a generic alluvial fan from an engineering viewpoint, and this definition makes it clear that flood hazards on alluvial fans are due to a wide range of hydraulic processes that involve sediment movement and transport. Many of these processes are not yet well-quantified. Finally, Schumm et al. (1996), in a study of alluvial fan flooding for the National Research Council (NRC 1996a), proposed the following definition:

"Alluvial fan flooding is a type of flood hazard that occurs only on alluvial fans. It is characterized by flow path uncertainty so great that this uncertainty cannot be set aside in realistic assessments of flood risk or in the reliable mitigation of the hazard. An alluvial fan flooding hazard is indicated by three related criteria: (a) flow path uncertainty below the hydrographic apex, (b) abrupt deposition and ensuing erosion of sediment as a stream or debris-flow loses its competence to carry material eroded from a steeper, upstream source area, and (c) an environment where the combination of sediment availability, slope, and topography creates an ultra hazardous conditions for which elevation on fill will not reliably mitigate the risk."

An alluvial fan is a surface attempting to reach equilibrium with the long-term spectrum of precipitation and runoff events and will attempt to reach a new equilibrium in response to deviations from the existing surface. Engineers, primarily trained in temperate environments, often attempt a comprehensive control of the drainage—sediment transport problem without developing an appreciation of the geomorphic viewpoint of the situation (Schick 1974; French and Keaton 1992; Keaton et al., 1990).

19.4.2 Background

Although the data on flow and precipitation in arid environments are generally sparse, the anecdotal record is replete with examples of the clear-water and sedimentation hazards associated with development on alluvial fans (McPhee 1989b). For example, in 1983, there was landslide-induced flooding at Ophir Creek, Nevada (Glancy and Bell 2000). Ophir Creek is a small, elongated watershed with an area of approximately 11.7 km^2 (4.5 mi^2) terminating in an alluvial fan. The total sediment deposited during this event was approximately

$555,000 \text{ m}^3$ (450 ac-ft), and the flood surge was estimated to have a peak flow of approximately $1,400 \text{ m}^3/\text{s}$ (50,000 ft $^3/\text{s}$). A wall of boulders, mud, trees, and water, 9 m (30 ft) high by 30 m (100 ft) wide destroyed structures outside of the estimated 100-yr regulatory floodplain; one life was lost.

Common sense, given the magnitude of these estimates, suggests that this was an extreme event; however, the historical record suggests a different answer. From the historical record, Glancy and Bell (2000) discovered that significant flooding had taken place on the Ophir Creek alluvial fan in 1874, 1875, 1890, 1907, 1937, 1943, 1950, and 1963. It would appear that this single event in 1983 confirms the old adages that those who fail to learn from history are destined to repeat it. This 1983 event was recorded because it took place along a major transportation alignment in the proximity of two major urban areas. It is unknown how many similar or larger events took place in the arid and semiarid areas of the world in 1983 and were not recorded or even noticed.

From the definitions of an alluvial fan presented previously, it is important to note that alluvial fans are not features unique to the arid environment. Rather, alluvial fans are ubiquitous to all climatic environments (see Fig. 19-12 of alluvial fans in Venezuela), which leads to the following observations:

1. The interest of engineers and geologists in alluvial fans in arid and semiarid environments may be due to their prominence in these environments given the lack of vegetation and state of preservation due to the episodic nature of precipitation and runoff. For example, Anstey (1965) estimated that alluvial fans constitute approximately 30% of the land area in the southwestern United States.
2. The current and anticipated rates of development on these landforms throughout the world demand that adequate and cost-effective flood mitigation be provided to residents and property owners.
3. There are significant differences between the FEMA and geological definitions of alluvial fans. As noted by French et al. (1993), the regulatory definition itemizes the hydraulic processes that may occur on an *engineering time scale*, whereas the geological definition focuses on the process that led to the shape and location of the landform on a *geological time scale*. This contradiction of definitions is appropriate given that the engineer is concerned with an analysis of structures on an engineering time scale, whereas the geologist is concerned with the geomorphic processes that resulted in the landform regardless of time scales.

The foregoing observation leads to the conclusion that when an analysis of flood flows on an alluvial fan is undertaken, the engineer must be sensitive to the processes that are active on the landform under current, engineering time scales, but also should be very aware of the geomorphic processes that continually form and reform the alluvial fan.

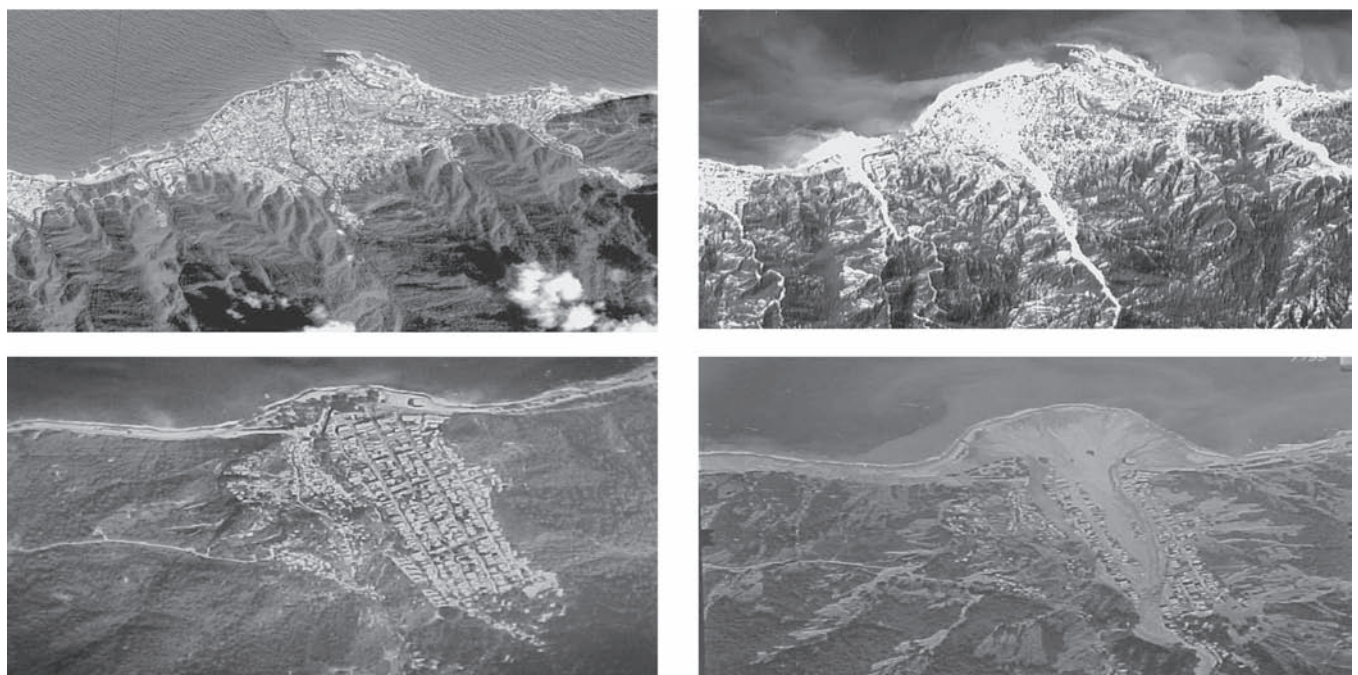


Fig. 19-12. SPOT Satellite images taken before and after the events of December 1999 of the alluvial fans in San Julián (above) and Carmen de Uria (below), Venezuela.

As Parker (1999) noted, the disparity between the engineering and geological time scales on alluvial fans can lead to significant misunderstandings regarding risk. For example, the fan-delta system on the Mississippi River south of Baton Rouge has avulsed several times to form multiple deltaic lobes over the past 5,000 years. However, over the lifetime of one engineer there was likely no change, which gives the illusion of stability (Parker 1999). It is pertinent to note that a lay discussion of this particular issue is provided in McPhee (1989a).

19.4.3 Early Developments

Attention to and focus on alluvial fan flooding and sedimentation issues in the engineering literature began with the publication of a probabilistic approach to identify regulatory flood hazard on alluvial fans (Dawdy 1979). The work by Dawdy was partially based on earlier results regarding channels formed by rare flood events on the surfaces of alluvial fans in the Albuquerque, New Mexico area, which were subsequently published (Magura and Wood 1980). These initial approaches to identifying flood hazard on alluvial fans were followed by others (*e.g.*, Edwards and Thielman 1984), and the establishment, by the regulators (*e.g.*, FEMA 1985), of guidance specifically for the evaluation of flood hazard on alluvial fans. These early papers dealt exclusively with the clear-water hazard on alluvial fans and did not incorporate the work and knowledge that the geoscience community had gained from decades of studying sediment processes on these landforms. Also, they

did not acknowledge that not all alluvial fans are active alluvial fans and that sound engineering judgment and new technical approaches were required to properly evaluate the clear-water and sediment hazard issues on these landforms.

The original FEMA (1985) approach to delineating flood hazard on alluvial fans contained the following key assumptions: (1) alluvial fan flooding is conveyed at critical depth in flow-formed channels governed by regime equations of depth, velocity, and discharge at the apex; (2) the location of the flood channel is unpredictable; (3) topographic relief and urbanization on the fan are minimal; and (4) the hazard is due only to clear-water flows. These and other implied assumptions were discussed by French (1987). In the view of many competent professionals, this generic approach to alluvial fan flood hazard incorporated assumptions that were not valid on all alluvial fans and, in some cases, had been misapplied (*e.g.*, Fuller 1990; Pearthree 1991; and Pearthree et al. 1991). This controversy over the use of a generic model to identify alluvial fan flood hazards led the Flood Control District of Maricopa County, Arizona (FCDMC), to undertake a study of alluvial fans (FCDMC 1992). The results of this study were published in French et al. (1993). The measurable characteristics and expected hydraulic processes during flood events on the types of alluvial fans identified during the FCDMC study are shown in Tables 19-4 and 19-5.

The early studies neglected the need to address not only clear water but also water transporting a wide range of sediment loads. Dependent on the concentration of sediment relative to the water, flood flows on an alluvial fan can be

Table 19-4 Measurable Alluvial Fan Characteristics

Active alluvial fan	Distributary flow system	FEMA alluvial fan	Inactive alluvial fan
Abandoned discontinuous channels	Discontinuous channels	Continuous channels	Continuous channels
Channel capacity decreases downstream	No definite trend in channel capacity	Cumulative capacity constant downfan	Channel capacity increases downstream
Channel flow changes to sheetflow	Channel and sheetflow	Channelized flow (no overbank or sheetflow)	Channelized flow (overbank flow possible)
Debris-flow possible	Minor (or no) debris-flow	Debris-flow important	No debris-flow
Frequent channel movement	Rare channel movement	Unpredictable channel location	Stable channels
Low channel capacity	Variable channel capacity	Channel capacity equals flow rate	High channel capacity
No calcrete	Calcrete horizons possible	No calcrete	Calcrete horizons
No (or buried) desert varnish	Varnished surfaces possible	No (or buried) desert varnish	Varnished surfaces possible
No surface reddening of soils	Minor reddening of soils	No surface reddening of soils	Surface reddening of soils
Overall deposition	Local erosion and deposition	Overall deposition	Overall erosion
Radiating channel pattern changes to sheetflow area	Radiating channel pattern changes to tributary	Single or multiple channels	Tributary drainage pattern
Slope decrease downstream	Slope increase at apex	Slope not a factor above bifurcation point	Slope variable
Stream capture or avulsions?	Channel movement by stream capture	Channel movement by avulsions	No channel movement
Uniform topography (low crenulation index)	Medium to low topographic relief (medium to low crenulation index)	Uniform topography (low crenulation index)	Topographic relief (high crenulation index)
Uniform vegetation in floodplain	Diverse vegetative community	Uniform vegetation in floodplain	Diverse vegetative community
Variable channel geometry	Variable channel geometry	Regular channel geometry	Regular channel geometry
Weak soil development	Variable soil development	Weak soil development	Strong soil development

Note: In a specific application not all of the characteristics noted may be present.

a fluvial flow, a hyper-concentrated flow, a mudflow, or a debris-flow; and in each of these situations a different modeling approach is required.

19.4.4 Current Developments

In response to the controversies raised over the use and misuse of the probabilistic method of identifying flood hazards promulgated in FEMA (1991), the National Research Council undertook a study of alluvial fan flooding (NRC 1996a). Although the report provides valuable data and insights, there are many issues that may be unresolved. In particular, the report relied mainly on the experience of the geosciences community but did not take full advantage of the valuable experience available in the engineering community. It is clear that cooperative input from both the geosciences and engineering fields is necessary to effectively study and analyze alluvial fan flooding. The NRC report did not consider also

the alluvial fan development situation in what was then, and remains, one of the fastest growing, and most arid states in the United States—Nevada. It is in this state where alluvial fans are currently both primary engineering research and legal issues. The U.S. Department of Energy, Nevada Operations Office, has likely dedicated more resources to identifying and evaluating flood hazards on alluvial fans and arid region hydrology than most other Federal Agencies combined.

In addition, there are now two-dimensional models available for modeling flows on alluvial fans. FLO-2D (O'Brien 1999) is a two-dimensional hydrodynamic model designed for both clear water and sediment-laden flood flows on alluvial fans. An application of FLO-2D by Bello et al. (2003) is presented later in section 19.6.3.6 of this chapter. Important new experimental-field scale advances regarding alluvial fans have also been recently published; for example by Parker et al. (1998a and 1998b) and Whipple et al. (1998). Progress has also been made with the linking of channel process with

Table 19-5 Expected Hydraulic Processes during Flood Events

Active alluvial fan	Distributary flow system	FEMA alluvial fan	Inactive alluvial fan
Channel movement possible	Channel movement rare	Unpredictable channel location	Channel location stable
Channel, overbank, and sheetflow	Channel, overbank, and sheetflow	All flow channelized	Channel, overbank, and sheetflow
Debris-flows important	Debris-flows not important	Debris-flows not considered	Debris-flows not important
Flows along existing and new channels	Flows along existing channels	Flow cuts new channel	Flow along existing channel
Flow attenuation	Flow attenuation	No flow attenuation	Flow attenuation likely
Net deposition on surface	Local deposition and erosion	Deposition not considered	Net erosion on surface
On-fan watershed flooding	On-fan watershed flooding	On-fan watersheds not considered	On-fan watershed flooding
Probable sediment bulking	Probable sediment bulking	No sediment bulking	Probable sediment bulking
Stream capture or avulsions?	Rare stream capture or avulsions	Channel movement by avulsions	No avulsions
Topography influences flow	Topography influences flow	Flow not affected by topography	Topography controls flow

Note: In a specific application not all of the characteristics noted may be present.

large-scale morphodynamic changes in fluvial fan-deltas such as the Mississippi delta (Sun et al., 2002) as well as in the use of physical models to assess flooding risks in alluvial fans (Cazanacli et al., 2002) and the limitations of such physical models (French and Miller, 2003). Physical modeling of sedimentation processes is addressed in *Appendix C-Sediment Transport Scaling for Physical Models* of this manual.

19.4.5 Conclusions

Although much has been done regarding the accurate and reliable definition of flood hazard on alluvial fans on an engineering time scale, still much remains to be accomplished. For example, even the basic definition of an engineering time scale remains to be defined. French et al. (1993) arbitrarily defined an engineering time scale to be 1,000 yr or less and a geologic time scale to be 10,000 yr or more. Although this definition provides a 9,000 yr difference, it is pertinent to observe that in the arid environment, engineers may be required to predict, given Federal requirements, the performance of flood mitigation structures for up to 10,000 yr. From the engineering viewpoint, predicting the performance of facilities 10,000 yr into the future involves pure speculation; however, under regulatory guidance specific to some types of waste management sites, this period is considered an engineering time scale. For example, by definition, an alluvial fan is an aggradational landscape feature on a geologic time scale; however, there are no guarantees that a channel could not be incised through a facility in response to a major event that occurs within an engineering time period,

given that the facility design period (or likelihood of a rare event that has the same probability of occurring) may be up to 10,000 yr. That is, the Dawdy (1979) or random channel movement across an alluvial fan surface is correct on a geologic time scale, which accounts for the symmetrical depositional shape of the fan.

The challenge facing the research community is that of producing results that are useful to the regulators, the practitioners, and the public. Modern researchers in engineering and science have to understand the need to show how their results relate and pertain to a larger world. At the same time, regulators ought to become more flexible and use good engineering judgment rather than rigidly adhering to a single approach to defining flood hazard on alluvial fans. The need to move away from rigidity was one of the recommendations of Schumm et al. (1996) that struck a common cord in the professional community.

The engineering community has to remember that alluvial fan flooding is a cutting-edge technology. Hazard evaluations in this field require field investigations by engineers together with colleagues who have expertise in geosciences and risk analysis. As shown above, it is also very important to search for historical records that might help in conducting flood hazard risk analysis. The accurate identification of flood hazard and mitigation of flood hazard on alluvial fans must be a shared experience between the engineers, geologist and geomorphologists to ensure that the public will be afforded the best technologically feasible level of protection and to avoid potential litigation issues. Readers can find more material on alluvial fans in Chapter 18, *Engineering Geomorphology*, while legal issues associated with flood

and sedimentation hazards are addressed in Chapter 20—*Sedimentation Law*.

or bio-technical procedures or a combination of these methods.

19.5 METHODS TO MITIGATE THE CONSEQUENCES OF SEDIMENTATION HAZARDS

19.5.1 Background

Reliable assessment and mitigation of hydraulic and sedimentation hazards depend on the engineers' ability to understand and describe in written and mathematical forms the physical processes that govern the fluvial system they are dealing with. As presented under 19.2, *Sedimentation Hazards—History and Magnitude*, significant hazardous conditions and natural disasters associated with sedimentation processes have occurred throughout recorded history. Today, however, engineers and scientists have greater access to data, information, and knowledge regarding where, when and how such events may occur. New procedures and mathematical modeling tools have evolved as aids to better assess present conditions and forecast future conditions. However, it must be recognized that the present state-of-the-science and our understanding of mobile boundary hydraulic processes related to different types of sedimentation hazards and mud and debris-flow processes are still limited. Exacerbated by our having few or no measured field data, these complex processes often evade theoretical attempts to characterize flow depth, location, orientation, velocity, sediment- and debris carrying capacity, and event predictability with a high degree of accuracy.

Methods for assessing and mitigating the consequences of severe sedimentation hazards, including mud and debris-flows, fall into three general approaches and levels of effort:

- *Hazard mapping and avoidance*—e.g., perform a hazard mapping study and have people not live there if it is mapped as a likely hazard zone; or if people already live there, help them to understand the risk and require that they buy hazard insurance. This approach focuses on avoidance of hazards, not mitigation.
- *Apply currently accepted hazard assessment and mitigation design procedures*; e.g., if you wish to develop in a hazard zone, apply currently accepted assessment procedures to define hazards and their levels of risk, and then apply appropriate design procedures to develop structural or nonstructural methods for mitigating the hazards.
- *Apply new state-of-the-science procedures*; e.g., if you wish to evaluate the risk of hazards or wish to develop in a hazard zone, you may elect to apply innovative methods including hazard forecasting, risk assessment, and process-simulation modeling and apply new design concepts to mitigate the hazards. New mitigation methods may include structural, nonstructural,

19.5.2 Hazard Mapping

Prior to the mid-1990's, there was very little guidance available for evaluating site-specific conditions or the mapping of flood hazards on alluvial fans or of hazards directly related to ultrahazardous sedimentation processes. As of the year 2000, however, hazard-mapping procedures predominantly follow those supported and documented by the Federal Emergency Management Agency (FEMA 1990; 1995; 2000), Federal Register (1989) guidelines and the National Research Council (NRC 1996a). FEMA prepares Flood Insurance Rate Maps (FIRMS) of flood hazard areas based on the results of Flood Insurance Studies (FIS). Those studies determine the areas with a 1% annual chance of being inundated (by water). The flood is called the *base (100-year) flood* by FEMA. The FIS must evaluate the existing flood conveyance system, including installed flood-control measures. Determination of the inundated area may depend on whether flood-control measures protect part of the floodplain. With increased development in the United States and other countries of the world, more people are being exposed to extreme flood hazards associated with flash floods, mud and debris-flows, high flow velocity, channel avulsion, severe erosion, and channel migration and episodic alluvial fan processes. FEMA (2000) recently expanded their guidance regarding the identification and mapping of traditional flood hazards to include procedures for flood hazards occurring on alluvial fans, *irrespective of the level of fan-forming activity* (see Section 19.4).

19.5.3 Currently Accepted Hazard Assessment and Mitigation Design Procedures

Most *accepted* assessment and design procedures depend on empiricism, experience, field observation, and the application of traditional clear-water assessment methods that have been modified to account for flow bulking, sediment dynamics, and the unpredictable and often episodic nature of sedimentation processes leading to hazardous flow conditions. These accepted practices have come into general usage because of their simplicity and relative accuracy. Accepted practices used primarily for the design of flood control channels are emphasized in this chapter. The most accepted and best documented sediment hazard assessment and design procedures are documented by the following federal agencies: the U.S. Army Corps of Engineers (USACE 1989; 1991; 1993; 1994), the HEC (1993), the Federal Highway Administration (FHWA, 2001), and the U.S. Department of Agriculture (1992; 1996). In the relatively new area of evaluating significant sedimentation hazards, and mud and debris-flows, sufficient time and proven testing has not yet occurred for accepted design practices to emerge.

19.5.4 State of the Science Procedures

New state-of-the-science procedures are often related to new computer simulation models or untested design concepts that may implement hybrid techniques, bio-technical flow diversion or stream stabilization measures. In such cases, the latest research has not yet been fully tested or documented sufficiently to become general practice. State-of-the-science procedures can be applied, but they, as well as the accepted practices, need to be thoroughly checked against real data and a reasonable range of possible hazard scenarios to cover all likely sedimentation and flow conditions the project area may experience during its lifetime. New procedures are most often presented in technical and trade journals or conference proceedings. For the most part these newly developed procedures are relatively untested and have not yet become general practice.

The following discussions are aimed at providing guidance to engineers and flood-hazard managers for planning and assessing the adequacy of flood-control measures exposed to significant sedimentation hazards and mud and debris-flows. This section is not intended to be a design manual for mitigation of sedimentation problems. It is intended to summarize general procedures for assessing flood hazards and for developing reasonable mitigation alternatives. A following section will list several accepted methods for hazard mitigation. Readers should also read Chapter 20—*Sedimentation Law*, for recent interpretations of pertinent court decisions regarding standards of practice and prudent levels of assessment and design.

19.5.5 General Approach

The following general approach is suggested to assess and develop sedimentation hazard mitigation alternatives. The approach consists of three phases of work:

Phase 1: Problem identification, preliminary assessment and design

- Perform site assessment and geomorphic analysis of project area
- Define hydrologic, hydraulic and sedimentation processes and hazards
- Perform surveys and hazard mapping if required
- Develop preliminary alternatives for hazard mitigation
- Perform preliminary engineering and environmental evaluation of alternatives for hazard mitigation
- Initiate the regulatory and environmental process
- Perform screening of preliminary alternatives to select a preferred alternative(s)
- Perform feasibility level design of preferred alternative(s)
- Prepare draft environmental documents (EIR and/or EIS)
- Seek public involvement and consensus

Phase 2: Prepare plans, specifications, and estimates (PS&E) along with CEQA/NEPA documentation and permitting

- Perform detailed design and environmental analyses
- Prepare final plans and specifications
- Prepare cost estimates
- Prepare final CEQA and NEPA documentation
- Respond to public comments
- Define project-related mitigation requirements
- Obtain regulatory permits
- Finalize project authorization and funding

Phase 3: Project construction, project mitigation, and monitoring

- Construct project
- Perform project-related mitigation
- Initiate project monitoring program

Phase 1 is perhaps the most important phase because it must identify the underlying physical processes affecting the site and properly define existing and potential hazards as well as other project constraints related to regulatory or environmental concerns if mitigation activities were to occur. It is essential that hazard mitigation alternatives not only reduce or eliminate identified hazards, but also not result in the initiation of other problems or impacts for areas upstream or downstream of the proposed project site (channel stability, scour, and significant changes in the hydrologic regime, environmental impacts, or significant project maintenance requirements). It is, therefore essential to perform a thorough regional assessment of the area's geomorphology, hydrology, hydraulics and sedimentation characteristics and compare those *existing* (baseline) characteristics to proposed *with-project conditions* to avoid project-induced impacts. MacArthur, et al., (1993) recommend that "reliance and single all-purpose model or computer program should be avoided," and they outline 14 elements of a multi-phased modeling and assessment approach for evaluating special sediment hazards. Environmental regulations require equal detail regarding the evaluation of potential impacts on the environment or endangered species.

19.5.6 Guidance

Detailed guidance on how to conduct planning and design studies for mitigation of flood hazards is found in many state and federal guidelines. Section 1–6 in the USACE (1991), manual *Hydraulic Design of Flood Control Channels (Engineering Manual 1110-2-1601)* outlines steps for conducting preliminary investigations for selection of type of improvement for mitigation of flooding hazards. The Corps emphasizes the need for careful consideration of the physical characteristics of the site, its history of flooding, and the nature of aggradation and degradation, debris transportation,

bank erosion, cutoffs, and bar formation. Other hydrologic, hydraulic, and economic aspects of the project are also important.

Engineering Manual 1110-2-1416, River Hydraulics (USACE 1993), states that “effective analysis of river problems requires recognition and understanding of the governing processes in the river system. There are two basic items that must always be considered in river hydraulics analyses: the characteristics of the flow in the river, and the geomorphic behavior of the river channel.” These two components are sometimes treated separately, however, in alluvial channels and floodplains (zones with movable boundaries) the flow and the shape of the boundary are interrelated. This is especially true during severe events occurring on movable boundaries such as alluvial fans.

Engineering Manual 1110-2-4000, Sedimentation Investigations of Rivers and Reservoirs (USACE 1989) outlines procedures for conducting staged sedimentation studies, including (1) sediment impact assessments, (2) detailed sedimentation studies, and (3) feature design sedimentation studies for the final design and location of project features. *EM 1110-2-4000* discusses the approach, data requirements, analyses, validation requirements, and design procedures for conducting thorough sedimentation investigations and designs. The manual discusses the importance of and procedures for identifying potential river sedimentation problems, and associating those problems with project purposes and presents methods for analyzing them at various levels of detail.

Engineering Manual 1110-2-1418, Channel Stability Assessment for Flood Control Projects, provides guidance for determining potential channel instability and sedimentation effects (potential problems) in flood control projects. “It is intended to facilitate consideration of the type and severity of stability and sedimentation problems, the need for and scope of further hydraulic studies to address those problems, and design features to promote channel stability. The concept of channel stability implies that the plan, cross-section, and longitudinal profile of the channel are economically maintainable within tolerable limits over the life of the project” (USACE 1994). Principles of stability and the causes and forms of instability and sedimentation problems are discussed.

The HEC (1993) prepared a report for the Federal Emergency Management Agency on *Assessment of Structural Flood-Control Measures on Alluvial Fans*. The report summarizes key geomorphic aspects of alluvial fans and discusses their unique hydrologic and hydraulic characteristics. It also discusses the effects of channel avulsion, occurrence of mud and debris-flows, channel incision or entrenchment, and an alluvial fan’s capacity to carry and deposit sediments during various flood events. The Flood Insurance Administration requires an assessment of the effectiveness of various structural approaches to flood control in alluvial fan special flood hazard areas (SFHAs),

(HEC, 1993). This report documents how installed flood-control measures have performed during major floods and presents current methods for assessing the performance and adequacy of the measures. HEC did not investigate nonstructural measures or procedures for mapping of alluvial fans as part of their study. The report is not intended to be a design manual. It is aimed at providing guidance to floodplain managers and engineers in assessing the adequacy of structural flood-control measures on alluvial fans (primarily improved channels, flow diversions, bypasses, and detention storage facilities) to protect against the Base Flood (HEC, 1993).

19.5.7 Examples of Structural Flow, Sediment and Debris Management Measures

HEC (1993) presents several case studies of flooding problems and in some cases, failures of flood-control project features that were exposed to high flow, sedimentation, and/or mud- and debris-flow conditions. Types of bank protection, flow diversion, and debris and sediment management measures include the following:

Bank Protection Works:

- Works designed to stabilize erodible channel banks and protect them from high-energy flows
- Pipe-and-wire fences
- Riprap (dumped rock)
- Rock paving (hand-placed)
- Wire and rock mattresses
- Gunite slope paving
- Reinforced concrete open channels
- Reinforced concrete closed conduits
- Bio-technical bank stabilization and erosion control measures (see USDA 1996)

Debris Barriers:

- Structures, usually located in the watershed, that stop or reduce the movement of debris down the channel system
- Debris fences (typically vertical beams or rails anchored in a foundation, sometimes with wire or cable reinforcement, oriented perpendicular to expected debris-flows)
- Debris barrier walls, typically referred to as fire barriers in southern California and built across canyon mouths following fires to retard debris-flow induced by heavy rains on the burned watershed (LACFCD, 1979).

Crib Barriers:

- Series of check dams across a channel constructed from concrete, rock, or logs, which retard flows, capture sediment and debris, and may provide seasonal wetland areas, and help stabilize the toe of canyon side slopes (see LACFCD 1959 for sketches and designs).

Debris Basins:

- Facilities designed to capture, store and settle out coarse material and trash resulting from a major storm event
- Guidance for Debris Basin design may be found in (LACFD 1979)

Sediment Traps and Sediment Retention Structures:

- Sediment traps are constructed depressions in a channel, stream bed or floodway that encourage rapid accumulation of bed load sediments during high flows. The Corps of Engineers occasionally installs sediment traps in high bed load river systems in locations where sediment removal can be managed more effectively and with the least amount of impacts to the environment.
- Sediment retention structures (similar to debris barriers and basins) are designed to capture, store, and settle out sediment materials from major storm events. Perhaps the most documented large-scale sediment retention structure was designed and constructed by the Portland District Corps of Engineers on the Toutle River downstream of Mount St. Helens following its eruption in 1980 (HEC 1985). The structure was designed to retain annual sediment loads, as well as significant mud and debris-flows that could move down-valley from areas affected by the eruption of Mount St. Helens.

Other Sediment Control Structures:

- Constructed wetlands
- Vegetative filter strips and strategic planting of riparian vegetation
- Porous structures: small check dams, filter fences and straw bales

Retention Basins:

- Storage structures (usually uncontrolled) designed to reduce the peak flood flow from a drainage basin. Such structures can also (often by default) capture sediment and debris, which may affect their original design performance. A well-documented debris basin project with a spillway and concrete-lined flood control channel and energy dissipater is discussed by the Los Angeles District Corps of Engineers; see (USACE 1983; 1988).

Operation of Small Dams:

- Existing small dams also work as retention basins during large storm events unless they are operated to remain full for water supply, hydropower, or other reasons
- Outlet and storage capacity are typically reduced by sediment and debris accumulation

Flood Control Channels:

- Engineered works designed to pass flood flows more efficiently than natural, unimproved channels, thereby reducing flood stages.
- Unlined channels
- Lined channels
- Maintained and stabilized natural channels

Diversions and Bypasses:

- Constructed channels designed to provide additional flow capacity during floods, or designed to direct flows away from developed areas

Floodwalls:

- Vertical walls, usually constructed with reinforced concrete and typically oriented parallel to a stream or channel to prevent overtopping flows from leaving the channel and entering developed areas.

Levees:

- Usually constructed of earthen and rock materials, oriented parallel to the stream or channel; designed to prevent overflows into developed areas
- Single-levee projects (one side of channel only)
- Double-levee projects (both sides of channel)
- Set-back levees (levees set back on the floodplain a measurable distance from the main channel to allow controlled flows on the confined floodplain, although preventing overflows into developed areas)

Floodwalls and Dikes:

- Often used in conjunction with other flow or debris diversion structures
- May be placed across a channel, floodplain or alluvial fan to direct flow away from developed areas or direct flow into bypass or retention facilities

HEC (1993) discusses special problems related to sediment transport issues, including sediment accumulation, scour and debris. Evaluation and design procedures for these processes are documented in (USACE 1989; 1994). HEC (1993) also states:

“Every factor affecting the nature of flood and debris problems, plus the development and its susceptibility to flooding, affect the feasibility of flood-reduction options. There is no cookbook approach to developing an effective flood reduction project. Planning and design of flood-control (*and sediment and debris control*) structures . . . must always consider **the effect of all possible flows on the structure as well as the effects the structure may have on the flow locally and downstream**. While FIA criteria are based on the 1-percent chance flood, the proper design of any flood-control project must consider project

performance for the entire range of floods, including floods larger than the Base Flood."

19.6 MATHEMATICAL MODELING OF MUDFLOWS AND DEBRIS-FLOWS

19.6.1 Introduction

Modeling mud flows and debris-flows has long been an interest of hydraulic and sedimentation engineers. Because of the complicated rheological structure of these flows, solving the fully dynamic equations for unsteady, non-uniform, non-Newtonian flows is still a complicated endeavor. Consequently, basic concepts of open-channel hydraulics are often applied to the simulation of mud flows. Parameters such as momentum and energy coefficients, Manning's n , and Darcy-Weisbach resistance coefficients are usually defined with the help of velocity profiles defined by different rheological models. Such approach includes the work of MacArthur and Schamber (1986), Wright and Krone (1987), O'Brien et al. (1993), Hungr (1995), and Brufau et al. (2000), Lenzi et al (2004) and Zanuttigh and Lambert (2004) among others. Literature reviews by Mainali and Rajaratnam (1991), Hutter et al. (1996), and Iverson (1997) show a great deal of work on modeling debris-flows and mud flows. However, due to the complicated composition and rheological constitutive relation of mud flows and debris-flows, a quantitative understanding of the fluid mechanics and the associated mathematics of these flows is still incomplete (Hunt, 1994; Huang and Garcia, 1997b).

From a sedimentation engineering point of view, two problems that are of particular interest: the routing of mud and debris-flows in steep mountain areas and the flooding of an alluvial fan with mud and debris (e.g. Parsons et al. 2001). These two problems are addressed here with (1) a one-dimensional kinematic-wave model (Choi and Garcia, 1993) and (2) a two-dimensional water flood and mudflow model (Bello et al. 2003).

19.6.2 Kinematic-Wave Approach to Debris-Flow Routing (Choi and Garcia, 1993)

19.6.2.1 Introduction A simple kinematic-wave model for debris-flow routing is presented. This model requires only a limited number of boundary conditions, making it suitable for the simulation of mudflows and debris-flows, for which direct observations are only rarely available. Observations of debris-flow surges at Kamikamihori Valley, Japan, are used to test the model. In spite of the crude approximations involved in the selection of values for the model parameters, reasonable agreement between observed and computed values is found. The following material is based on the analysis presented by Choi and Garcia (1993).

A similar approach was proposed also by Arattano and Savage (1992) as well as Takahashi (1991).

19.6.2.2 Depth-Averaged Equations of Motion The dynamic equations describing a one-dimensional, unsteady debris-flow in a wide channel, where no sediment erosion or deposition occurs are (Chen 1986)

$$\frac{\partial h}{\partial t} + \frac{\partial(h\bar{u})}{\partial x} = 0 \quad (19-9)$$

$$\frac{\partial(h\bar{u})}{\partial t} + \frac{\partial(\beta_*h\bar{u}^2)}{\partial x} = gh \sin \theta - gh \frac{\partial h}{\partial x} \cos \theta - \frac{\tau_0}{\rho} \quad (19-10)$$

Where

- t = time;
- x = space coordinate along downstream direction;
- h = flow depth;
- \bar{u} = depth-averaged velocity;
- θ = bed-slope angle;
- τ_0 = bed shear stress;
- g = acceleration of gravity;
- ρ = density of the water-sediment mixture; and
- β_* = momentum correction coefficient.

In principle, for a given set of boundary conditions, if the momentum correction factor could be estimated and the bed shear stress could be related to flow variables through an appropriate resistance coefficient (e.g. Darcy-Weisbach, Manning's n), the one-dimensional dynamic equations for unsteady water flow shown above could be applied to debris-flow routing (Schamber and MacArthur 1985; Iverson and Denlinger 2001). However, the kind of computational work involved in solving such equations requires a level of expertise that is not always at hand. Thus, simple routing schemes such as the one presented here, in spite of their limitations, can provide a useful tool (Takahashi 1991; Arattano and Savage 1992).

19.6.2.3 Rheological Equations To model debris-flows, a rheological model or constitutive equation for sediment-water mixture is needed. Here, the approach suggested by Chen (1988) is followed. Water-sediment mixture can be treated as a material that satisfies Coulomb's yield criterion

$$\tau = \tau_y + \sigma \tan \phi \quad (19-11)$$

where

- τ = shear stress;
- σ = normal stress;

τ_y = yield stress; and

ϕ = angle of internal friction of the mixture.

A simple rheological relation between the normal stress and shear rate is given by the semiempirical relation $\sigma = \lambda_c(du/dz)^\eta$, where λ_c is a constant of proportionality;

u = longitudinal velocity component;

z = direction upward normal to the bed; and

η = exponent.

Substitution of the expression for σ into Eq. (19-11) gives

$$\tau = \tau_y + \mu(du/dz)^\eta \quad (19-12)$$

where

$$\mu = \lambda_c \tan\theta.$$

The parameters μ and η are normally referred to as the consistency index and the flow behavior index, respectively (Chen 1988). Then, if τ and τ_y are expressed as $\tau = \rho g S_0(h - z)$ and $\tau_y = \rho g S_0(h - z_0)$, respectively,

where

z_0 = depth corresponding to the yield stress, and
 S_0 = bed slope,

we obtain from Eq. (19-12) the following expressions for the velocity gradient

$$du/dz = \left[\frac{\rho g S_0(z_0 - z)}{\mu} \right]^{1/\eta} \quad \text{for } 0 \leq z \leq z_0 \quad (19-13a)$$

$$du/dz = 0 \quad \text{for } z_0 \leq z \leq h \quad (19-13b)$$

Integrating the above equation in the z -direction normal to the bed, we have

$$u(z) = \frac{\eta}{\eta+1} \left(\frac{\rho g S_0}{\mu} \right)^{1/\eta} z_0^{\frac{\eta+1}{\eta}} \left[1 - \left(1 - \frac{z}{z_0} \right)^{\frac{\eta+1}{\eta}} \right] \quad (19-14a)$$

for $0 \leq z \leq z_0$

$$u(z) = \frac{\eta}{\eta+1} \left(\frac{\rho g S_0}{\mu} \right)^{1/\eta} z_0^{\frac{\eta+1}{\eta}} \quad \text{for } z_0 \leq z \leq h \quad (19-14b)$$

Using the expression for u in the two regions, an equation for the depth-averaged velocity is obtained, as follows:

$$\bar{u} = \frac{1}{h} \int_0^h u(z) dz = \frac{\eta}{\eta+1} \left(\frac{\rho g S_0}{\mu} \right)^{1/\eta} (i)^{\frac{\eta+1}{\eta}} \left[1 - \frac{\eta}{2\eta+1} i \right] h^{\frac{\eta+1}{\eta}} \quad (19-15)$$

In this equation, the parameter $i = z_0/h$, indicates the relative strength of the yield stress τ_y against the bed shear stress τ_0 .

A data base on experimental observations of non-Newtonian, open-channel flow can be found in Haldenwang and Slatter (2006). It could be used to estimate the parameters of the model presented above as well as the assumptions made in its derivation.

19.6.2.4 Kinematic Wave Approximation The kinematic wave approximation is frequently used in open-channel flow routing when the inertial and pressure terms in the momentum equation can be neglected with respect to others. In steep mountain streams, where mud and debris-flows take place, backwater effects are negligible, so this approximation is quite reasonable. The main advantages of using a kinematic wave model are not only the simplicity of the equation itself but also the number of boundary conditions needed. The hyperbolic nature of the dynamic equations requires upstream and downstream boundary conditions, which in the case of catastrophic events such as debris-flows are only rarely available. Because the mean flow velocity \bar{u} has been expressed as a function of the flow depth h in Eq. (19-15), it is possible to introduce the kinematic wave approximation for debris-flow routing by expressing the specific flow discharge $q = \bar{u}h$ as

$$q = \alpha h^\beta \quad (19-16)$$

where

$$\alpha = \frac{\eta}{\eta+1} \left(\frac{\rho g S_0}{\mu} \right)^{1/\eta} (i)^{\frac{\eta+1}{\eta}} \left[1 - \frac{\eta}{2\eta+1} i \right] \quad (19-17a)$$

and

$$\beta = \frac{2\eta+1}{\eta} \quad (19-17b)$$

Substitution of Eq. (19-16) into Eq. (19-9) yields

$$\frac{\partial h}{\partial t} + \alpha \beta h^{\beta-1} \frac{\partial h}{\partial x} = 0 \quad (19-18)$$

For the numerical solution of Eq. (19-18), the algorithm proposed by Li et al. (1975), which consists of a second-order nonlinear scheme combined with a linear scheme, can be used. The nonlinear scheme ensures convergence, whereas the linear portion of the scheme speeds up the computations. This numerical scheme is unconditionally stable and conserves mass. Time and space derivatives are approximated by using a forward time and centered space (FTCS) scheme, and $h = (h_{j+1}^n + h_j^{n+1})/2$ is used in Eq. (19-18). Then, a finite-difference equation for a linear kinematic wave is obtained as follows:

$$\frac{h_{j+1}^{n+1} - h_j^n}{\Delta t} + \alpha \beta \left(\frac{h_{j+1}^n + h_j^{n+1}}{2} \right)^{\beta-1} \left(\frac{h_{j+1}^{n+1} - h_j^{n+1}}{\Delta x} \right) = 0 \quad (19-19)$$

By solving Eq. (19-19), values of h_{j+1}^{n+1} can be obtained explicitly, which, in turn, can be used as initial estimates in the application of the nonlinear portion of the algorithm. For the nonlinear algorithm, one can use h_{j+1}^{n+1} directly. Then the finite-difference form of Eq. (19-18) becomes

$$\frac{\Delta x}{\Delta t} h_{j+1}^{n+1} + \alpha(h_{j+1}^{n+1})^\beta = \left(\frac{h_{j+1}^{n+1} - h_j^{n+1}}{\Delta x} \right) = \frac{\Delta x}{\Delta t} h_{j+1}^n + \alpha(h_j^{n+1})^\beta \quad (19-20)$$

where all the values on the right-hand side of Eq. (19-20) are known. This is a nonlinear equation in h_{j+1}^{n+1} ; therefore a numerical technique such as the Newton-Raphson algorithm can be used to solve it. This numerical solution was verified by Choi and García (1993) with the help of an analytical expression for a simple kinematic wave given by Whitham (1974).

In mountain areas, where slopes are pronounced, back-water effects are negligible and the kinematic wave approximation can be expected to work quite well for the routing of mudflows and debris flows. Rickenmann (1991) has proposed an experimentally-derived equation to estimate sediment transport by hyperconcentrated flows (fine-material slurry) on steep slopes (larger than 10%) than can be readily adapted for use with the approach presented above to estimate the propagation of sediment waves.

19.6.2.5 Model Application Data collected by Japanese scientists in the mountainous area of the Yakedake volcano were used to apply the kinematic wave model. Among the data collected, the first surge of debris-flows on July 21, 1985 at Kamikamihori Valley was used (Suwa 1989). A longitudinal view of Kamikamihori valley is shown in Fig. 19-13. To measure hydrologic and hydraulic parameters, on-line

systems were installed. Flow rate, maximum flow depth, and surface velocity were recorded at dam #6. According to the observed data, the frontal velocity ranged between 10 and 20 m/s in the upper reaches of the valley, where the slope angle is 20 to 30°. At the downstream end, the frontal velocity had a smaller value of 1 to 10 m/s. The bulk density of the debris mixture was between 1.5 and 2.0 tn/m³, corresponding to volume concentrations of solid particles between 40 and 80%.

For the upstream boundary condition, a simple step function was assumed, as shown in Fig. 19-14. The duration time was determined by trial and error after the calculated discharge was compared with the observed one. The longitudinal domain was discretized into 13 intervals according to the main surveying points, which are shown as dots in Fig. 19-13, and a time increment $\Delta t = 4$ s was used. A debris mixture density of $\rho = 1,750$ kg/m³, and a dynamic viscosity or consistency index of $\mu = 2,000$ poise were used as input data. The value of μ was chosen after an inspection of the data on sampled debris-flows provided by Costa (1984). A constant value of the flow behavior index $\eta = 1$ (i.e., Bingham plastic) was used in the computation. In Fig. 19-15, the computational results (solid line) are compared with the observed values (dashed line) at the site of dam #6. The agreement is fairly reasonable, taking into account the uncertainty about the model parameters, as well as the lack of more detailed field observations. The computational results at the downstream end (point 14), where the time taken for the debris-flow surge to arrive is about 100 s, are shown in Fig. 19-16. The computed hydrograph shows that the rising stage has a fairly steep slope, and the hydrograph tail after the peak value is long. Similar behavior is observed in the analytical solutions obtained by Takahashi (1991, p. 97) using kinematic wave theory. There, the slope of the rising stage in both the depth and discharge hydrographs is approximately 90°, and the depth hydrograph also has a very long tail.

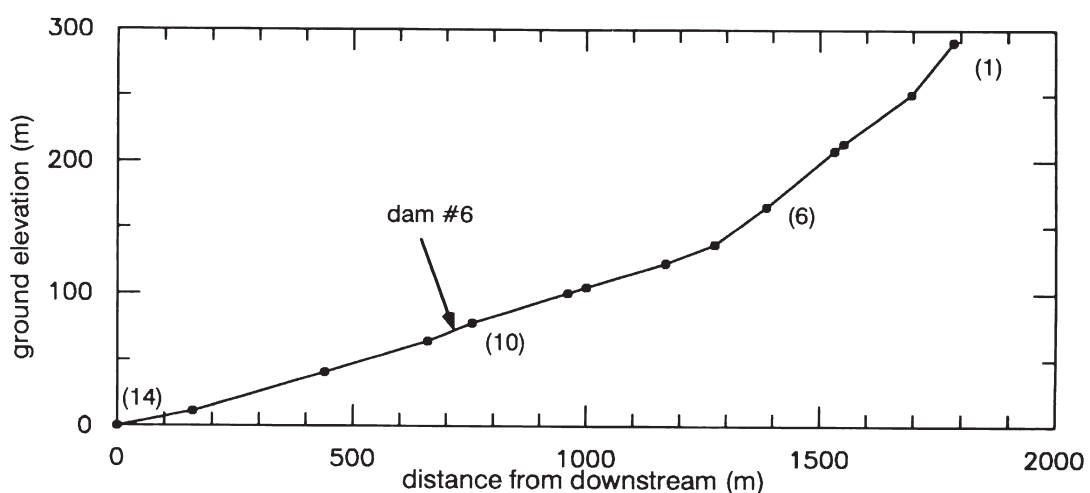


Fig. 19-13. Longitudinal profile of Kamikamihori Valley (Choi and Garcia 1993).

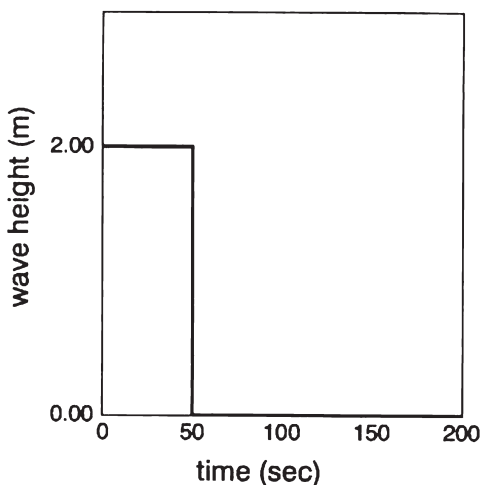


Fig. 19-14. Input Hydrograph at Upstream End (Choi and García 1993).

19.6.2.6 Conclusion The kinematic wave approximation has been applied to debris-flow routing. A nonlinear algorithm was used to compute the numerical solution. Comparison of model predictions against field observations gives encouraging results. It should be clear that the proposed model can provide only an approximate, yet useful, tool to compute the propagation of debris-flows. As new knowledge is gained about the rheological properties of debris and mud flows, it should be possible to incorporate it readily into the simple structure of the kinematic wave model (e.g. Whipple 1997).

There are more sophisticated models to predict the propagation of debris-flow surges, which include the dynamics of the pore-pressure evolution inside the flow (e.g., Savage and Iverson 2003). Although these models provide substantial insight into the mechanics of debris-flows (Savage and Hutter, 1989; 1991), their practical use is still limited to idealized conditions (Tubino and Lanzoni, 1993).

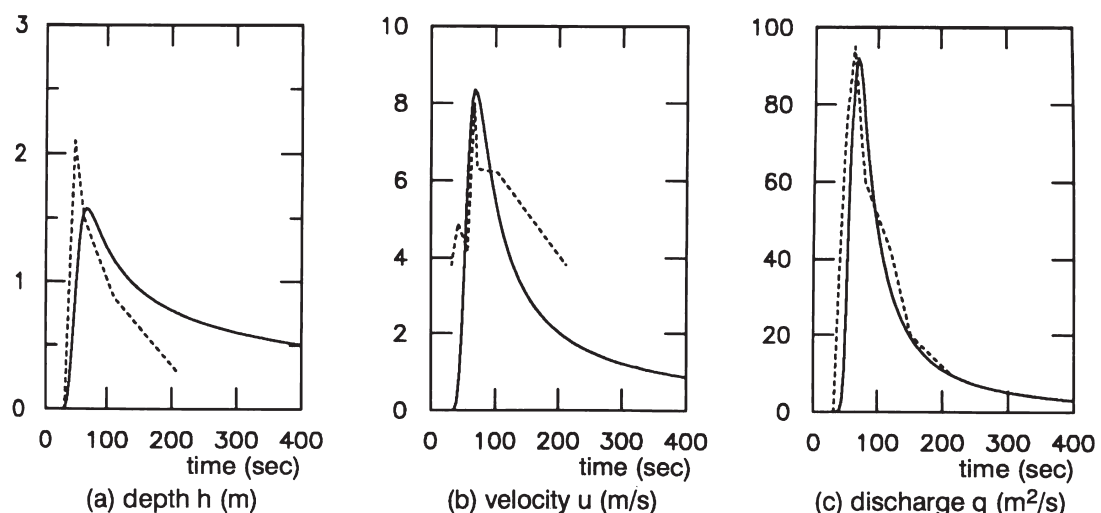


Fig. 19-15. Downstream Hydrograph at dam #6 upper (Choi and Garcia 1993).

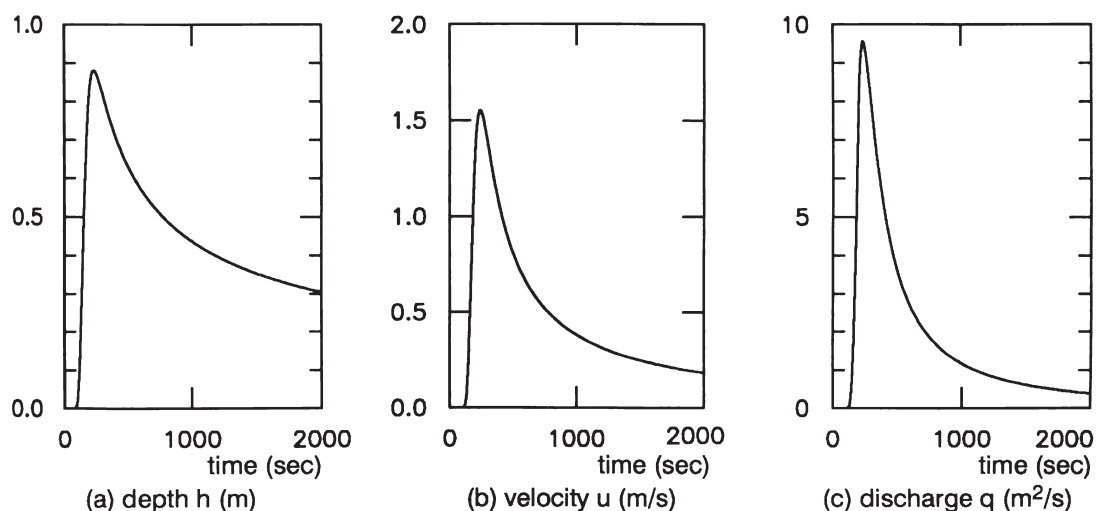


Fig. 19-16. Downstream Flow Hydrograph at Pt. #14 (Choi and Garcia 1993).

19.6.3 Simulation of Flooding and Debris-Flows in the Cerro Grande River, Venezuela (Bello et al. 2003)

19.6.3.1 Introduction During the first two weeks of December 1999, intermittent rainfall during a particularly wet rainy season saturated the steep watersheds of the north coast of Venezuela (Wieczorek et al. 2001). Then torrential rainfalls over a 3-day period (December 14–16) spawned landslides throughout the upper watersheds of the Cerro Grande River. Landslides were also observed on the steeper hill slopes of the lower watersheds. Mud-floods, debris-flows and flood surges destroyed much of the town of Tanaguarena. Tanaguarena was only one of about twenty coastal tourist communities developed on alluvial fans that were devastated by the flooding and debris-flows. Over 15,000 people perished during this 3-day period. Floods swept through these communities with frontal debris waves, a series of hour-long flood waves, and surges of flood waters and debris. The Cerro Grande River is located in the north coastal range of Venezuela and flows in a south-north direction into the Caribbean Sea. The highest elevation in the watershed is 2,750 m and the river course descends steeply to sea level in a horizontal distance of 10.5 km. The average slope of the Cerro Grande River is 20.2% and the area of the watershed is 23 km². The Cerro Grande River is ephemeral, with flows usually occurring in response to short-duration high-intensity rainfalls. Prior to December 1999, aerial photos showed a vegetated watershed. Much of the middle of the basin is a rainforest ecosystem. The following material is based on the work presented at the “International Seminar on the Debris-flow Disaster of December 1999,” Institute of Fluid Mechanics, Universidad Central de Venezuela, Caracas, Venezuela, in 2000 (López and García 2000). More detailed information can be found in Bello et al. (2003).

19.6.3.2 Description of the Flood Tanaguarena is a residential coastal community with two- and three-story houses, buildings and a private resort (Club Tanaguarena). Many of the buildings were constructed within the confined river canyon or on the short alluvial fan leading to the ocean. The alluvial fan extends approximately 400 m out into the ocean from the foot of the mountain slope (Fig. 19-17). According to local reports, flows were approaching bank-full on December 14. On December 15, the river started to inundate the houses along the left bank, and in the early hours of December 16, right overbank flooding ensued and flooded many of the houses in canyon. People climbed to the rooftops to escape the mud-floods and debris that were coming in surges down the river channel. Cars and urban debris were swept up by the flood waves and deposited in the ocean or along the coastal streets. The flood receded in the final hours of December 16. Average sediment deposition in the river canyon was about 2 to 3 m and essentially buried most of the standing houses to the rafters. Water level marks as high as 7 m were observed in some of the buildings. The debris surges destroyed approximately 60% of the structures

in town of Tanaguarena and resulted in approximately 100 fatalities. The mining operation (Cantera Cerro Grande) reported damages in excess of \$3 million in lost structures and equipment.

Damages were incurred through a combination of river flood inundation and alluvial fan unconfined flooding. Upstream of the mining operation, the canyon-confined flooding functioned as a sediment transport zone, delivering source area sediment from the upper watershed. Downstream of the mining operation in the canyon and onto the alluvial fan, a geomorphic sediment deposition zone was apparent. Structures in the canyon sustained impact damage from debris and boulders in surges. Some structures were completely destroyed by impact, scour, and exposure to high-velocity flows. Foundations were undermined by scour and collapsed. High-velocity surges with boulders and debris were experienced across the entire canyon bottom as the channel conveyance capacity was lost. The structures that remained standing were buried in a coarse grain mixture of boulders, cobbles, sand, and debris (Bello et al. 2003).

On the alluvial fan, structures were inundated with water and buried by sand deposition. Boulders, debris and cars were piled against buildings and some buildings sustained impact and scour damage. Video footage of flood events along the coast indicated a long duration (hours) of high flows punctuated by surges of sediment and debris related to upstream hillslope and debris dam failure. Streets became important flood conveyance channels that isolated portions of the community and cut off emergency access (Bello et al. 2003).

19.6.3.3 Rainfall Data and Frequency Analysis Only two rainfall gauging stations were operating in the State of Vargas in December 1999: Maiquetia (43 m above sea level), located about 15 km west of Cerro Grande, and Mamo (81 m above sea level,) located 20 km west of Cerro Grande. Precipitation data indicate that a low-intensity but continuous rainfall occurred between December 1 and December 13, totaling 293 mm at Maiquetia. Rainfall intensity increased during December 14 to 16. Maiquetia station reported 911 mm during these three days, with a total precipitation of 1,207 mm for the first 17 days of December. At Mamo, however, the cumulative value for the same 17-day period was 438 mm.

Over a period of record of 51 yr, Maiquetia station recorded the following rainfall data (excluding 1999): annual average rainfall of 523 mm; annual maximum rainfall of 961 mm (1951); and annual minimum rainfall of 205 mm. The log Pearson III frequency distribution indicates that the return period of the 1999 storm, without including the 1999 data, is greater than 1,000 yr. When the 1999 storm total rainfall (410 mm) is included in the analysis, the return period is approximately 270 yr.

19.6.3.4 Estimated 1999 Flood Hydrograph Using estimates of the peak stage from high water marks upstream of the Cerro Grande water intake weir, Zhang et al. (2000)

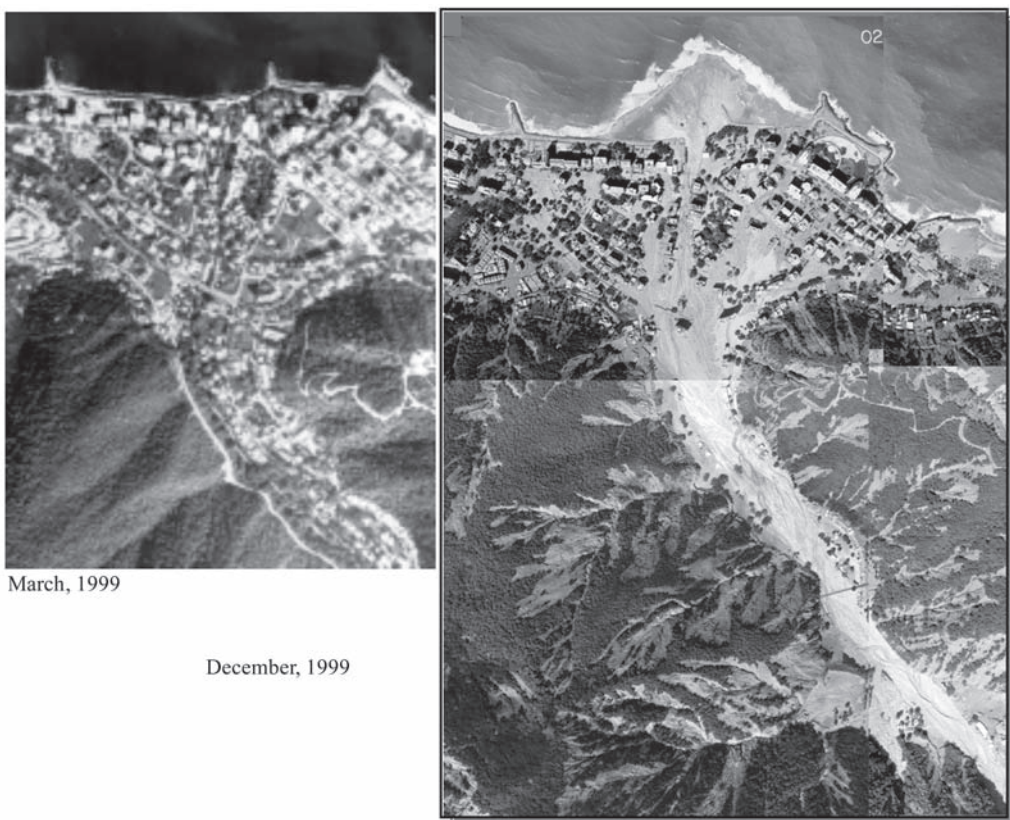


Fig. 19-17. Comparison of Cerro Grande alluvial fan before and after the Dec. 1999 flood disaster—SPOT Satellite images (Bello et al. 2003).

estimated the debris-flow peak of the December 16, 1999 event to be equal to $1,250 \text{ m}^3/\text{s}$ (Bello et al., 2003). Based on observations of the water damage and sediment deposition in the canyon and on the alluvial fan, it is assumed that the 1999 flood had an average sediment concentration of 35 to 40% by volume. Using this sediment bulking factor, the estimated water peak discharge was $800 \text{ m}^3/\text{s}$. Personal observations indicate that the peak discharge probably ranged from 800 to $1,200 \text{ m}^3/\text{s}$.

To obtain a flow hydrograph for the 1999 storm, an HEC-1 hydrologic model was prepared. The HEC-1 simulation was based on the 3-day period of maximum precipitation (December 14–16). Soils were considered to be partially saturated due to the 293 mm of rainfall reported in the previous days of December. HEC-1 loss parameters were calibrated to generate a peak water clear water discharge of $800 \text{ m}^3/\text{s}$. The effects of flow bulking are considered next.

Fig. 19-18 displays the HEC-1 simulated flood hydrograph for the Cerro Grande basin. The 3-day flood consisted of a series of approximately five major flood waves. These flood waves reflect the flood description reported by the local citizens. The rainfall intensity that created the flood waves were so high that the peak discharge was insensitive

to loss rate. It is unlikely that the peak rainfall intensities measured at the Maiquetia Station gauge (at sea level) were experienced in the upper Cerro Grande Basin. Although the distance from the rain gauge to the basin is only about 15 km, the elevation effects on the rainfall distribution over the entire watershed were not considered (2,000 m elevation variation). The rainfall peak intensities used in this analysis may be conservatively high. Assuming a sediment concentration that varied with discharge during the storm, the debris-flow hydrograph for the 1999 storm was predicted as shown in Fig. 19-19.

The steeply rising flood waves shown in Fig. 19-18 and 19-19 were also punctuated by debris and sediment surges related to failure of naturally forming debris dams, periodic landslides, hillslope sloughing into the channel, bank failures and roll waves phenomena. Each flood wave and debris surge had a fluid matrix with highly non-uniform sediment concentration ranging from perhaps 15 to 40% by volume.

Although tremendous quantities of sediment were delivered from the upper and middle watershed to the depositional zones in the canyon and on the alluvial fan, mudflows as characterized by viscous concrete-like consistency (see Fig. 19-9) did not occur on the fan. There was so much excess

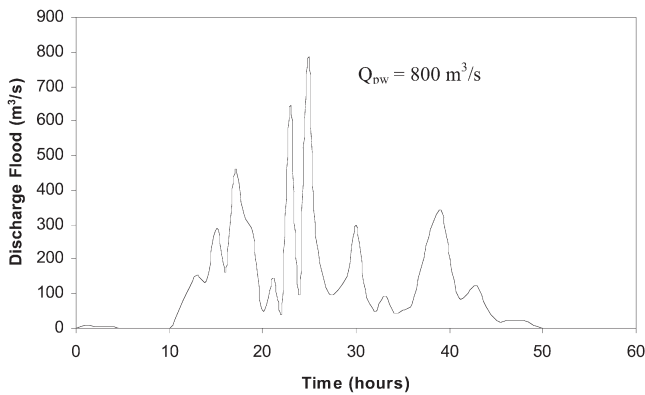


Fig. 19-18. Cerro Grande HEC-1 simulated flood hydrograph, December 15–16, 1999 (Bello et al. 2003).

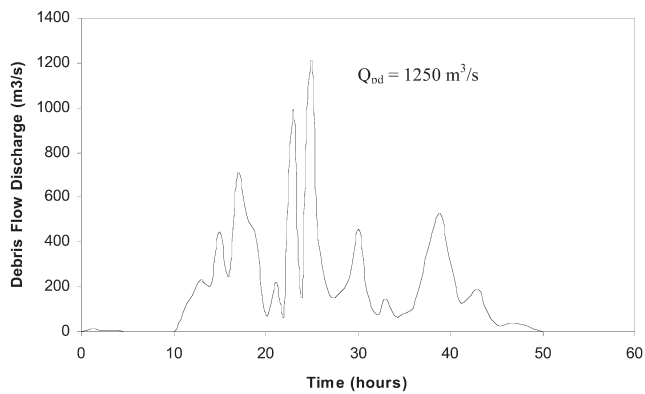


Fig. 19-19. Cerro Grande simulated debris-flow hydrograph, December 15–16, 1999 (Bello et al. 2003).

rainfall during this three-day storm that the flood waves, debris frontal waves and roll waves behaved essentially as water flood phenomena in the deposition zone. The depositional zone was essentially devoid of fine sediment (silts and clays), and there was little evidence of mudflow features such as levees, bouldery mud snouts, and undulating mud surfaces, which usually characterize mudflow alluvial fans.

Evidence indicates that near the source where the landslides and hillslope failures coalesced into moving fluid phenomena as they entered the water courses, mudflows were common. Generally, on western United States alluvial fans, mudflows occur in response to relatively frequent rainfall events with 5- to 50-yr return periods. Less frequent floods such as the 100-yr have too much water, compared to the available sediment supply, to generate long-duration mudflows. Once the watershed has a chance to recover from this catastrophic event, a process that could take several years, the Cerro Grande upper basin may be capable of producing mudflows for frequent return-period storms.

19.6.3.5 Channel Morphological Response A comparison between longitudinal profiles in the 2000 m Cerro Grande canyon reach before and after the 1999 storm is shown in Fig. 19-20. The slope of the channel bed did not significantly change; it varies from between 3 and 4% in the canyon to 2.5% on the fan. The alluvial fan extended into the sea about 140 m from the original mouth of the river. The sediment deposition along the river profile was 4 m to 5 m in the valley and 2 to 3 m on the alluvial fan.

Observation of the aerial photo of December 1999 (Fig. 19-17) indicates that in the lower canyon, where buildings were located, the river channel was obliterated and flows extended across the canyon floor. There was so much sediment moving as bed load and in flood waves that the flows became braided. During rising and recessional limbs of the five major flood waves, the flows followed multiple channel paths through the urbanized area. The area of sediment deposition extended about 1500 m east and west along the coast. Based on field observations and aerial photos, the amount of sediment accumulation was estimated to be on the order of 1.5 million cubic meters. This sediment deposition volume compares with 7.6 million cubic meters of water in the storm runoff hydrograph. Obviously most of the sediment conveyed by the flood washed into the ocean and is unaccounted for in deposition estimates.

19.6.3.6 Mud and Debris-Flow Modeling The FLO-2D model (O'Brien, 1999) was applied to simulate flooding in Cerro Grande canyon on the alluvial fan (Bello et al., 2003). FLO-2D is a two-dimensional flood-routing model that can simulate flows over complex topographies and roughness on urbanized alluvial fans and river floodplains and has a component to compute the channel-floodplain flow exchange. Hyperconcentrated sediment flows such as mudflows and the transition from water flows to fully developed mud and debris-flows can be simulated. Data requirements include a digital terrain model, channel geometry, estimates of channel and floodplain roughness, inflow flood hydrographs or rainfall, and rheological properties of the sediment-water mixture. The model is based on a finite difference solution of the two-dimensional Saint-Venant equations for non-Newtonian fluids.

A total of 1322 grid elements (50 m square) constituted the model flow domain covering the Cerro Grande canyon and urbanized alluvial fan area. This area is essentially the entire depositional area for the watershed, and the inflow node may be considered the fan apex even though the point is well upstream of the canyon mouth. The grid system coordinates and elevations were based on 1984 5-m contour mapping (Bello et al., 2003).

Other FLO-2D input data included the inflow hydrograph, channel geometry, estimates of sediment parameters and concentration and urban components (streets and buildings). In the absence of flow matrix samples, a number of simulations with temporal variations in the sediment concentration were attempted. It is apparent from the deposits that the fluid

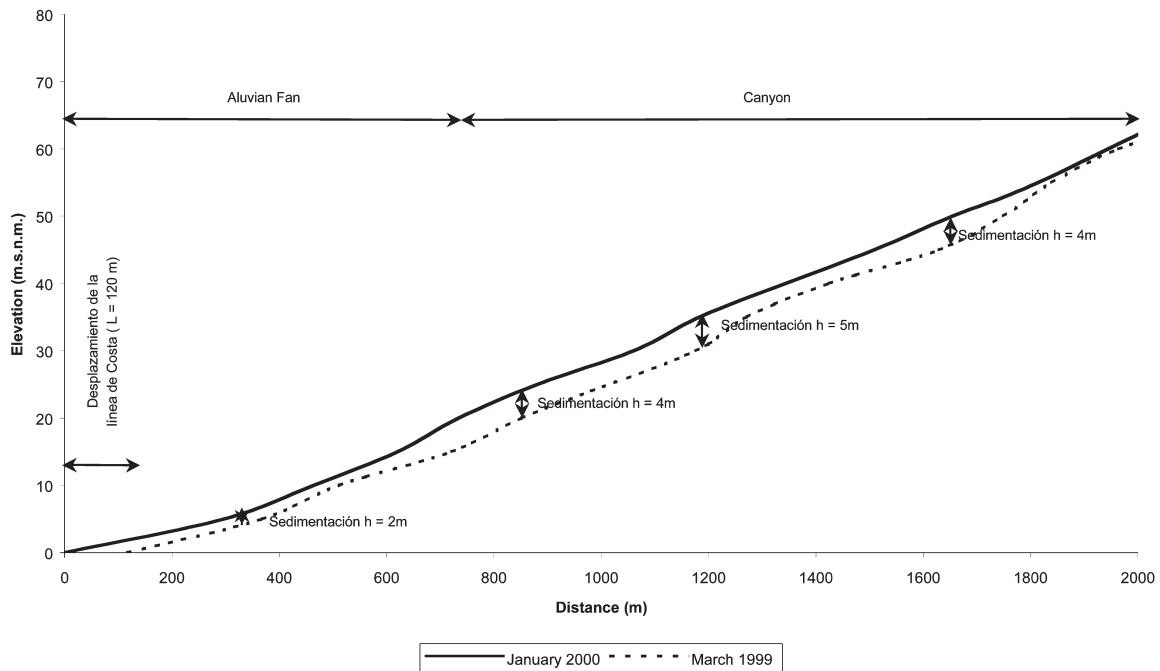


Fig. 19-20. Longitudinal profiles of bottom elevation along the canyon and the alluvial fan before and after the flooding. Up to 5 meters of sediment accumulated at some locations (Bello et al. 2003).

matrix sediment concentration was highly variable especially during the flood waves perhaps reaching concentrations as high as 40 to 45% by volume. During the low-flow periods between the flood waves, the sediment concentrations may have been less than 20% by volume. The average sediment concentration was probably on the order of 30 to 35% by volume. Sediment parameters related to flow viscosity and yield stress were estimated from analysis of actual debris-flows in the United States (O'Brien et al. 1993). A rigid-bed analysis with potential deposition on the fan was simulated. The fluid matrix was assumed to be a continuum and conventional bed-load and suspended-load sediment transport were not simulated.

The volume of flood was so large in 3 days that the effect of the streets and building obstructions on the predicted area of inundation was relatively minimal. These model features are important to local hydraulic conditions such as maximum flow depth and velocity, but were not analyzed in the existing-conditions simulation. Floodplain roughness n-values of 0.05 to 0.06 and channel n-values ranging from 0.032 near the ocean to 0.062 near the fan apex were assumed.

19.6.3.7 Simulation Results Predicted maximum flows depth ranged from 3.0 to 6.0 m on the canyon floodplain and 1.5 m to 4.0 m on the alluvial fan (Bello et al. 2003). Flow depths were greater in the channel, although during the actual flood the channel ceased to function. Alluvial fan velocities were predicted in the general range from 1 to 2 m s^{-1} with velocities as high as 5 m s^{-1} in the canyon area. Again channel velocities were slightly greater. The predicted

channel discharge constituted only about 16% of the actual maximum discharge. In other words, most of the flood volume was distributed over the alluvial fan surface.

The key to the accuracy of the Cerro Grande flood simulation is the area of inundation and predicted flow depth as a function of the estimated bulk volume. The total volume of the inflow hydrograph was approximately 23.35 million m^3 (34.91 million m^3 bulked with sediment). The predicted area of inundation on the alluvial fan was 8,093,000 m^2 (Fig. 19-21).

19.6.3.8 Conclusions The December 1999 rainstorm was a severe flood event that none of the coastal communities were prepared for. Inadequate or nonexistent zoning and planning resulted in the construction of buildings along the Cerro Grande channel within the 100-yr floodplain. Although the flood event exceeded the 100-yr flood estimate, there was only limited flood protection from channel conveyance against more frequent floods. Once the channel capacity was lost to sediment deposition early in the three days of flooding, structures on the alluvial fan were subjected to the full flood event.

The frequency analysis of two rain gauges with relatively long records of 50 yr or more indicated that the December 1999 flood was on the order of a 250-yr flood event or higher for a 3 day storm. Simulating the rainfall with the HEC-1 hydrologic model revealed that the flooding occurred in a series of at least five major flood waves over the 3-day period, as was reported by local citizens. By applying the HEC-1 model and the rainfall distribution recorded at the Macuto



Fig. 19-21. General area of inundation of the Cerro Grande Canyon and Alluvial Fan estimated by Bello et al. (2003).

Station, which is closer than the Maquetia Station to the Cerro Grande basin, a hydrograph for the 1999 flood event was estimated at the fan apex. This hydrograph was used in the FLO-2D model to route the 1999 flood as both channel and unconfined flows. The bulked sediment hydrograph was estimated from properties of the limited sediment data and estimates of sediment concentration (Bello et al. 2003).

Flood damages were incurred by flood scour, debris impact and flood inundation in the Cerro Grande canyon. Sediment deposition and flood inundation were the primary hazards on the alluvial fan. There was so much sediment moving as bed load and in mud-flood surges that the channel was obliterated and the flows braided across the canyon floor.

FLO-2D results indicated that the model was able to replicate the general area of inundation and to reproduce the flow depth pattern of the 1999 flood and debris-flow event in Cerro Grande. Predicted flow velocities were also in the general range of anticipated maximum velocities.

The importance of replicating the 1999 flood relates to the possibility of expanding the simulation for mitigation design (Bello et al. 2003). Although the 1999 event was an infrequent flood, simulating the flood event still has practical applications. In mitigation design, flood timing, duration, magnitude, and flood wave attenuation are important.

As a result of this study, a methodology was developed to delineate hazards maps due to mud and debris-flow events,

based on the application of the FLO-2D model (García et al. 2003). The methodology was tested in 23 sites in the Caracas and Vargas state region in Venezuela. The model results compared very well to the maximum flow depths and areas of inundation observed during the December 1999 Vargas mud and debris-flow disaster. The hazard maps are being used by planners of the Venezuelan Ministry of the Environment and Natural Resources to design emergency plans and new land use policies.

Many more applications of debris flow simulations models, including several case studies and potential mitigation measures, can be found in Rickenmann and Chen (2003). Predictive models that have been used for engineering purposes, besides those presented above include those advanced by MacArthur and Schamber (1986), Han and Wang (1997) and Laigle and Coussot (1996). Modeling of hyperconcentrated flows and hazard mitigation measures will continue to be extremely challenging problems for the engineering and geosciences community (García and Zech 2007).

Because of the impact that this catastrophic event had on human lives as well as on infrastructure and water resources, the appendix to this chapter is devoted to the case of Mount St. Helens.

REFERENCES

- Aguirre-Pe, J., Quisca, S. and Plachco, F. P. (1995) "Tests and Numerical One-dimensional Modelling of a High-viscosity Fluid Dam-break Wave." *Journal of Hydraulic Research, IAHR*, 33 (1), 17–26.
- Anstey, R. L., (1965). "Physical characteristics of alluvial fans." *Technical Rep. ES-20*. U.S. Army Natick Laboratories, Natick, Mass.
- Arattano, M., and Savage, W., (1992). "Kinematic wave theory for debris flow microform." Open file Rep. 92–290, U.S. Geological Survey, Denver, CO.
- Askew, Arthur J. (1997). "Water in the International Decade for Natural Disaster Reduction. *Proc., Conference on Destructive Water: Water-Caused Natural Disasters, Their Abatement and Control*, IAHS Publication No. 239, International Association of Hydrological Sciences, Wallingford, U.K.
- Bagnold, R. A. (1954) "Experiments on a gravity-free dispersion of a large solid sphere in a Newtonian fluid under shear." *Proceedings of the Royal Society Of London, Series A* 225, 49–63.
- Bagnold, R. A. (1956). "Flow of cohesionless grains in fluids." *Phil. Trans. Roy. Soc. Lond.* 249(964), 235–297.
- Bello, M. E., Lopez, J. L., Garcia-Martinez, R., and O'Brien, J. S. (2003). "Simulation of flooding and debris flows in the Cerro Grande River," *Acta Cientifica Venezolana*, Vol. 54, Suplemento No 1, 22–32.
- Beverage, J. P., and Culbertson, J. K. (1964) "Hyperconcentrations of suspended sediment." *Journal of the Hydraulics Division, ASCE*, 90 (HY6), 117–126.
- Bin, Y. & Huilin, Z. (2000) Direct determination of rheological characteristics of debris-flow, *J. Hydraulic Engineering*, 126, pp. 158–159.

- Bigio, E. R. and Cannon, S. H. (2001). "Compilation of post-wildfire runoff-event data from the western United States." *Open File Rep. 01-0474*, U.S. Geological Survey, Denver, CO.
- Bradley, J. B., and McCutcheon, S. C. (1987). "Influence of large suspended-sediment concentrations in rivers." In *Sediment Transport in Gravel-bed Rivers*, Thorne, C. R., Bathurst, J. C., and Hey, R. D., eds., Wiley, New York.
- Brufau, P., Garcia-Navarro, P., Ghilardi, P., Natale, L., and Savi, F. (2000). "1-D mathematical Modeling of Debris-Flow," *Journal of Hydraulic Research* 38(6), 435–446.
- Campbell, R. H. (1975). "Soil slips, debris-flows, and rainstorms in Santa Monica Mountains and vicinity, southern California." *Professional Paper 851*, U.S. Geological Survey U.S. Govt. Printing Office, Washington, D.C.
- Cannon, S. H., and Ellen, S. (1985). "Rainfall conditions for abundant debris-flow avalanches: San Francisco Bay region, California." *California Geology* (December), 38(12), 267–272.
- Cazanacli, D., Paola, C. and Parker, G. (2002). "Experimental steep, braided flow: application to flooding risk on fans." *Journal of Hydraulic Engineering*, ASCE, 128(3), 322–330.
- Chassie, R. G., and Goughnour, R. D. (1976). "National highway landslide experience." *Highway Focus*, 8(1), 1–9.
- Chen, C. L. (1988). Generalized viscoplastic modeling of debris-flow." *Journal of Hydraulic Engineering*, ASCE, 114 (3), 237–258.
- Chen, C. L., ed. (1997). *Proceedings of the First International Conference on Debris-flow Hazards Mitigation: mechanics, prediction, and assessment*, ASCE, New York.
- Chen, C. L. and Ling, C. H. (1997). "Resistance formulas in hydraulics-based models for routing debris flows," Proceedings of the First International Conference on Debris-Flows Hazards Mitigation: Mechanics, Prediction and Assessment. San Francisco, CA, August 7–9, 1997: 360–372. New York: ASCE.
- Choi, S. U., and Garcia, M. H. (1993). "Kinematic wave approximation for debris-flow routing." *Proc., XXV IAHR Congress*, Vol. B-3–4, 94–101, Japan Society of Civil Engineers, Tokyo, Japan.
- Chow, V. T., (1959). "Open-Channel Hydraulics." McGraw-Hill, New York, 680p.
- Contreras, S. M., and Davies, T.R.H. (2000). "Coarse-grained debris-flows: Hysteresis and time-dependent rheology." *Journal of Hydraulic Engineering* 126 (12), 938–941.
- Costa, J. E. (1984). "Chapter 9: Physical geomorphology of debris-flow." *Development and applications of geomorphology*, J. E. Costa and P. J. Fleisher, eds., Springer, New York.
- Coussot, P. (1992), "Rhéologie des Laves Torrentielles." *Collection Etude, serie Montagne, n 5*, INPG, Grenoble, France.
- Coussot, P. (1994). "Steady, laminar, flow of concentrated mud suspensions in open channel." *Journal of Hydraulic Research* 32, 535–539.
- Coussot, P. (1997). *Mudflow rheology and dynamics*, IAHR Monograph Series, Balkema, The Netherlands.
- Coussot, P., Laigle, D., Arattano, M., Deganutti, A. and Marchi, L. (1998). "Direct determination of rheological characteristics of debris-flow." *Journal of Hydraulic Engineering*, ASCE 124(8), 865–868.
- Davies, T. R. (1997). "Using hydro science and hydro technical engineering to reduce debris-flow hazards." *Proc., First International Conference Debris-flow Hazards Mitigation: Mechanics, Prediction and Assessment*, ASCE, New York, 787–809.
- Davies, T.R.H. (1986). "Large debris-flows: A macroviscous phenomenon." *Acta Mechanica* 63: 161–178.
- Davies, T.R.H. (1988). "Debris-flow surges—A laboratory investigation." *Mitt. 96*, Versuchsanstalt fur Wasserbau, Hydrologie und Glaziologie, ETH, Zurich, Switzerland.
- Dawdy, D. R. (1979). "Flood frequency estimates on alluvial fans." *Journal of the Hydraulics Division, ASCE, Proceedings* 105 (HYII), 1407–1413.
- Denlinger, R. P., and Iverson, R. M. (2001). "Flow of variably fluidized granular masses across three-dimensional terrain. 3: Numerical predictions and experimental tests." *Journal of Geophysical Research* 106(B1), 553–566.
- Dent, J. D. and Lang, T. E. (1983). "A biviscous modified bingham model of snow avalanche motion." *Annals Glaciology*, 4, 42–46.
- Doehring, D. O. (1970). "Discrimination of pediments and alluvial fans from topographic maps." *Bulletin of the Geological Society of America*, 81: 3109–3115.
- Dominique, L., and Coussot, P. (1997). "Numerical modeling of mudflow." *Journal of Hydraulic Engineering*, ASCE 123(11), 617–623.
- Edwards, K. L., and Thielman, J. (1984). "Alluvial fans: Novel flood challenge." *Civil Engineering*, ASCE 54(11), 66–68.
- Egashira, S., Miyamoto, K., and T. Itoh, (1997). "Constitutive equations of debris-flows and their applicability." *Proc., First International Conference on Debris-Flow Hazard Mitigation: Mechanic, Prediction, and Assessment*, C. L. Chen, ed., ACSE, New York, 340–349.
- Engelund, F., and Wan, Z. (1984). "Instability of hyperconcentrated flow." *Journal of Hydraulic Engineering*, ASCE 110(3), 219–223.
- Fan, J. and Dou, G. (1980). "Sediment transport mechanics." *Proceedings of International Symposium on River Sedimentation*, Guanghua Press, Beijing, China, pp. 1167–1177.
- Federal Emergency Management Agency (FEMA). (1985). "Flood insurance study: Guidelines and specifications for study contractors." *FEMA 37*, Federal Emergency Management Agency, Washington, D.C.
- Federal Emergency Management Agency (FEMA). (1990). *FAN: An alluvial fan flooding computer program user's manual and program disk*, FEMA, Washington D.C.
- Federal Emergency Management Agency (FEMA). (1991). Flood Insurance Study: Guidelines and Specifications for Study Contractors. (FEMA 37) Washington, D.C. 100 pp.
- Federal Emergency Management Agency (1994). "Engineering principles and practices for retrofitting flood prone residential buildings," chapter 4 (draft), Washington, D.C.
- Federal Emergency Management Agency (FEMA). (1995). "Flood insurance study guidelines and specification for study contractors." *FEMA 37*, FEMA, Washington, D.C.
- Federal Emergency Management Agency (FEMA). (2000). *Guidelines for Determining Flood Hazards on Alluvial Fans*. Federal Emergency Management Agency, Washington, D.C.
- Federal Highway Administration. (2001). Bridge scour and stream instability countermeasures experience, selection, and design guidance. *Hydraulic Engineering Circular No. 23*, NHI-01-0003.
- Federal Register. (1989). *44 CFR Parts 59, 60 and 65, Rules and Regulations*, Vol. 54, No. 156, August, 1989, Washington, D.C.

- Flood Control District of Maricopa County (FCDMC). (1992). "Alluvial fan data collection and monitoring study." *Prepared for Flood Control District of Maricopa County, Phoenix, AZ*, CH2M-Hill, Tempe, AZ. and R. H. French, Las Vegas, NV.
- French, R. H. (1989). "Effect of the length of record on estimates of annual precipitation in Nevada." *Journal of Hydraulic Engineering, ASCE* 115(4), 493–506.
- French, R. H. (1987). *Hydraulic processes on alluvial fans*, Elsevier Science, Amsterdam.
- French, R. H., Fuller, J. E., and Waters, S. (1993). "Alluvial fan: Proposed new process-oriented definitions for arid Southwest." *Journal of Water Resources Planning and Management, ASCE*, 119 (5), 588–598.
- French, R. H. and Keaton, J. R. (1992). "Successful interactions between hydraulic engineering and geomorphology in identifying flood hazard areas in the southwestern United States." *Proc., 1992 Hydraulic Engineering Sessions at Water Forum '92*, ASCE, New York, 581–586.
- French, R., and Miller, J. (2003). Discussion on "Experimental steep, braided flow: application to flooding risk on fans." By Cazanacli et al, *Journal of Hydraulic Engineering, ASCE*, 129(11), 920–922.
- Fuller, J. E. (1990). "Misapplication of the FEMA alluvial fan model: A case history." *Proc., 1990 International Symposium Hydraulics/Hydrology of Arid Lands*, R. H. French, ed., ASCE, New York, 367–372.
- García, R., et al. (2003). "Hazard mapping for debris-flow events in the alluvial fans of northern Venezuela." *Proc., Third International Conference on Debris-Flow Hazards Mitigation: Mechanics, Prediction, and Assessment*, Rickenmann, D. and Chen, C. L. eds., 589–599.
- García, M. H., and Zech, Y., eds. (2007). "Dan-break flow experiments and real-case data: A database from the European IMPACT Research Program." *Journal of Hydraulic Research* 45, Special issue.
- Glancy, P.A. and Bell, J.W. (2000). *Landslide-induced flooding at Ophir Creek, Washoe County, Western Nevada, May 30, 1983. Professional Paper 1617*, U.S. Geological Survey, Carson City, Nev.
- Govier, G. W., Shook, C. A., and Lilge, E. O. (1957) "The properties of water suspension of finely subdivided magnetite, galena, and ferrosilicon." *Transactions of the Canadian Institute of Mining Metallurgy* 60, 147–54.
- Haldenwang, R. and Slatter, P. (2006). "Experimental procedure and database for non-Newtonian open-channel flow." *Journal of Hydraulic Research, IAHR*, 44(2), 283–287.
- Hanes, D., and Bowen, A. (1985). "A granular-fluid model for steady intense bedload transport." *Journal of Geophysical Research* 90 (C5), 9149–9158.
- Han, G. and Wang, D. (1996). "Numerical modeling of Anhui debris flow." *J. Hydr. Engrg., ASCE*, 122(5), 262–265.
- Huang, X., and García, M. H. (1997a). "Asymptotic solution for Bingham debris-flows." *Proc., First International Conference on Debris-Flow Hazard Mitigation: Mechanics, Prediction, and Assessment*, C. L. Chen, ed., ASCE, New York, 561–575.
- Huang, X., and García, M. H. (1997b). "A perturbation solution for Bingham plastic mud flows." *Journal of Hydraulic Engineering, ASCE* 123(11), 984–996.
- Huang, X., and García, M. H. (1998). "A Herschel-Bulkley model for mud flows down a slope", *Journal of Fluid Mechanics* 374, 305–333.
- Hungr, O. (1995). "A model for the runout analysis of rapid flow slides, debris-flows, and avalanches." *Canadian Geotechnical Journal* 32(4), 610–623.
- Hunt, B. (1994). "Newtonian fluid mechanics of debris-flows and avalanches." *Journal of Hydraulic Engineering, ASCE* 120, 1350–1363.
- Hutter, K., Svendsen, B., and Rickenmann, D. (1996). "Debris-flow modeling: A review." *Continuum Mechanics and Thermodynamics* 8, 1–35.
- Hutchinson, J. N. (1988). "Morphological and geotechnical parameters of landslides in relation to geology and hydrogeology," in *Landslides*, Proceedings of the Fifth International Symposium on Landslides, Bonnard, C. (Editor), Lausanne, Switzerland, Balkema Publishers, The Netherlands, pp. 3–35.
- Hydrologic Engineering Center (HEC). (1985). "Toutle River Mudflow Investigation." *Special Projects Rep. No. 85-3, prepared for the Portland District Corps of Engineers* by MacArthur, Hamilton, and Schamber, Hydrologic Engineering Center, Davis, Calif.
- Hydrologic Engineering Center (HEC). (1993). "Assessment of structural flood-control measures on alluvial fans." *Prepared for FEMA*, Hydrologic Engineering Center, Davis, Calif.
- Imran, J., Parker, G., Locat, J., and Lee, H. (2001). "A 1D numerical model of muddy subaqueous and subaerial debris-flows." *Journal of Hydraulic Engineering, ASCE* 127(11), 959–968.
- International Federation of Red Cross and Red Crescent Societies (IFRCRCS). (2001). *World disasters report 2001*, Kluwer Academic, Boston.
- Iverson, R. M. (1985). "A constitutive equation for mass-movement behavior." *Journal of Geology* 93, 143–160.
- Iverson, R. M. (1997). "The physics of debris-flows." *Reviews of Geophysics*, American Geophysical Union, Washington D.C., 35(3), 245–296.
- Iverson, R. M. (2003). "The debris-flow rheology myth." *Proc., Third International Conference on Debris-flow Hazards Mitigation: Mechanics, Prediction, and Assessment*, Rickenmann, D. and Chen, C. L. eds., 303–314.
- Iverson, R. M., Costa, J. E., and LaHusen, R. G. (1992). "Debris-flow flume at H. J. Andrews Experimental Forest, Oregon." *Open-File Rep. 92-483*, U.S. Geological Survey, Reston, VA.
- Iverson, R. M., and Denlinger, R. P. (2001). "Mechanics of debris-flows and debris-laden flash floods." *Proc., Seventh Federal Interagency Sedimentation Conference*, Subcommittee on Sedimentation, Reno, Nevada, IV:1–8.
- Jeyapalan, J. K., Duncan, J. M., and Seed, H. B. (1983). "Analysis of flow failures of mine tailings." *Journal of Geotechnical Engineering, ASCE*, 109(2), 150–171.
- Johnson, A. M. (1970). *Physical processes in geology*. Freeman, Cooper & Company, San Francisco, CA, 577p.
- Julien, P. Y. (1995). *Erosion and sedimentation*, Cambridge University Press, New York.
- Julien, P. Y., and Lan, Y. Q. (1991). "Rheology of hyperconcentrations." *Journal of Hydraulic Engineering, ASCE* 115(3), 346–53.
- Julien, P. Y. and O'Brien, J. S. (1997). "On the importance of mud-flow and debris-flow: Rheology in structural design." *Proc., First International Conference on Debris-Flow Hazards Mitigation: Mechanics, Prediction and Assessment*, Chen, C. L. ed., ASCE, New York 350–359.
- Julien, P. Y. and Leon, C. A. (2000). "Mud floods, mudflows and debris flows: classification, rheology and structural design."

- International Seminar on the Debris-flow Disaster of December 1999*, Institute of Fluid Mechanics, University of Central Venezuela, Caracas, Venezuela (CD ROM).
- Keaton, J. R., Shlemon, R. J., French, R. H., and Dawdy, D. R. (1990). "Piedmont-fan flood hazard analysis from geomorphology and surface water hydrology, Hudspeth County, Texas." *Proc., 1990 International Symposium Hydraulics/Hydrology of Arid Lands*, R. H. French, ed., ASCE, New York, 356–360.
- Krohn, J. P. and Slosson J. S. (1976). "Landslide potential in the United States." *California Geology* 29 (10), 224–231.
- Krone, R. B. (1963). "A study of rheologic properties of estuarial sediments." *Ser. Rep. 63–8*, Hydraulic Engineering Laboratory and Sanitary Research Laboratory, University of California, Berkeley, CA.
- Krone, R., and Wright, V. (1987). "Laboratory and numerical study of mud and debris-flows." Vol. 1 and 2, Report of Department of Civil Engineering, University of California, Davis.
- Laigle, D. and Coussot, P. (1997). "Numerical modeling of mud-flow." *J. Hydr. Engrg.*, ASCE, 123(7), 617–623.
- Lanzoni, S. and Seminara G., (1993). "Debris waves." *Proc., XXV IAHR Congress*, Vol. B-3–4, 79–85, Japan Society of Civil Engineers, Tokyo, Japan.
- Larsen, M. C., Wieczorek, G. F., Eaton, L. S., Morgan, B. A., and Torres-Sierra H. (2001). "Natural hazards on alluvial fans: The Venezuela debris-flow and flash flood disaster." *Fact Sheet FS103–0*, U.S. Geological Survey.
- Lecce, S. A. (1990), "The alluvial fan problem." *Alluvial Fans: A Field Approach*, A. H. Rachoki and M. Church, eds., Wiley, New York.
- Lenzi, M. A., Comiti, F., and Marion, A. (2004). "Local Scouring at Bed Sills in a Mountain River: Plima River, Italian Alps." *J. Hydr. Engrg.*, ASCE, 130(3), 267–269.
- Li, R. M., Simons, D. B., and Stevens, M. A. (1975), "Nonlinear kinematic wave approximation for water routing." *Water Resources Research* 11 (2), 245–252.
- Liu, K. F., and Mei, C. C. (1989). "Slow spreading of a sheet of Bingham fluid on an inclined plane." *Journal of Fluid Mechanics* 207, 505–529.
- Locat, J. (1997). "Normalized rheological behavior of fine muds and their flow properties in a pseudo plastic regime." *Proc., First International Conference on Debris-Flow Hazards Mitigation: Mechanics, Prediction, and Assessment*, C. L. Chen, ed., ASCE, New York, 260–269.
- López J. L., and García, R. (2000). "Los Aludes Torrenciales de Diciembre de 1999 en Venezuela", Proceedings of Internacional Seminar, Instituto de Mecanica de Fluidos, Universidad Central de Venezuela, Caracas, Venezuela (CD ROM).
- López, J. L., Perez, D., and García, R. (2003). "Hydrologic and geomorphologic evaluation of the 1999 debris-flow event in Venezuela." *Proc., Third International Conference on Debris-Flow Hazards Mitigation: Mechanics, Prediction, and Assessment*, Rickenmann, D. and Chen, C. L., eds., 989–1000.
- Lorenzini, G., and Mazza, N. (2004). *Debris-flows: Phenomenology and rheological modelling*, WIT Press, Boston, MA.
- Los Angeles County Flood Control District (LACFCD). (1959). *Report on debris reduction studies for mountain watersheds of Los Angeles County*, Los Angeles County Flood Control District, Los Angeles.
- Los Angeles County Flood Control District (LACFCD). (1979). *Design manual, debris dams and basins*, Los Angeles County Flood Control District, Los Angeles.
- MacArthur, R. C., and Hamilton D. L. (1988). "Review of the U.S. Army Corps of Engineers involvement with alluvial fan flooding problems." *Technical Paper No. 124*, Hydrologic Engineering Center, Davis, Calif.
- MacArthur, R. C., Hamilton, D. L., Harvey, M. D. and Kekaula, H. W. (1992). "Analysis of special hazards and flooding problems in tropical island environments." *Proc., Environmental Engineering Sessions Water Forum '92*, ASCE, New York.
- MacArthur, R. C., Hamilton, D. L., and Branch, W. E. (1993). "Assessment Procedures for Lahars, Mudflows, Debris-Flows, and Debris Torrents." *Proc., National Conference of Hydraulic Engineering, Hydraulic Division*, ASCE, San Francisco, Calif.
- MacArthur, R. C., and Schamber, D. R. (1986). "Numerical Methods for Simulating Mudflows." *Proceedings of Third International Symposium on River Sedimentation*, Wang S. Y., Shen H. W. and Ding L. Z. (editors), School of Engineering, University of Mississippi, Mississippi.
- MacTigue, D. F., (1982). "A nonlinear constitutive model for granular material." *Journal of Applied Mechanics Transations*, ASME 49(6), 291–296.
- Magura, L. M. and Wood, D. E. (1980). "Flood hazard identification and flood plain management on alluvial fans." *AWRA, Water Resources Bulletin* 16(1), 55–62.
- Mainali, A. and Rajaratnam, N. (1991). "Hydraulics of debris-flows: A review." *Tech. Rep. WRE 91–2*, Department Civil Engineering, University of Alberta, Edmonton, Al., Canada
- Mainali, A. and Rajaratnam, N. (1994). "Experimental study of debris-flows." *Journal of Hydraulic Engineering*, ASCE 120(1), 104–123.
- Major, J. J., and Iverson, R. M. (1999). "Debris-flow deposition-effects of pore-fluid pressure and friction concentrated at flow margins." *Geological Society of America Bulletin* 111, 1424–1434.
- Major, J. J., and Pierson, T. C. (1992). "Debris-flow rheology: Experimental analysis of fine-grained slurries." *Water Resources Research* 28, 841–857.
- McPhee, J. (1989a). "Atchafalaya." *The control of nature*, Farrar, Straus and Giroux, New York, 3–92.
- McPhee, J. (1989b). "Los Angeles against the mountains." *The control of nature*, Farrar, Straus and Giroux, New York, 183–272.
- Migniot, P. C. (1968). "A study of the physical properties of various forms of very fine sediment and their behavior under hydrodynamic action." *La Houille Blanche* 7, 591–620.
- Mih, W. C. (1999). "High concentration granular shear flow." *Journal of Hydraulic Research* 37(2), 229–248.
- National Research Council (NRC). (1982). "Selecting a Methodology for Delineating Mudslides Hazard Areas for National Flood Insurance Program," National Academy of Sciences Report by the Advisory Board on the Build Environment, Washington, D.C.
- National Research Council (NRC). (1989). "Reducing disasters' toll." *The United States decade for natural disaster reduction*, National Academy Press, Washington, D.C.
- National Research Council (NRC). (1996a). *Alluvial fan flooding*, National Academy Press, Washington, D.C.
- National Research Council (NRC). (1996b). "Landslides: Investigation and mitigation." *Special Rep. 247*, Transportation Research Board, National Research Council, Washington, D.C.
- Neill, C. R. assoc. ed. (1989). "Hydrology of floods in Canada: A guide to planning and design", National Research Council, Canada.

- O'Brien, J. S. (1986). Physical processes, rheology and modeling of mud flows. (PhD Dissertation). Department of Civil Engineering, Colorado State University, 155 pp.
- O'Brien, J. S., and Julien, P. Y. (1985) "Physical properties and mechanics of hyper-concentrated sediment flows." in *Proc., ASCE Specialty Conference on Delineation of Landslides, Flash Flood and Debris-Flow Hazards*, Bowles, D. (Editor), Utah Water Research Laboratory, Utah State University, Logan, Utah, 260–279.
- O'Brien, J. S., and Julien, P. Y. (1988). "Laboratory analysis of mudflow properties." *Journal of Hydraulic Engineering, ASCE* 114, 877–887.
- O'Brien, J. S., Julien, P. Y., and Fullerton, W. T. (1993). "Two dimensional water flood and mudflow simulation." *Journal of Hydraulic Engineering, ASCE* 119(2), 244–261.
- O'Brien, J. S. (1999). *FLO-2D users manual*, Tetra Tech ISG, Nutrioso, Ariz.
- Parker, G. (1999). "Progress in the modeling of alluvial fans." *Journal of Hydraulic Research, IAHR*, 37 (Special Issue), 805–825.
- Parker, G., Paola, C., Whipple, K. X., and Mohrig, D. (1998a). "Alluvial fans formed by channelized fluvial and sheet flow. I: Theory." *Journal of Hydraulic Engineering, ASCE*, 124(10), 985–995.
- Parker, G., et al. (1998b). "Alluvial fans formed by channelized fluvial and sheet flow. II: Application." *Journal of Hydraulic Engineering, ASCE* 124(10), 996–1004.
- Parsons, J. D., Whipple, K. X., and Simioni, A. (2001). "Experimental study of the grain-flow, fluid-mud transition in debris-flows." *Journal of Geology* 109, 427–447.
- Pearthreee, P. A. (1991). "Geologic insights into flood hazards in piedmont areas of Arizona." *Arizona Geology*, 21(4), 1–5.
- Pearthreee, P. A., Demsey, K. A., Onken, J., Vincent, K. R. and House, P. K. (1991). "Geomorphic assessment of flood prone areas on the southern piedmont of the Tortolita Mountains, Pima County, Arizona." *Open-File Rep. 91-11*, Arizona Geologic Survey, Tucson, Ariz.
- Phillips, Ch. J., Davies, T.R.H. (1991). Determining rheological parameters of debris flow material. *Geomorphology*, 4, 101–110.
- Pierson, T. C., and Costa, J. E. (1984). "A rheological classification of subaerial sediment-water flows." *97th Annual Meeting, Geological Society of America*, Vol. 16, No. 6, p. 623.
- Pierson, T. C., and Costa, J. E. (1987). "A rheological classification of subaerial sediment-water flows." *Reviews in Engineering Geology*, 7, 1–12.
- Qian, N., and Wan, Z. (1986). *A critical review of the research on the hyperconcentrated flow in China*, International Research and Training Centre on Erosion and Sedimentation, Beijing.
- Rickenmann, D. (1991). "Hyperconcentrated flow and sediment transport at steep slopes." *Journal of Hydraulic Engineering, ASCE*, Vol. 117, No. 11, 1419–1439.
- Rickenmann, D. (1999). "Empirical Relationships for Debris Flows." *Natural Hazards*, 19: 47–77.
- Rickenmann, D., and Chen, C-L., eds. (2003). *Proc., Third International Conference on Debris-Flow Hazards Mitigation: Mechanics, Prediction, and Assessment (Vols. 1 and 2)*, Davos, Switzerland, Sept 2003, Millpress Science Publishers, Rotterdam, The Netherlands. 1335 p.
- Rubin, C., Yezer, B.A.M., Hussain, Q., and Webb, A. (1986). "Summary of Major Natural Disaster Incidents in the United States: 1965 to 1985." Washington, D.C. Federal Emergency Management Agency (FEMA).
- Savage, S. B. (1984). "The mechanics of rapid granular flows." *Advances in Applied Mechanics* 24, 289–366.
- Savage, S. B., and Hutter, K. (1989). "The motion of a finite mass of granular material down a rough incline." *Journal of Fluid Mechanics*, 199, 177–215.
- Savage, S. B., and McKeown, S. (1983). "Shear stresses developed during rapid shear of concentrated suspension of large spherical particles between concentric cylinders." *Journal of Fluid Mechanics* 137, 453–72.
- Savage, S. B., and Iverson, R. M. (2003) "Surge dynamics coupled to pore-pressure evolution in debris-flows." *Proc., Third International Conference on Debris-Flow Hazards Mitigation: Mechanics, Prediction, and Assessment*, Rickenmann, D. and Chen, C. L., eds., 503–514, Millpress Science Publishers, Rotterdam, The Netherlands.
- Savage, S. B., and Hutter, K. (1991). "The dynamics of avalanches of granular materials from initiation to runout. I: Analysis." *Acta Mechanica* 86, 201–223.
- Schamber, D. R., and MacArthur, R. C. (1985). "One-dimensional model for mud flows." *Proc., Conference on Hydraulics and Hydrology in the Small Computer Age*, ASCE, New York.
- Schatzmann, M., Fischer, P., and Bezzola, G. R. (2003). "Rheological behavior of fine and large particle suspensions." *Journal of Hydraulic Engineering, ASCE* 129(10), 796–803.
- Schick, A. P. (1974). "Alluvial fans and desert roads—A problem in applied geomorphology." *Abhandlungen der Akademie der Wissenschaften in Gottingen Mathematisch-Physikalische Klasse* 29, 418–425.
- Schumm, S. A., et al. (1996). *Alluvial fan flooding*, Committee on Alluvial Fan Flooding, Water Science and Technology Board, Commission on Geosciences, Environment, and Resources, National Research Council, National Academy Press, Washington, D.C.
- Schuster, R. L., and Flemming, R. W. (1986). "Economic Losses and Fatalities Due to Landslides." *Bulletin of the Association of Engineering Geologists* 23(1), 11–18.
- Sharpe, C.F.S. (1938) *Landslides and related phenomenon*, Columbia University Press, New York, 137pp.
- Shen, H., and Ackermann, N. L. (1982). "Constitutive relations for fluid-solid mixtures." *Journal of Engineering Mechanics, ASCE*, 108(5), 748–763.
- Singh, Vijay P. (1996). *Hydrology of disasters*, Kluwer, Dordrecht, The Netherlands.
- Sun, T., Paola, C., and Parker, G. (2002). "Fluvial fan-deltas: Linking channel processes with large-scale morphodynamics." *Water Resources Research, AGU*, 38(2), doi:10.1029/2001WR000284, 2002.
- Suwa, H. (1988). "Focusing Mechanism of Large Boulders to a Debris-flow Front". *Trans. Jpn. Geomorphol. Union*, 9, 151–178.
- Suwa, H. (1989). "Field observation of debris-flows." *Proc., Japan-China Joint Seminar on Natural Hazard Mitigation*, Kyoto, Japan.
- Takahashi, T. (1978). "Mechanical characteristics of debris-flows." *Journal of Hydraulic Engineering, ASCE* 104 (HY3), 381–396.
- Takahashi, T. (1980) "Debris-flow on a prismatic channel." *Journal of Hydraulic Engineering, ASCE* 106 (HY8), 1153–1169.

- Takahashi, T. (1981b). "Estimation of potential debris-flows and their hazardous zones: Soft countermeasures for a disaster." *Natural Disaster Science*, 3(1), 57–89.
- Takahashi, T. (1981). Debris-flow, *Ann. Rev. Fluid Mechanics*, 13, pp. 57–77.
- Takahashi, T. (1991). *Debris-flow*, IAHR Monograph Series, Balkema, Rotterdam, The Netherlands.
- Tubino, M., and S. Lanzoni (1993). Rheology of debris flows: experimental observations and modelling problems. *Excerpta* 7, 201–236.
- United Nations. (1996). *Mud flows: Experiences and lessons learned from major disasters*, Department of Humanitarian Affairs, New York, 139.
- U.S. Army Corps of Engineers (USACE). (1994). "Engineering and design—Channel stability assessment of flood control projects." *Engineering Manual No. 1110-2-1418*, Department of the Army, Washington, D.C.
- U.S. Army Corps of Engineers (USACE). (1983). *Magnesia Spring Canyon—Detailed project report for flood control, Riverside County*, USACE, Los Angeles District, Los Angeles.
- U.S. Army Corps of Engineers (USACE). (1988). *Special report—White water river flood warning system and preparedness plan, White water river basin*, USACE, Los Angeles District, Los Angeles.
- U.S. Army Corps of Engineers (USACE). (1989). "Engineering and design—Sedimentation investigations of rivers and reservoirs." *Engineering Manual No. 1110-2-4000*, Department of the Army, Washington, D.C.
- U.S. Army Corps of Engineers (USACE). (1993). "Engineering and design—River hydraulics." *Engineering Manual No. 1110-2-1416*, Department of the Army, Washington, D.C.
- U.S. Army Corps of Engineers (USACE). (1991). "Engineering and design—Hydraulic design of flood control channels." *Engineering Manual No. 1110-2-1601*, Department of the Army, Washington, D.C.
- U.S. Department of Agriculture (USDA). (1992). "Chapter 18—Soil bioengineering for upland slope protection and erosion reduction." *National Engineering Field Handbook Series (EFH-650-18) 210-VI*, Soil Conservation Service, U.S. Department of Agriculture, Washington, D.C.
- U.S. Department of Agriculture (USDA). (1996). "Chapter 16—Streambank and shoreline protection." *National Engineering Handbook Series (NEH-650-16) 210-VI*, Soil Conservation Service, U.S. Department of Agriculture, Washington, D.C.
- Vanoni, Vito A., ed. (1975). *Sedimentation Engineering, Manual No. 54*, American Society of Civil Engineers, NY.
- Vanoni, Vito A., ed. (2006). *Sedimentation Engineering, Manual No. 54, Classic Edition*, American Society of Civil Engineers, Reston, VA.
- Varnes, D. J. (1958). "Landslide types and processes." *Landslides and engineering practice*, Special Rep. 29, Eckel, E. B., ed., Special Report 29: 20–47, Highway Research Board, Washington, D.C.
- Walling, D. E., Davies, T. R., and Hasholt, B. (1992). "Erosion, debris-flows and environment in mountain regions." *Proc., Chengdu Symposium*, Publication No. 209, International Association of Hydrological Sciences, Wallingford, U.K.
- Wan, Z. (1982). "Bed material movement in hyperconcentrated flows." *Series paper 31*, Institute of Hydrodynamics and Hydraulic Engineering, Technical University of Denmark, Lyngby.
- Wan, Z., and Wang, Z. (1994). "Hyperconcentrated flows." *IAHR Monograph*, Balkema, Rotterdam, The Netherlands.
- Whipple, K. X. (1997). "Open-channel flow of Bingham fluids: Applications in debris-flow research." *Journal of Geology* 105, 243–262.
- Whipple, K. X., Parker, G., Paola, C., and Mohrig, D. (1998). "Channel dynamics, sediment transport, and the slope of alluvial fans: Experimental study." *Journal of Geology* 106, 677–693.
- Whitham, G. B. (1974). *Linear and nonlinear waves*, Wiley-Interscience, New York.
- Wieczorek, G. F., Larsen, M. C., Eaton, L. S., Morgan, B. A., and Blair, J. L. (2001). "Debris-flow and flooding hazards associated with the December 1999 storm in coastal Venezuela and strategies for mitigation." *Open File Rep. 01-0144*, U.S. Geological Survey, Denver, CO.
- Wieczorek, G. F. and Naeser, N. D. eds., (2000). *Proc., Second International Conference on Debris-Flow Hazards Mitigation: Mechanics, Prediction, and Assessment*. Taipei, Taiwan. Rotterdam: Balkema.
- Wilson, R. C., and Wieczorek, G. F. (1995). "Rainfall thresholds for the initiation of debris-flows at La Honda, California." *Environmental and Engineering Geoscience* 1(1), 11–27.
- Winterwerp, J. C., de Groot, M. B., Masterbergen, D. R., and Verwoert, H. (1990). "Hyperconcentrated sand-water mixture flows over flat-bed." *Journal of Hydraulic Engineering, ASCE* 116(1), 36–54.
- Woo, H. S., Julien, P. Y., and Richardson, E. V. (1988). "Suspension of large concentrations of sands." *Journal of Hydraulic Engineering, ASCE* 114(8), 888–898.
- Wright, V., and Krone, R. (1987). "Laboratory and numerical study of mud and debris-flows." in Proceedings of Technical Session A on XXII International Association for Hydraulic Research Congress., IAHR, W. R. White (Editor), Ecole Politehnique Federale de Lausanne, Lausanne, Switzerland,
- Youd, T. L. (1978). "Major cause of earthquake damage is ground failure." *Civil Engineering, ASCE* 48, (4), 47–51.
- Zanuttigh, B. and Lamberti, A. (2004). Analysis of Debris Wave Development with One-Dimensional Shallow-Water Equations. *J. Hydr. Engrg., ASCE*, Volume 130, Issue 4, pp. 293–304.
- Zanuttigh, B. and DiPaolo, A. (2006). "Experimental analysis of the segregation of dry avalanches and implications for debris flows." *Journal of Hydraulic Research, IAHR*, Vol. 44, No. 6, 796–806.
- Zhang S., Lopez, J. L., Garcia R., and Perez D. (2000). "Basin characteristics of large scale debris-flows in Vargas Region, Venezuela, December 16, 1999." *International Seminar on the Debris-flow Disaster of December 1999*, Institute of Fluid Mechanics, University of Central Venezuela, Caracas, Venezuela (CD ROM).

APPENDIX CHAPTER 19

Case Study Mount St. Helens—20 Years Later

INTRODUCTION AND CHRONOLOGY

On 18 May 1980, just before a magmatic blast signaled the onset of the Mount St. Helens eruption (Fig. 1 shows eruption and after effects), an earthquake triggered a major slope failure on the north flank of the mountain. Sliding off the cone, some 2.8 billion cu m (3.7 billion cu yd) of rock, ice and other material avalanched into the upper North Fork Toutle River Valley removing the upper 404 m (1,324 ft) of the mountain and depositing material over an area of 596 sq km (230 sq mi) (USACE, 1999). The resultant debris avalanche buried the upper 27 km (17 mi) of the North Fork Toutle River to an average depth of 46 m (150 ft). Melting snow and glacial ice combined with water from North Fork Toutle River and possibly Spirit Lake to produce mudflows. These swept down the valley, incorporating logs and debris, raising valley floors and diverting streams. Moving downstream into the Toutle and Cowlitz rivers, the mudflows destroyed bridges, inundated buildings, caused widespread flooding along the river banks and blocked the main navigation channel in the Columbia River (see Fig. 2).

Within 24 hours, the mudflows deposited some 38 million cu m (50 million cu yd) of sediment in the lower 37 km (23 mi) of the Cowlitz River including overbank areas, and an additional 38 million cu m (50 million cu yd) into the Columbia River upstream and downstream from Longview, WA. Infilling in the lower Cowlitz as much as 4.6 m (15 ft) in some places reduced the river channel hydraulic capacity by nearly 80% the discharge at bank-full capacity decreased from a pre-eruption level of 1,982 cms (70,000 cfs) to less than 368 cms (13,000 cfs). Downstream at the mouth of the Cowlitz, the Columbia River channel, normally maintained at a 12.2-m (40-ft) depth, shrank to less than 4.6 m (15 ft). Thirty-one deep draft vessels were trapped in upstream harbors; some fifty ships enroute to the area had to be diverted to other ports.

In the aftermath of the eruption, the U.S. Army Corps of Engineers coordinated efforts with other federal, state and local agencies to provide flood protection for the urban

areas and to remove sediment deposited in the river channels. Work was started to strengthen or construct levees at Castle Rock, Lexington, Longview and Kelso, Washington. Pipeline and hopper dredges began to remove sediment from the Columbia almost immediately; by July pipeline dredges and other equipment were at work on the lower Cowlitz and Toutle to restore flood carrying capacity. By the end of November some 10.7 million cu m (14 million cu yd) of sediment had been removed from the Columbia, and nearly 26 million cu m (34 million cu yd) from the Cowlitz and Toutle Rivers.

But while these initial recovery efforts were underway, the long-term effects of the emplacement of the debris avalanche were being assessed. Preliminary estimates ranged widely as to the amount of sediment the avalanche would deliver annually, but it was believed that it would be years before the basin would reach a state of dynamic equilibrium. For one thing, the eruption had left the upper valley devoid of stabilizing vegetation. As channels slowly evolved to carry off impounded water or storm runoff, they would also deliver blast deposits, ash and sediment downstream for an indeterminate time.

During the fall of 1980, two debris retention structures were built on the North and South Forks of the Toutle to trap sediment so that it could be removed from the river system. The larger structure, DRS N-1, was built just downstream of the debris avalanche on the North Fork of the Toutle. At nearly 2.4 km (1.5 miles) wide, it was designed to retain 4.6 million cu m (6 million cu yd) of sediment. The other structure, located on the South Fork, was 152 m (500 ft) wide with a capacity of 457,700 cu m (600,000 cu yd). To supplement the two structures, a dozen sediment stabilization basins, or sumps, were to be excavated in the North Fork, South Fork and Lower Toutle Rivers.

By the end of November 1980, when the winter storm season began in earnest, it became clear that the potential for continued sedimentation problems had not been overestimated. Erosion of the abutment at the Interstate 5 bridge over the Toutle River necessitated emergency repairs to



Fig. 1. Mount St. Helens eruption and after effects.

Figure created by WEST Consultants, Inc. based on the following:

- Upper left photograph. Photo source: USGS Cascades Volcano Observatory
- Upper right photograph. Photo source: WEST Consultants, Inc.
- Center photograph. Photo source: WEST Consultants, Inc.
- Lower left photograph. Photo source: WEST Consultants, Inc.
- Lower right photograph. Photo source: USGS Cascades Volcano Observatory

avoid extended closure of the main north-south highway. The south impoundment area of the N-1 debris retaining structure, completed in October, was already two-thirds full with an estimated 1.1 million cu m (1.5 million cu yd) of sediment. The smaller S-1 structure was completely filled and passing excess sediment over its spillway.

On 25 December 1980 a heavy but not uncommon winter storm occurred, with rainfall estimated in excess of 3.5 in. (8.9 cm) in the upper basin. The peak stage on the Cowlitz at Castle Rock produced by the storm was 5.73 m (18.8 ft), at a discharge of 1359 cms (48,000 cfs). Due to the storm a substantial amount of sediment moved into the Cowlitz from the Toutle, reducing hydraulic capacity: a shift of more than 0.6 m (2 ft) in the rating curve gave the first indication of the quantity of sediment that could be delivered by a single

storm. With approximately 1.5 million cu m (2 million cu yd) of sediment impounded behind N-1—despite operation and maintenance dredging of some 11,500 cu m (15,000 cu yd) a day—the south spillway of the debris retaining structure washed out, opening a breach 76 m (250 ft) long and 7.6 m (25 ft) deep.

Repairs on N-1 were initiated, and during the winter months other measures were taken to mitigate the sedimentation problems in the Toutle-Cowlitz-Columbia System. Contractors continued to dredge the sediment stabilization basins, but because of limited funding, many of the other basins could not be maintained. These filled quickly; moreover, lateral shifting of the river eroded the dredged material storage piles. Further downstream bank erosion during periods of high water necessitated revetment work

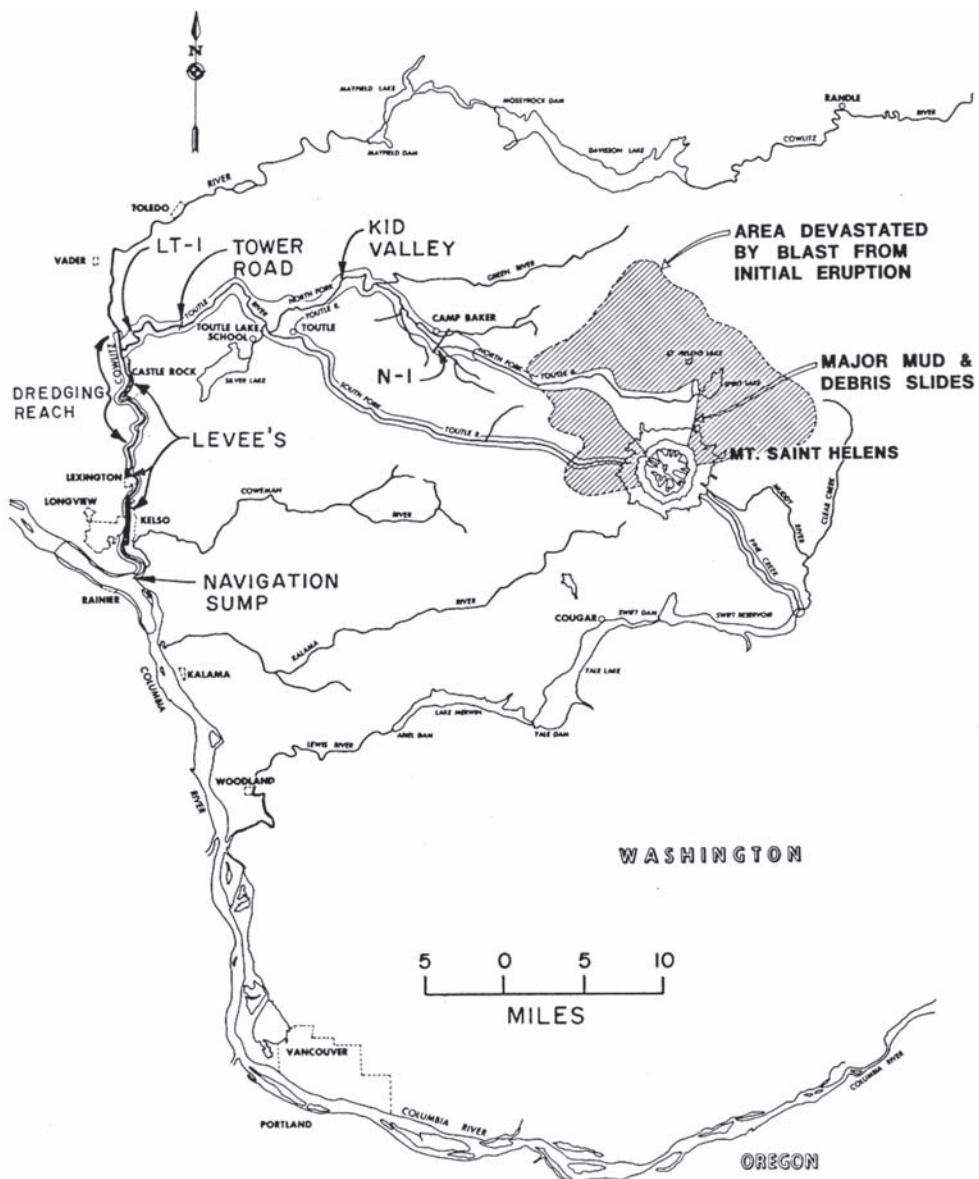


Fig. 2. Area Map—Mount St. Helens eruption impacts.

Source: U.S. Army Corps of Engineers (USACE), Portland District, *Mt. St. Helens Cowlitz and Toutle Rivers Sedimentation Study*, September 1984.

at Cowlitz River Kilometer 20.6 and 21.7 (Mile 12.8 and 13.5). At the mouth of the Cowlitz, a sump was excavated in January to trap sediment being delivered to the Columbia.

By mid-May 1981, a year after the eruption, 9.8 million cu m (12.9 million cu yd) of sediment had been dredged from the Toutle River, 42.7 million cu m (55.8 million cu yd) from the Cowlitz, and 15.4 million cu m (20.1 million cu yd) from the Columbia. At the debris retaining structures upstream, operation and maintenance dredging had removed 1.1 million cu m (1.4 million cu yd) from S-l, and 3.7 million cu m (4.8 million cu yd) from N-l. A roller-compacted concrete spillway replaced the gabion spillway that had

breached in December, and an estimated 2.3 million cu m (3 million cu yd) of sediment was trapped in the N-l north and south impoundment areas. Above the debris retaining structures, several small lakes blocked by the debris avalanche had overtopped, and concern grew about the potential flood threat posed by other impounded bodies of water. During the summer, a 670-m-long (2,200-ft) channel was dug to provide outlets for a lake in Coldwater Canyon, and another channel was begun at a lake, which had formed on South Castle Creek.

At the end of water year 1981, aggradation was continuing in the Toutle and Cowlitz rivers. River channels tended to widen and shift in response to the sudden change in sediment

load and size, and channel depth and slope. Aggradation was exacerbated by erosion of river banks and dredged material disposal piles in some areas, and changes in channel alignment were an ongoing cause for concern at bridge locations, particularly at the I-5 Bridge. However, except for work at the mouth of the Cowlitz, mechanical removal of sediment from the Toutle-Cowlitz system had virtually ceased. Excavating at sediment stabilization sites had been completed by the end of May. All 13 of the original contractors dredging on the Cowlitz from kilometer 14.5 to 34.6 (mile 9.0 to 21.5) and the mouth of the Toutle had completed their work. Maintenance dredging of sediment impounded areas at N-1 and S-1 stopped at the end of September.

Water year 1982 was an extremely "wet" year. High sediment delivery to the Cowlitz River continued and, without channel dredging, aggradation of the channel was significant. Changes of the thalweg elevations from the original eruption through 1982 are shown in Fig. 3. Large amounts of deposition were noted, particularly in the January and February 1982 storm events. Very high concentrations were measured in February. Small mudflows were also noted in the debris avalanche during this period. The N-1 spillway failed in February and the structure was overtapped, as it was full prior to the event.

A major mudflow occurred on 19 March 1982. At that time, an explosive eruption was vented out of the southeast portion of the dome. A fraction of this blast melted ice and snow on the crater walls and ponded water behind the dome. This pond filled rapidly and breached. Subsequently, the floodwaters eroded sediment from the debris avalanche, becoming transformed into a mudflow. Two pulses of this flow entered the N-1 debris retaining structure, which trapped an estimated two-thirds of the flow volume. Fig. 4 shows the magnitudes of the 1982 water year bed material yields for mudflows, hyperconcentrated flows and "normal flows",

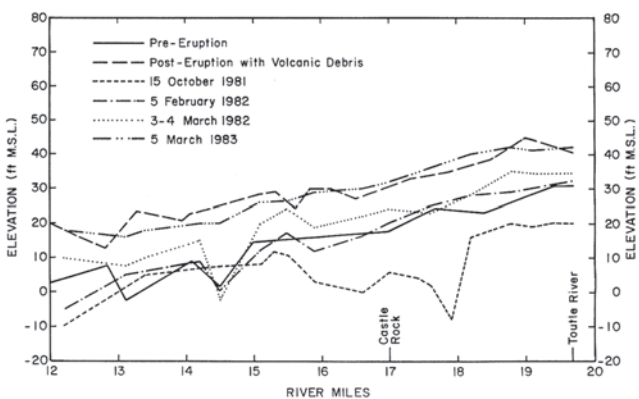


Fig. 3. Cowlitz River thalweg changes (in English Units).
Source: U.S. Army Corps of Engineers (USACE), Portland District, Mt. St. Helens Cowlitz and Toutle Rivers Sedimentation Study, September 1984.

those not related to the March 1982 mudflow. Pierson and Scott (1985) have documented additional information on this event.

From 1983 until the mid-1990s nature was kinder. None of these seasons were wet; in fact they were quite dry. The U.S. Army Corps of Engineers again dredged portions of the Cowlitz and operated sumps at the mouth of both the Toutle and Cowlitz Rivers during this period. Significant floods occurred during the mid-1990s; their impacts will be discussed later in this Appendix.

The Mount St. Helens Project was formulated to control the projected movement of sediment from the debris avalanche along the North Fork Toutle River and to maintain an optimized level of flood protection downstream along the lower Cowlitz River. A major element of the Mount

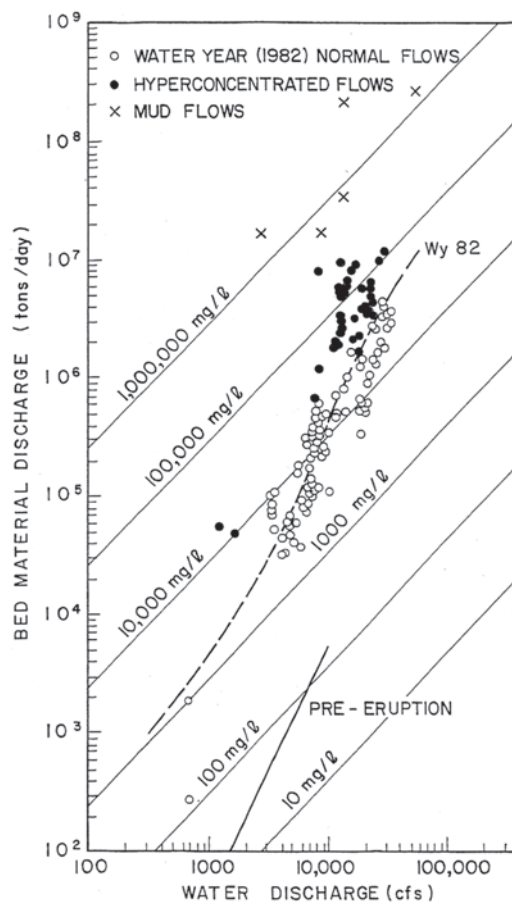


Fig. 4. Comparison of measured bed material transport rates of the Toutle River Highway 99 Gauging Station (in English Units).

Source: Jeffrey Brent Bradley. (1986). "Hydraulics and bed material transport at high fine suspended sediment concentrations," Dissertation Ph.D., Colorado State University, Fort Collins, Colorado.

St. Helens Project is the Sediment Retention Structure (SRS) located at river kilometer 21.2 (RM 13.2) of the North Fork of the Toutle River. The SRS dam is 54.8 m (180 ft) high and has an estimated capacity of 197 million cu m (258 million cu yd). Construction was completed in 1987. The debris avalanche along the North Fork Toutle River has been evolving since 1980 and differs significantly from when the original SRS design was completed. Sediment deposits upstream of the SRS reached the elevation of the SRS spillway crest between November 1997 and March 1998 (see Fig. 5). The uppermost row of outlet pipes on the SRS was closed in April 1998.

WATERSHED RECOVERY

Since the 1980 eruption, the Toutle River basin has adjusted itself in various ways. These adjustments include recovery of the watershed, vegetation, and development of the channel system. These ecological and morphological changes alter the hydrologic, hydraulic and sediment transport characteristics of the basin. Available data and information were evaluated to assess the extent and rate of watershed recovery. The objective of the analysis was to estimate the long-term trend of sediment supply from the debris avalanche to the North Fork Toutle River. Elements of the analysis included evaluation of historic cross-section data, channel profile comparisons, historic aerial photography comparisons, and computer-based evaluations of digital elevation models of the North Fork Toutle River basin for different time periods.

Historic cross-section survey information was evaluated to identify trends in channel cross-section development, such as channel widening and channel degradation. The rate at which channel cross-section development has occurred



Fig. 5. Sediment deposits behind the SRS.
Source: WEST Consultants, Inc.

and whether or not the channel has stabilized was assessed. Surveyed cross-sections (USGS, 2000) along the North Fork Toutle, South Fork Toutle, and Toutle Rivers were utilized in the analysis. Cross-sections have been repeatedly surveyed at more than 100 locations along these three rivers. Cross-section surveys began as early as 1980, and have been resurveyed periodically up through 1999. Typical results are shown in Fig. 6. Cross-sections on the North Fork Toutle, South Fork Toutle, and Toutle Rivers show a general trend of increased cross-sectional area since the eruption. A majority of the cross-sections have had a significant amount of stream bank erosion and channel degradation. As a result, many locations show an increase in channel width and lowering of the thalweg elevation.

A profile analysis was performed for the North Fork Toutle River, Castle Creek, and Coldwater Creek in order to identify changes in the channel slope and thalweg elevation. Digital Terrain Models (DTMs) (CENWP 2000) of the North Fork Toutle River above the SRS for the years 1987 and 1999 were used in the analysis. Profiles were extracted from the two DTMs along the path of the 1999 channel starting at the upstream end of Loowit Creek, near the crater, down to the SRS along the North Fork Toutle River.

The profile analysis shows that the North Fork Toutle River, Coldwater Creek, and Castle Creek have all degraded between 1987 and 1999, except between the N-1 debris dam and the SRS. The most degradation on the North Fork Toutle River occurred near the Coldwater/Castle Creek confluence, and was as much as 12.2 m (40 ft). Up to 12.2 m (40 ft) of degradation was also observed on Coldwater Creek, and up to 18.3 m (60 ft) of degradation was observed on Castle Creek. More than 30 m (100 ft) of aggradation was observed upstream of the SRS. Even though the channels degraded significantly, the overall slope of the channels changed very little between 1987 and 1999, except near the SRS. Fig. 7 and Fig. 8 show changes in the North Fork Toutle River, Coldwater Creek and Castle Creek profiles, respectively.

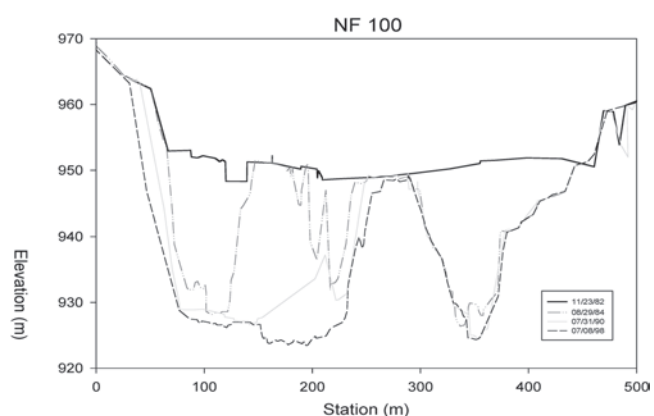


Fig. 6. Typical cross section data for the North Fork Toutle River.
Source: WEST Consultants, Inc.

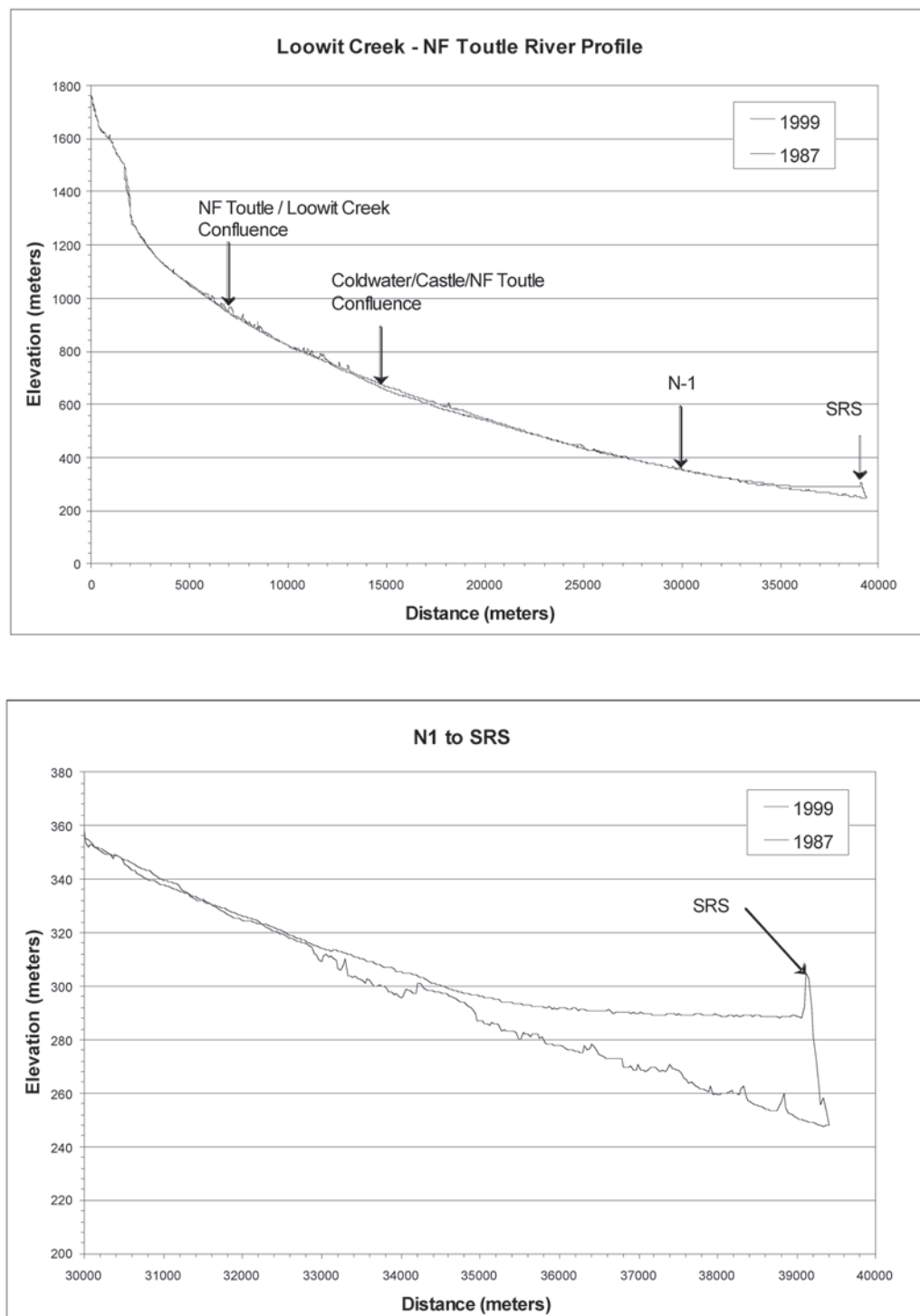


Fig. 7. Loowit Creek—N.F. Toutle River channel profiles.
Source: WEST Consultants, Inc.

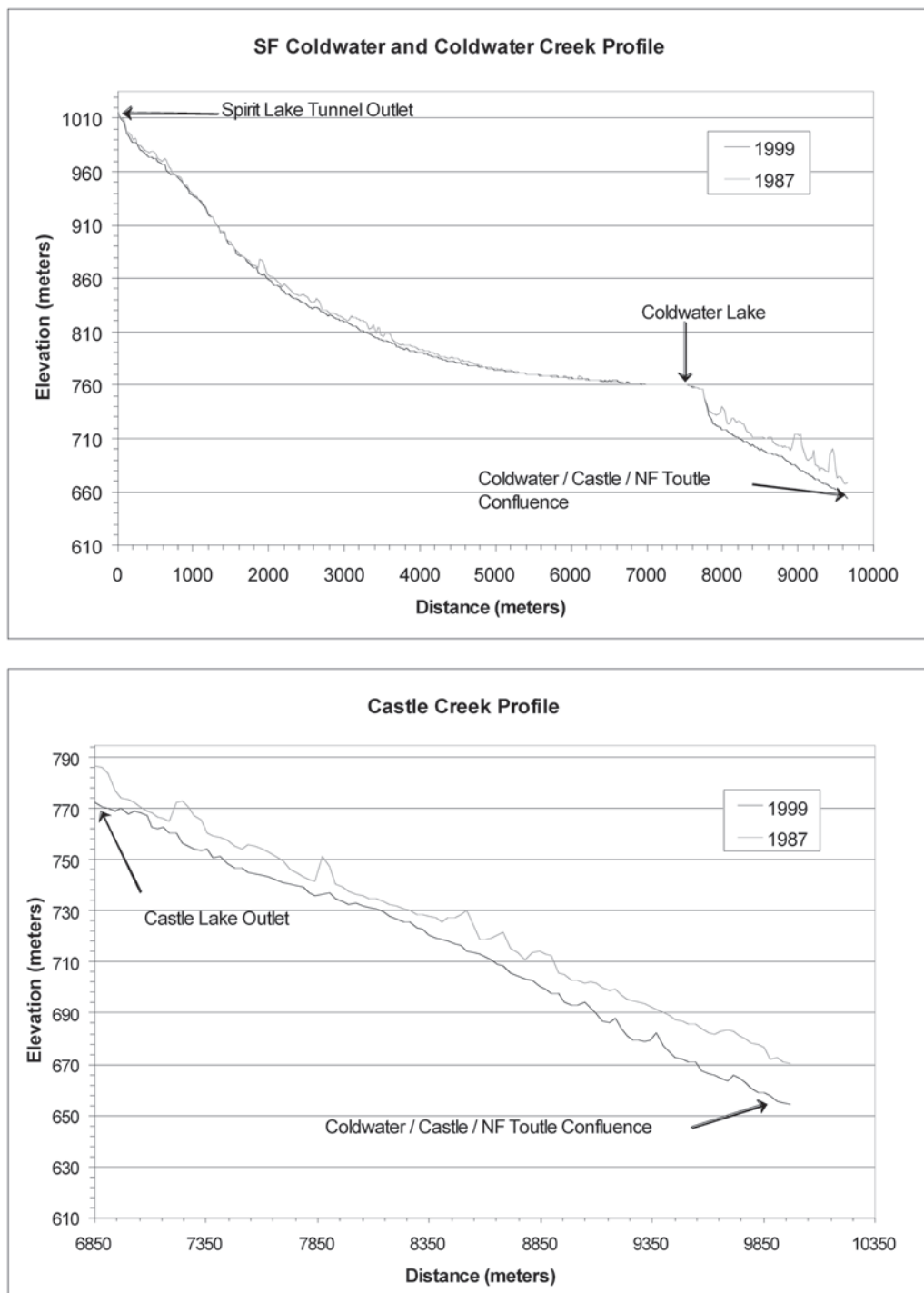


Fig. 8. Coldwater Creek and Castle Creek profiles.
Source: WEST Consultants, Inc.

A plan form analysis was made to observe the condition of sediment erosion and deposition upstream of the SRS. The analysis was made to observe and document geomorphic changes in the river valley over time and evaluate how the occurrence and severity of these channel changes has progressed since the eruption. To perform the analysis, historic aerial photography for the years 1980, 1982, 1983, 1984, 1985, 1987, and 1999 were compared. Analysis of the historical aerial photography indicates that the basin is beginning to recover. The majority of the channels were historically braided since the eruption; however, in many places the density of braided channels has declined, and at a few locations a single thread channel has formed. This would indicate that these channels have become more stable. The emergence of vegetation seen in the 1999 aerial photography adjacent to many of the channels provides additional evidence that watershed recovery is beginning to occur. However, the floodplains remain virtually unvegetated, indicating a continued lack of channel stability. The density and aerial extent of vegetation generally increases in the downstream direction.

The majority of the debris avalanche lacks any significant vegetation while nearer to the SRS there are trees growing on the hillslopes, the floodplain fringe, and even portions of the floodplain. This is likely due to several factors, including

lack of sufficient soil nutrients, and soil moisture to promote vegetative growth on the debris avalanche, reduced impacts from the eruptive blast in the downstream direction, and replanting of private forest land outside of the volcanic monument. Additional evidence of watershed recovery can be seen by the stability and extensive vegetation of the delta formation in Coldwater Lake. This would indicate that South Coldwater Creek has started to stabilize.

While there are some indications of hydro-geomorphic recovery, the aerial photograph analysis also provides clear evidence that recovery is very slow. Watershed recovery to pre-eruption conditions has not occurred. The channels continue to shift and widen, and large-scale degradation and bank erosion is still occurring in many areas, as evidenced by the changes in channel plan form and the massive volume of sediment trapped behind the SRS since its completion in 1987.

SEDIMENT SOURCES

Digital Terrain Models (DTMs) developed from aerial photography for the years 1987 (pre-SRS) and 1999 in the form of Triangulated Irregular Networks (TINs) were analyzed to estimate the total erosion on the debris avalanche upstream of the SRS as well as the total deposition behind the SRS over

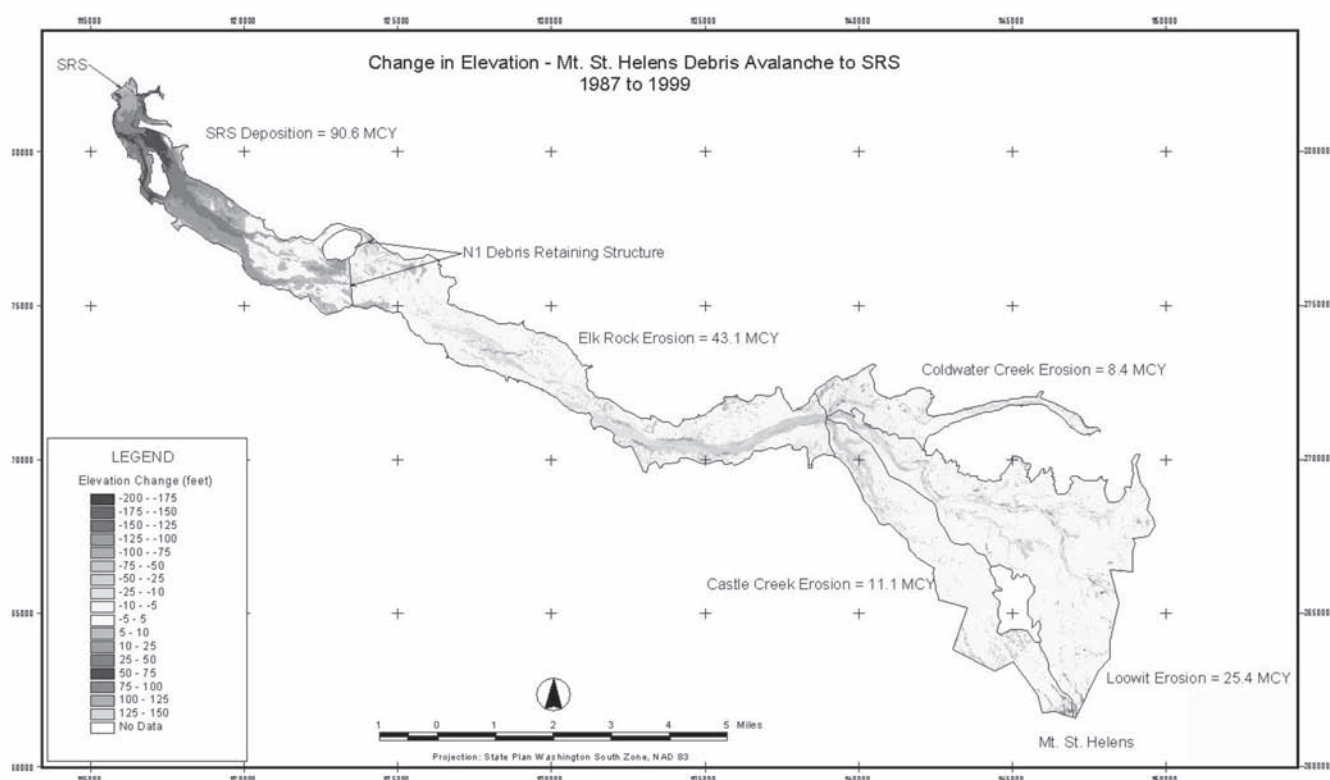


Fig. 9. Elevation difference grid showing locations of erosion and deposition (in English Units).
Source: WEST Consultants, Inc.

the involved time period. Erosion estimates were defined for each of the primary sediment sources (sub-areas) on the debris avalanche. These sub-areas were categorized as Elk Rock, Coldwater Creek, Castle Creek and Loowit Creek. Deposition estimates were developed for the North Fork Toutle River between the SRS and N-1 Debris Retention Structure.

The two TINs were converted to overlapping grids with 10 ft by 10 ft cells. The grids were clipped to contain only the data pertinent to the analysis (only the locations of deposition or erosion as seen in the 1999 aerial photography). An elevation difference grid was developed by subtracting the 1987 grid surface from the 1999 grid surface showing the location and magnitude of the changes in elevation that occurred between 1987 and 1999 (see Fig. 9). An extensive amount of deposition has occurred between the SRS and N-1 Debris Retaining Structure. In locations nearest the SRS deposition depths exceed 30m (100 ft). The majority of the debris avalanche erosion is associated with the North Fork Toutle River channel upstream of Elk Rock. The most extensive erosion typically occurs along the outside of channel

bends, where bank erosion has caused elevation changes of up to 55 m (180 ft). This suggests that bank erosion has played a major role in the contribution of sediment to the North Fork Toutle River. Site visit observations confirm this conclusion. Fig. 10 and Fig. 11 are 3-dimensional views of portions of the DTMs showing erosion from the debris avalanche and deposition behind the SRS.

The total erosion from the sediment source sub-areas were compared to the sediment deposition volume measured between the SRS and N-1 Debris Retaining Structure and the volume of sediment passing the Kid Valley gauge (assumed to be the same as the sediment passing the SRS) to evaluate data consistency. The total amount of erosion was measured to be 67.3 million cu m (88 million cu yd). When bulked by 16% to account for the reduction in density associated with deposition, the total erosion is estimated to be 78.1 million cu m (102.1 million cu yd). Total deposition measured between the SRS and N-1 is 69.3 million cu m (90.6 million cu yd). Suspended sediment passing the Kid Valley gauge was estimated to be 8.4 million cu m. (11 million cu yd). It is noted that the Green River enters the North Fork Toutle River above the Kid Valley gauge and would account for a small portion of the 8.4 million cu m (11 million cu yd) measured at the gauge. Between 1988 and 1998 the Green River was estimated to contribute approximately 0.5 million cu m (0.6 million cu yd) to the North Fork Toutle above Kid Valley. This estimate was based on suspended sediment discharge measurements made from 1988 and 1994 and correlation with the Tower Road suspended sediment record. Fig. 12 shows historical channel evolution at selected areas in the debris avalanche.

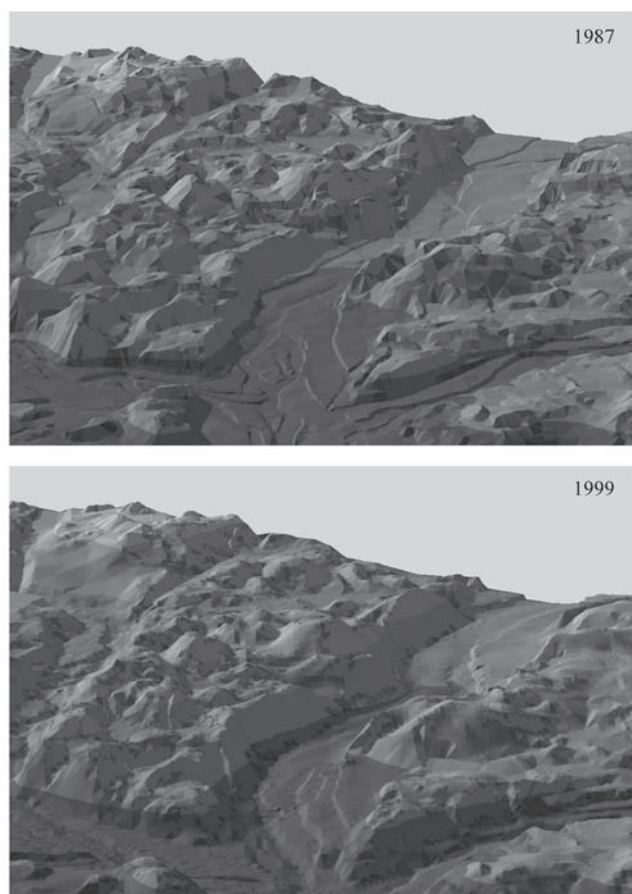


Fig. 10. Three-dimensional view of erosion from the debris avalanche at the Castle-Coldwater-N.F. Toutle confluence, 1987–Present.
Source: WEST Consultants, Inc.

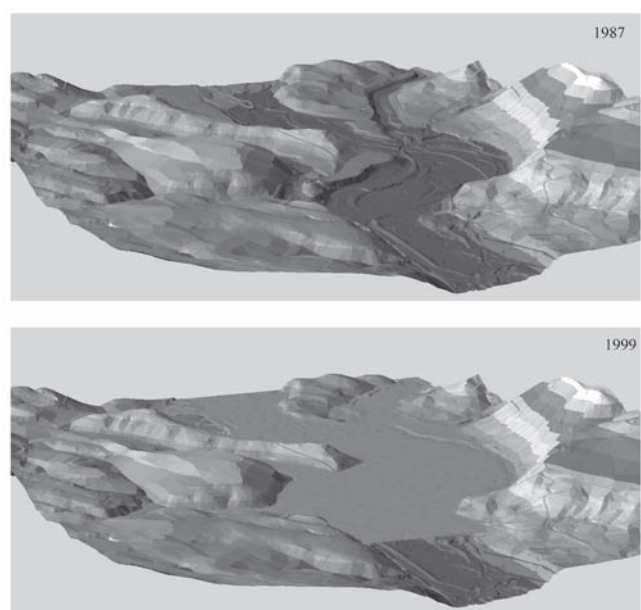


Fig. 11. Three-dimensional view of downstream portion of deposition behind the SRS, 1987–present.
Source: WEST Consultants, Inc.

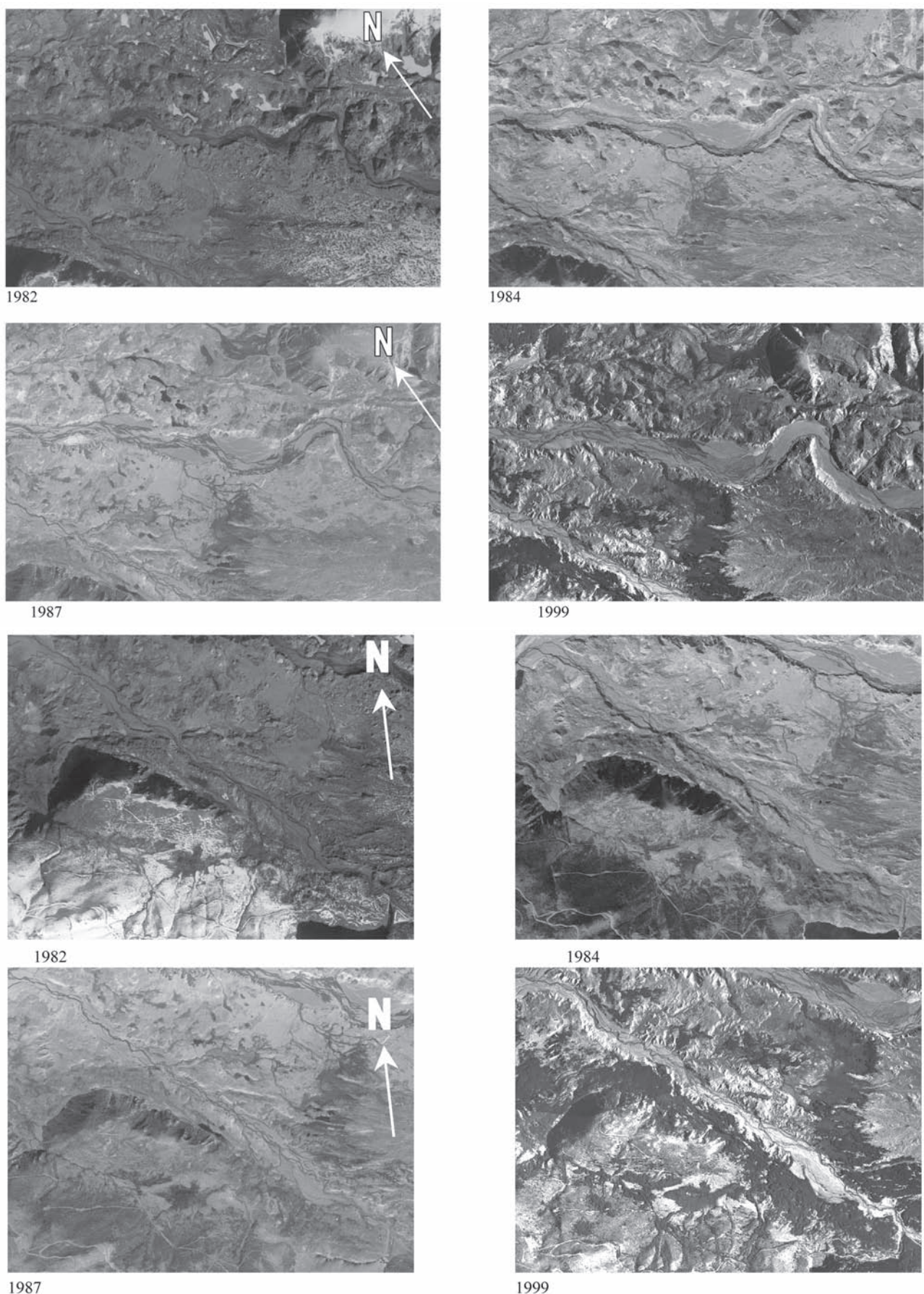


Fig. 12. Historical aerial photographs of the N.F. Toutle River upstream of the Castle Creek/Coldwater Creek Confluence.

Source: WEST Consultants, Inc. Based on historical aerial photography developed by the Corps of Engineers, Portland District.

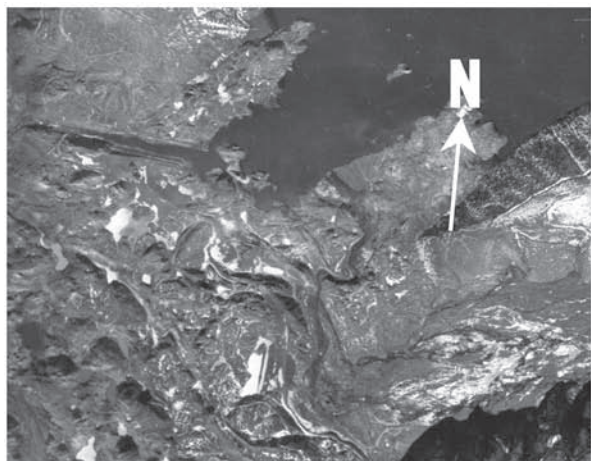
The total North Fork Toutle River suspended sediment load that passed the SRS (above the Green River) for water years 1988 through 1998 was estimated to be 7.95 million cu m (10.4 million cu yd). The deposition behind the SRS plus the estimate of suspended sediment that passed through the SRS totals 77.2 million cu m (101 million cu yd). This volume is approximately 1% less than the total erosion volume estimated for the sediment source sub-areas. The most significant source of sediment has been the Elk Rock and Loowit sub-areas, which have a combined total of approximately 78% of the total debris avalanche erosion since 1987. Castle Creek sub-area and Coldwater Creek sub-area make up approximately 12.6 and 9.5% of the total debris avalanche erosion, respectively.

SEDIMENT YIELD

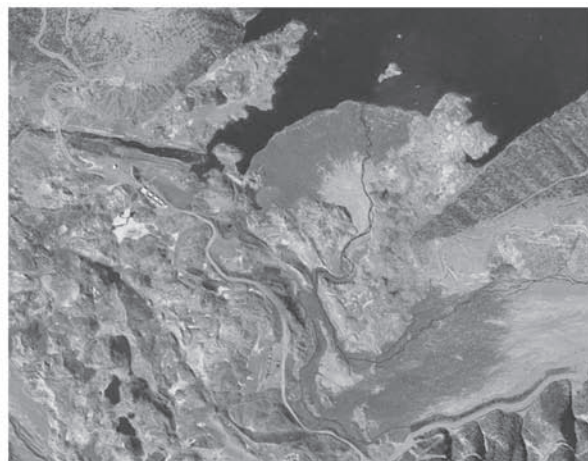
The average annual sediment yield of the debris avalanche will be influenced by the hydrologic and geomorphic recovery

of the watershed and its stream channels. The trend and rate of recovery could be expected to significantly affect the accuracy of the average annual sediment yield estimate. Measured sediment yields at the Toutle River at Tower Road Gage and deposition behind the SRS were used to evaluate existing trends in sediment yield.

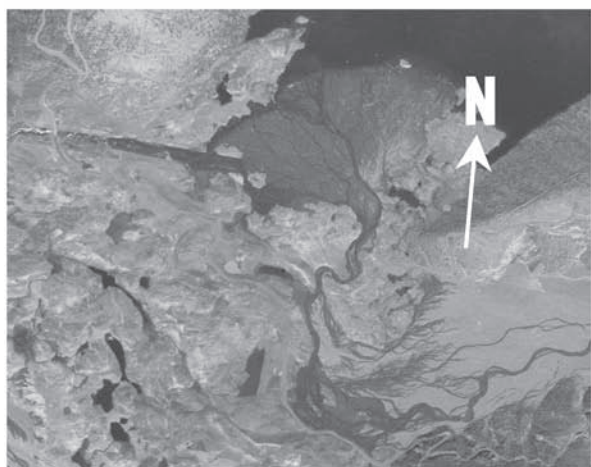
As seen in Fig. 13, annual sediment yields measured at Tower Road were significantly larger during the early 1980s, but then reduced fairly rapidly throughout the late 1980s and early 1990s. This would indicate that recovery in the watershed was causing a reduction in sediment supply to downstream areas. However, this time period was also a period of below average runoff. Total annual runoff was approximately 15% below normal for the period 1985 to 1995. A significant increase in sediment yield occurred during the 1996 and 1997 water years, as total annual runoff was approximately 45% above normal. This would indicate that sediment yield from the watershed is highly dependent upon the hydrology. Variability in the hydrologic cycle would tend to mask trends in the reduction of sediment yield. However, the fact that



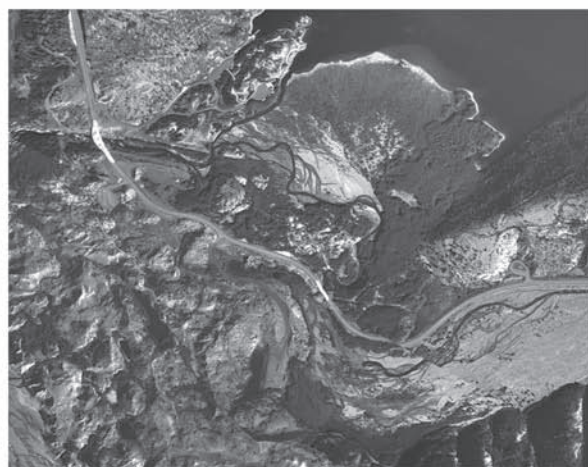
1982



1984



1987



1999

Fig. 12. Historical aerial photographs of the N.F. Toutle River upstream of the Castle Creek/Coldwater Creek Confluence.

Source: WEST Consultants, Inc. Based on historical aerial photography developed by the Corps of Engineers, Portland District. (*Continued*)

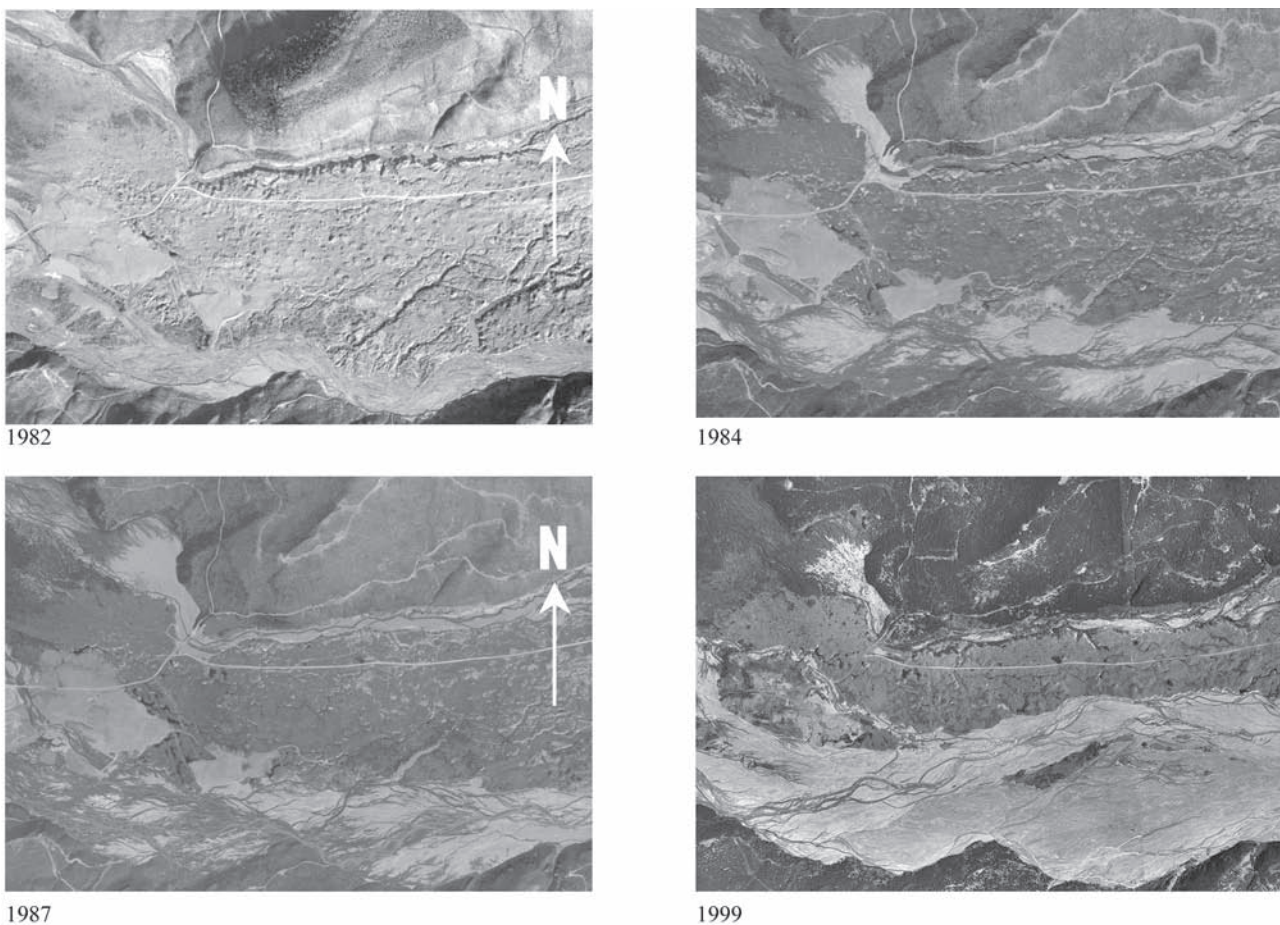


Fig. 12. Historical aerial photographs of the N.F. Toutle River upstream of the Castle Creek/Coldwater Creek Confluence.

Source: WEST Consultants, Inc. Based on historical aerial photography developed by the Corps of Engineers, Portland District. (*Continued*)

the sediment yields measured for 1996 and 1997, the largest water years of record, were less than those measured in 1982 and 1983 would indicate that some recovery has taken place. However, the sediment yield in 1996 was nearly the same as that which occurred in 1984, which further indicates the dependence of sediment yield on the involved hydrology. To account for the dependence between sediment yield and hydrology, the annual sediment yield was divided by the annual runoff to determine the yield of sediment per unit volume of runoff or average sediment concentration. As seen in Fig. 14, the yield of sediment in 1996 was approximately 8.6 kg per cu m (11.7 tn per acre-ft) of runoff while the yield in 1984 was approximately 11.3 kg per cu m (15.3 tn per acre-ft) of runoff, a reduction of approximately 24%, providing further evidence of watershed recovery.

The average annual sediment concentrations were accumulated on an annual basis to determine if a trend of decreasing average sediment concentration over time is occurring in the system (see Fig. 15). A trend line was fit to the cumulative concentration data to develop a sediment concentration decay

curve. By extrapolation, a future sediment yield curve can be developed and is shown in Fig. 16 (WEST Consultants 2002). Total sediment yield from the debris avalanche is estimated to be 344 million cu m (450 million cu yd) by the year 2035. This is approximately 55 and 31% less than estimates of 765 million cu m (1 billion) and 497 million cu m (650 million cu yd) made previously (USACE 1984).

CONCLUSIONS

A chronology of events has been presented at Mount St. Helens since the May 18, 1980 eruption to present. A further discussion of watershed recovery, sediment sources and sediment yields has also been presented to the reader. While there are some indications that watershed recovery has begun to occur, analyses of available data suggests that recovery has been very slow. Watershed recovery to pre-eruption conditions has not occurred. The channels continue to shift and widen, and large-scale degradation and

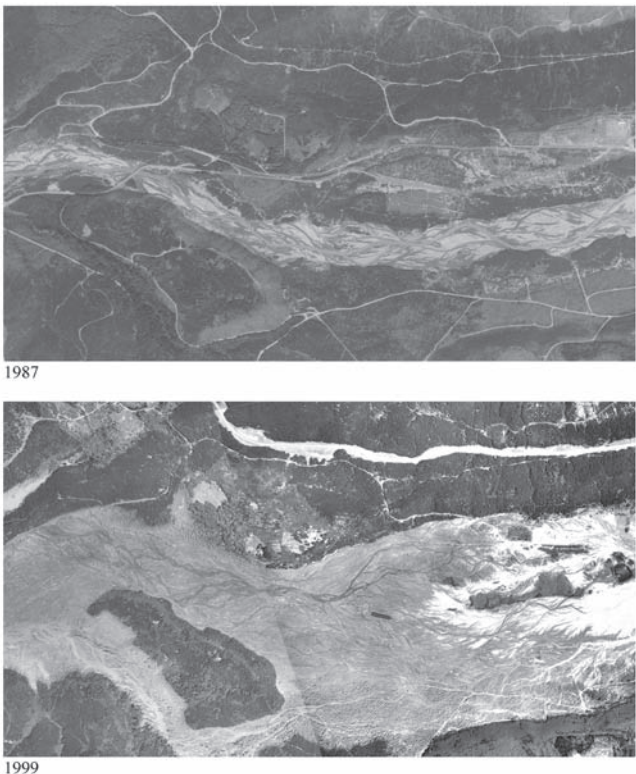


Fig. 12. Historical aerial photographs of the N.F. Toutle River upstream of the Castle Creek/Coldwater Creek Confluence.

Source: WEST Consultants, Inc. Based on historical aerial photography developed by the Corps of Engineers, Portland District. (*Continued*)

bank erosion is still occurring in many areas, as evidenced by the changes in channel plan form and the massive volume of sediment trapped behind the SRS since its completion in 1987. Additionally, the time period between the two most recent years of aerial photography (1987–1999) of 12 years combined with the occurrence of very high flows in 1996, makes it difficult to assess more recent hydrologic recovery. However, it is noted that the volume of sediment deposited behind the SRS during the 1996 water year was approximately two times larger than in any previous year since 1987. This would indicate that significant hydrologic recovery of the basin has not occurred in recent years as large flow events such as that which occurred in 1996 still have the ability to mobilize large volumes of sediment. However, it is expected that as watershed recovery progresses, sediment yields will decrease over time for similar flood events.

The SRS is currently filled with sediment to the spillway crest, though it is still a relatively horizontal deposit. There is still significant sediment storage behind the SRS for the sand and coarser fraction of the sediment load. Fine sediments that had been previously trapped by the SRS since its

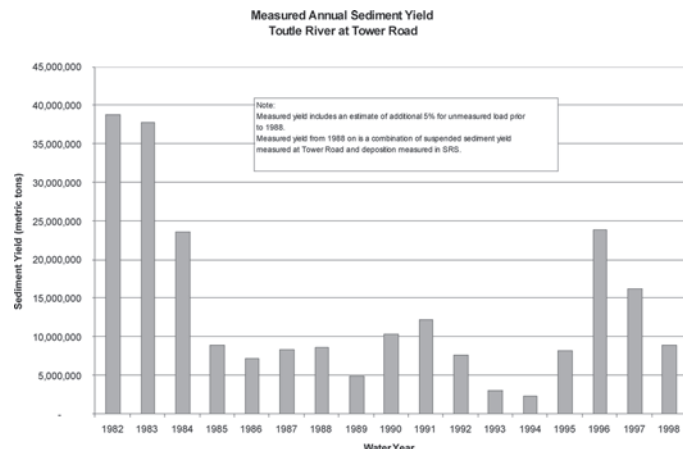


Fig. 13. Measured annual sediment yield from Toutle River at Tower Road.

Source: WEST Consultants, Inc.

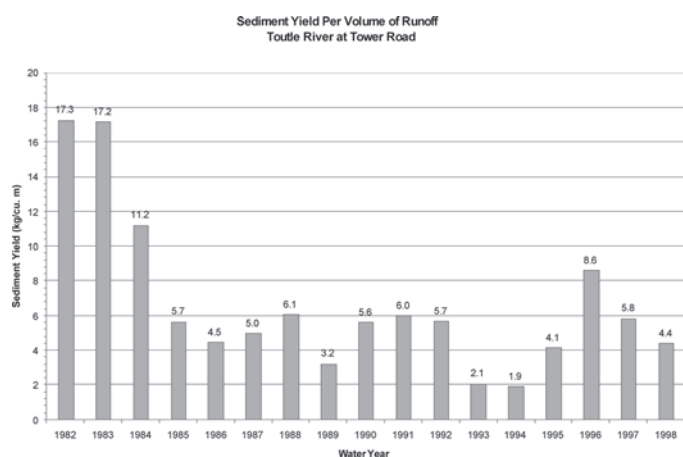


Fig. 14. Annual sediment yield per unit volume of runoff.

Source: WEST Consultants, Inc.

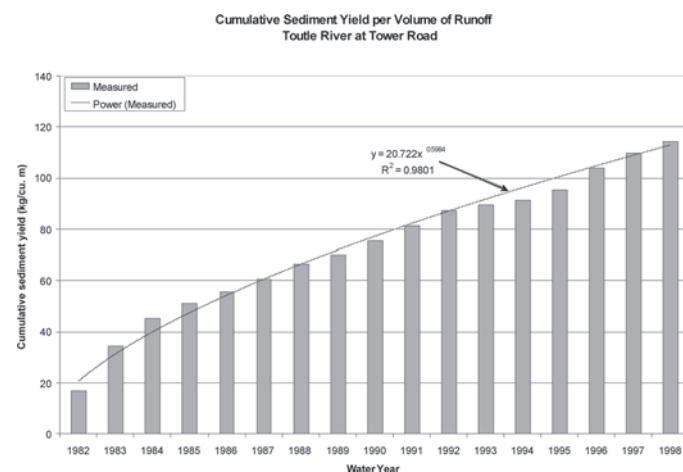


Fig. 15. Cumulative sediment yield per unit volume of runoff.

Source: WEST Consultants, Inc.

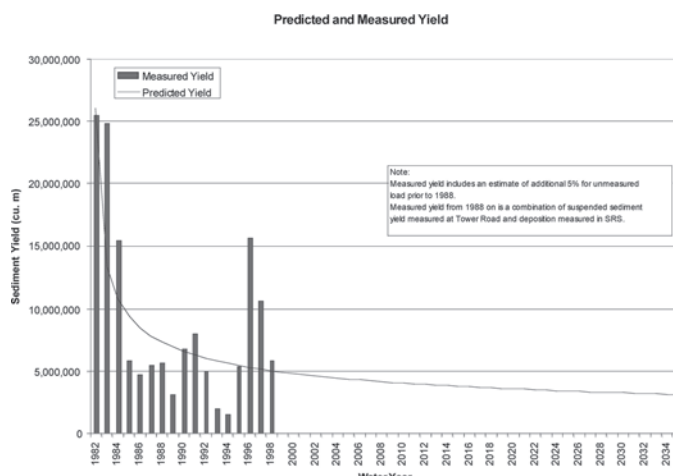


Fig. 16. Predicted and measured sediment yield.

Source: WEST Consultants, Inc.

1987 closure will now be passed downstream to the Toutle, Cowlitz and Columbia Rivers. It is expected that as the sediment deposits build behind the SRS, more and more of the coarse fraction of the sediment load will be passed over the spillway and be transported downstream by the Toutle and Cowlitz Rivers. Extremely high sediment transport rates should still be expected in the future.

REFERENCES

- Bradley, J. B. (1986). "Hydraulics and bed material transport at high fine suspended sediment concentrations." Ph.D. Dissertation, Department of Civil Engineering, Colorado State University, Fort Collins, CO.
- Pierson, T. C. and Scott, K. M., *Downstream Dilution of a Lahar: Transition from Debris Flow to Hyperconcentrated Flow*, Water Resources Research, American Geophysical Union, Vol. 21, No. 10, October 1985.
- Portland District Corps of Engineers (CENWP), Electronic File Transfer, May 2000.
- U.S. Army Corps of Engineers (USACE). *Corps Project Components*. Mt St. Helens, Washington. ASCE Tour. Portland District, Hydrologic, Coastal, and River Engineering Section, 1999.
- U.S. Army Corps of Engineers (USACE), Portland District, *Mt. St. Helens Cowlitz and Toutle Rivers Sedimentation Study*, September 1984.
- U.S. Army Corps of Engineers (USACE), *A Comprehensive Plan for Responding to the Long-Term Threat Created by the Eruption of Mount St. Helens*, Washington, Appendices, October 1983.
- U.S. Geological Survey (USGS) Cascades Volcano Observatory (CVO), Historic Cross Section Data for Toutle River, N. F. Toutle River and S. F. Toutle River, Electronic file transfer, 2000
- WEST Consultants, Inc., Mount St. Helens Engineering Reanalysis: Hydrologic Hydraulic, and Sediment Transport Analyses, April 12, 2002.